INSTITUTO POLITÉCNICO DE BRAGANÇA
Escola Superior de Tecnologia e Gestão

Generation of Phase Equilibrium Data in the Production of Ethyl Biodiesel using Non-Edible Vegetable Oils

FAHAD MUHAMMAD

Dissertation presented to

Escola Superior de Tecnologia e Gestão

Instituto Politécnico de Bragança

To obtain

Master's degree in Chemical Engineering

Supervisor:

Simão Pedro de Almeida Pinho

Co-Supervisor:

Lucie Coniglio-Jaubert

October, 2016

Acknowledgements

My greatest acknowledgement goes to that Supreme Being, Creator and Master of the day of Judgement who have bestowed me with the best of health and wisdom, guided me to the straight path and kept me alive to experience the blessed times we are living in.

I am highly grateful to have worked with so many wonderful people, who have assisted me in one way or another during my entire work. This short review will fall short in words to include everyone who had been the driving force in the accomplishment of my thesis.

My earnest gratitude to my supervisor, Prof. Simão Pedro de Almeida Pinho without his consent this work wouldn't have been initiated. He had been an excellent source of guidance in imparting knowledge. I have found him to be an expert in the domain of this work and the extent of his knowledge amused me to recognize his priceless possession. His significant assistance coupled with vast scientific insights helped me to understand the importance of this work which I hope will make a decent contribution to the scientific community world-wide. I appreciate all his efforts for being my mentor and a building block for my project.

The pragmatic approach needed for the completion of this work is also my primary source of information and this wouldn't have been possible without Prof. Lucie Coniglio Jaubert who was a constant motivator ever since the start of my work. She participated actively during my work and provided me with the appropriate working conditions from time to time. She built a bridge to elucidate the theoretical concepts in practical applications. I cannot thank her enough for her continuous support, understanding and patience during my stay in her lab. Throughout my internship, her kind behavior always inspired me and these few words will do no justice on her alluring personality. Also, I would like to thank Prof. Jean Noel Jaubert, I am delighted to have met such a wonderful person.

I confer my deepest thanks to my course co-ordinator, Prof. Filomena Barreiro for her encouragement to take this internship as an opportunity, thereby opening the gateways of bright prospects for my future. I deeply thank Prof. Filomena Barreiro together with Prof. Luis Pais for their persistent help.

I want to thank International Relations-Office-IPB, who earned exceptional mention here for their invaluable support in dealing with complex bureaucratic formalities throughout my

Erasmus stay. I am proud to have been part of this temple of education, ‘’Instituto Politecnico de Bragança’’. I want to thank all the academic and non-academic staff for their help.

My appreciation will be hollow in words, without mentioning Riskivector Unipessoal Lda Team for their supervision in all the affairs of my life. In particular, Vitor Daniel Pinho Laranjeira and Rasa Savodnikaite deserve special attention as they have erased that gray-zone which differentiates family and friends. I am thrilled to have met people of such caliber in this life.

I am also grateful to my family who had left no stone-unturned in their exceptional moral upbringing, ultimately rendering me to acquire the best of education in a foreign land.

Lastly, my sincere thanks to all my friends who have been around me in pursuit of my goals.

Table of Contents

List of Tables

List of Figures

LIST OF ABREVIATIONS

ASOG	Analytical Solution of Groups
BA	Balanites Aegyptiaca
BAEE	Balanites Aegyptiaca Ethyl Esters
DIPPR	Design Institute of Physical Properties
FAEEs	Fatty Acid Ethyl Esters
FAMEs	Fatty Acid Methyl Esters
FFAs	Free Fatty Acids
FID	Flame Ionization Detector
HC	Hydrocarbons
IS	Internal Standard
LLE	Liquid- Liquid Equilibrium
NEVO	Non- Edible Vegetable Oils
NIST	National Institute of Standards and Technology
NO_X	Nitrogen Oxides
NRTL	Non- Random Two Liquid Model
RHA	Rice Husk Ash
RTD	Resistance Thermometer Detector
SO_X	Sulphur Oxides
TCD	Thermal Conductivity Detector
UNIFAC	UNIQUAC Functional Group Activity Coefficients
UNIQUAC	UNIversal QUAsi Chemical Activity Coefficient
VLE	Vapour- Liquid Equilibrium

Abstract

The importance of fatty acid ethyl esters (FAEEs) in the various applications of chemical industries such as pharmaceutical, cosmetic, food and most recently, in the oil and gas industry for the production of biodiesel has driven this study to carry out phase equilibrium measurements composed of fatty acid esters together with a mixture of alcohols. The data collected from this study is of high importance for the design, optimization and operation of industrial facilities manufacturing these compounds for the production of biodiesel.

Pure component vapour pressures of two saturated fatty acid ethyl esters, ethyl hexanoate and ethyl octanoate and three alcohols namely, 1-pentanol, 1-octanol and 1-dodecanol were measured at pressures ranging from 7 kPa to 98 kPa and temperatures from (354 to 474) K using a dynamic apparatus. The experimental data (P-T) were smoothed using the Antoine equation and compared with the available literature values.

The objective also involved the study of vapor-liquid equilibria (VLE) data for three different binary system using a dynamic ebulliometer. The binary systems included ethanol + ethyl hexanoate, 1-pentanol + ethyl hexanoate and 1-pentanol + ethyl octanoate. The VLE data for each binary system was determined at two pressures ranging from (14.65 to 53.33) kPa. The experimental VLE data for each of the binary mixtures was represented by the NRTL five-parameter models together with Lyngby modified UNIFAC and Dortmund modified UNIFAC to understand the VLE behaviour of these mixtures.

Finally, multicomponent VLE was performed for a system comprising 1-octanol + 1-dodecanol + BAEE (Balanites Aegyptiaca ethyl esters) for a pressure range of 8 kPa to 12 kPa. The vapour pressures of fatty acid ethyl esters of balanites aegyptiaca (BAEE) involved in this multicomponent system was also evaluated using the DIPPR databank.

Chapter 1. Introduction

Fuels play a crucial role in the economy of every country and a large proportion of world's energy needs are fulfilled by petroleum, and its derivatives, such as coal and natural gas. With an unprecedented consumption of these natural resources in the areas of transportation, agricultural sector together with intensive industrialization and population growth have led to a sharp rise in the prices of these resources. Due to these reasons, the stocks of naturally available petroleum resources are being depleted and it is creating an imbalance in the production and consumption cycle at global level. In addition to the scarcity of these organic sources, they also create a negative impact on the ecosystem since burning of these fuels leads to emission of gaseous pollutants like CO_2, HC, NO_x, SO_x etc. which is an added elemental cause in global warming. The rapidly increasing and unstable prices, uncertainties concerning petroleum availability, increased environmental concern and the effect of greenhouse gases from the industries have aroused an attention in the quest for alternate sources for petroleum-based fuel including diesel fuel [1].

The challenges to meet its demand and to reduce the world's dependence on crude oil, biofuels have culminated and resulted in providing sustainable alternatives which not only reduce greenhouse gas emissions into the atmosphere, but also helps in improving engine performance thereby helping in attaining fuel efficiency and reducing exhaust emissions [2]. These biofuels which are mostly employed as an alternative resource to diesel engines, are the mono-alkyl esters of long chain fatty acids, derived either from vegetable oils or animal fats and alcohols, through transesterification with or without a catalyst. It is a renewable, biodegradable, non-toxic, portable, and readily available eco-friendly fuel. A biodiesel production may involve different means with a different potential feedstock. The use of edible vegetable oils, or the first generation feedstock, has been of great concern because they raise issues such as food versus fuel debate, that might cause starvation especially in the developing countries owing to shortage of agricultural production, creating a global imbalance to the market demand, rising of food prices and also not to forget the environmental problems triggered by utilizing much of the available arable land. This route of biodiesel production creates serious ecological problems as countries around the world would begin cutting down forests for plantation purposes. Hence, use of such a feedstock could cause deforestation and damage to the wildlife in the long run.

Therefore, non-edible vegetable oils (NEVO) have become more attractive and viable source for sustainable production of biodiesel. Non-edible vegetable oils are not suitable for human consumption due to the presence of some toxic compounds in the oils. NEVO crops use lands that are largely unproductive and those that are located in degraded forests and desolate areas. These crops can be planted on field/farm boundaries, fallow lands, and in public land such as along railways, roads and irrigation canals. This production route of biodiesel from non-edible oils can overcome the problems of food versus fuel, economic and environmental issues related to edible vegetables ultimately providing energy security [3].

Thus, more emphasis should be given to non-edible resources, owing to its inherent advantages of low cost compared to edible oil crops and also due to their wide versatility, natural availability, variety of plants producing these oils in large amounts all over the world. Lastly, the growing of these plants reduces concentrations of CO_2 in the atmosphere. However, as a serious drawback, most non-edible oils contain high content of free fatty acids (FFAs), which increase the biodiesel production cost [4].

1.1 Motivation

The ever increasing worldwide concern for environment protection and for the conservation of non-renewable natural resources have led to demonstrate the potential applications of fatty acid methyl esters (FAMEs) and fatty acid ethyl esters (FAEEs) as diesel substitutes and they are known as biodiesel. A wide range of resources could be used for ethanol production: starch, sugar, and cellulose containing raw materials, as well as wastes. Both ethanol and vegetable oils are renewable and environmentally benign. Additionally, ethanol has better solvent properties than methanol in biodiesel production.

The greatest potential of biofuels lies in its utilization of raw materials emerging mainly from non-edible crops, instead of edible ones, as they do not compete in terms of shortage of resources and also from other controversial issues of food chain. Although biodiesel has lot of advantages in relation to petroleum diesel, the high price of its production is the major barrier in its commercial applications. The use of cheap non-edible oils can be a way to improve the economy of biodiesel production at the industrial scale. Because of differences in climatic conditions of various countries, a considerable research has resulted in the achievement of best type of non-

edible vegetable oils for its efficient use in biodiesel production [4]. The current focus is to produce fuels with desired properties in both technically and economically attractive ways to support sustainability and protect the environment. Due to the abundance and variety of biomass feedstocks, as it brings a great deal of incompatibility of various biofuels and the combustion engines, therefore a more resilient and compatible production method is the need of the time [5]. The most efficient route should take into account, the sustainable method of fuel production in line with lowest level of carbon emissions, safe handling of the fuel, its impact on bio-diversity, resources which impedes food level and most importantly the cost and quality of the fuel.

For a rational design and operation of biodiesel production processes, it is essential to have quantitative and reliable information about the vapour-liquid equilibrium (VLE) and liquid-liquid equilibrium (LLE) of mixtures containing alcohols, fatty acid esters and glycerol, near or above the critical temperature of the alcohol [6]. An adequate description of the distribution of the transesterification products between the two immiscible phases, in a broad range of thermodynamic conditions, is essential for a correct study and design of equipment involved in the production and purification of biodiesel. However, the presence of polar compounds with strong associative interactions increases the complexity of these systems, limiting the use of conventional thermodynamic models. In addition, there is still a considerable lack of experimental equilibria data for the two phases formed during the transesterification [7].

The sustainable methods for production of biodiesel as an alternative to petroleum diesel require simulating the production process by using estimators involving thermodynamic and kinetic models. Regardless of the method one chooses, be it Supercritical/Low pressure/High pressure transesterification, the attainment of the accurate phase equilibrium data involving VLE or LLE are always essential. This data will later help to validate the previously selected thermodynamic model to simulate the process at its different stages of the reaction, separation and purification. Depending on the raw materials used, this oil can contain more or less unsaturated fatty acids ethyl esters in its composition. For example, ethyl oleate and ethyl linoleate are the main products from soybean oil and ethyl palmitate is the primary component in palm oil. Among the raw materials, the oleaginous seeds with high oil content (soybean, sunflower and rapeseed seeds) have gained much attention as a renewable raw material for biodiesel production due to their relatively high yield [8]. Due to the competition of edible oils for human use and biofuel

production, non-edible oils are becoming one of the leading raw materials for producing biodiesel.

As it will be shown in the section 3.2, a careful and extensive study on the available papers shows a considerable lack of VLE and LLE data related to ethanol ethyl esters. Therefore, due to the complexity of the conditions involved in VLE data generation, this work was inspired to make contributions in this ever-increasingly important field.

1.2 Objectives

Biodiesel fuels, mainly mixtures of fatty acid methyl or ethyl esters (FAMEs or FAEEs), have been the focus of significant media attention, industrial interest, and scientific research. These fuels are potential blending additives for petroleum-derived diesel fuels due to their overall performance, its impact on environment, safe handling, feedstock availability, and fuel quality.

One important objective of this work is to explore a well-founded and clear review on available alternatives between the various approaches for the production of biodiesel either by conventional routes, based on homogenous/heterogeneous catalysis under atmospheric pressure and ambient temperature, combined with dry purification, and the supercritical route without the use of catalyst.

Owing to time limitations, the specific objective of this work is restricted to the presentation of new important VLE phase equilibrium data for binary systems involved in ethyl biodiesel production obtained at two different pressures. A large body of new vapor pressure data of pure substances is also going to be measured in order to considerably increase the number of available data and check the accuracy of temperature and pressure measurements. The synthesis of an ethyl ester mixture from non-edible oil is also under attention.

Besides, to perform different consistency tests for the new data, the ability of excess free Gibbs energy model and group-contribution based approaches to describe the phase diagrams of these complex binary systems is going to be evaluated, as well as to represent real multicomponent mixtures.

Chapter 2. Processes for Biodiesel

In chemical terms, biodiesel is a mixture of fatty acid alkyl esters, most often methyl or ethyl esters obtained by alcoholysis of triacylglycerols from vegetable oils and animal fats. In general, vegetable oils can be converted into biofuels using any of the four methods: blending, micro-emulsions, pyrolysis and transesterification. Out of these methods, transesterification is widely applied because it offers the most promising solutions to problems related to high viscosity oil contained in vegetables [4].

Biodiesel, a blend of fatty acid alkyl esters, is industrially produced by the transesterification of fats or oils with alcohols (methanol/ethanol) in the presence of a catalyst, to produce fatty acid alkyl esters and a by-product, glycerol [7]. A catalyst is used to, initiate the reaction, increase the reaction rate and enhance the solubility of alcohol. Another method may include the supercritical process without the involvement of catalyst, essentially carried out at high temperature and pressure to compensate the absence of catalyst. The stoichiometry of the transesterification uses 1 mole of triglyceride for every 3 moles of ethanol to form 3 moles of esters and 1 mole of glycerol. The overall equation can be described in terms of three consecutive reversible reactions leading to intermediate diglycerides and monoglycerides shown in the scheme below [2]:

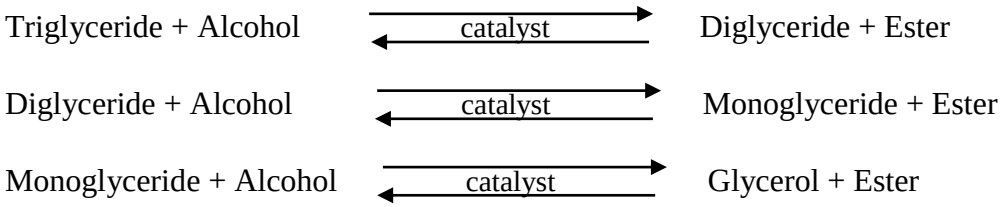

Scheme 1: Alcoholysis of triglycerides as a sequence of three consecutive reversible reactions.

A typical diesel engine cannot run by using a normal vegetable oil, as the high viscosity of these oils prevents its usage in proper functioning of the engine. Various methods for biodiesel production have been developed over the course of time, the prominent among them are pyrolysis, micro-emulsion, dilution & transesterification. A more detailed explanation for the production process is given in the paper by Atabani.*et.al*.[3].

The main sources of edible oils for biodiesel production are soybean, palm, rapeseed, sunflower, linseed and coconut oils. Whereas the non-edible vegetable oils (NEVO) sources include

Azadirachta indica (neem), Jatorpa curcas, Pongamia pinnata etc. Within the non-edible sources, Balanites Aegyptiaca(BA) popularly known as desert date is found to be a good candidate for its use as a feedstock in the biodiesel production, as it is known to produce significant amount of triglycerides and this tree can be cultivated in arid and semi-arid regions of the world, therefore it is found in abundant quantities in Africa and Asia. Annually, a typical Balanites Aegyptiaca Ethyl Esters (BAEE) tree produces 10,000 yellow colour fruits with each fruit weighing 5-8g consisting of pulp 28-33%. This pulp is mixed with water for several hours and later oven dried to remove the moisture ultimately producing the oil. Various quality parameters are taken into consideration to know the standard of the extracted oil, such as specific gravity, viscosity, refractive index, saponification, moisture content etc. before the transesterification reaction is carried out using alcohol as the reacting medium. Alcohol such as ethanol is used because of its physical and chemical advantages as the shortest chain alcohol can quickly react with the triglycerides in the presence of a catalyst [33].

Figure 1. A typical Balanites Aegyptica fruit and seeds

2.1 Conventional

Transesterification reaction can be catalysed by both homogeneous (alkalis and acids) and heterogeneous catalysts. Typically, a catalyst is essential to enhance the reaction speed and yield. In order to move the reaction towards the products, an excess of alcohol is used in the transesterification reaction. Different types of catalysts can be used such as sodium or potassium

hydroxides, sulphuric acid, ion exchange resins or lipases [7]. Transesterification through homogeneous catalysts show better results when the free fatty acid content is < 1 wt%, but they come with certain disadvantages such as expensive separation of the catalyst from the reaction mixture, generation of large amount of wastewater during separation and cleaning of catalyst and the products, formation of unwanted by-products. Transesterification by heterogeneous catalysts has no such disadvantages and shows better results when the vegetable oils contains free fatty acid (FFA) is > 1 wt% as they can be easily separated from the reaction products unlike homogenous catalysts. They are especially suitable for deep frying oils from restaurants and food processing industries because they prevent undesired saponification reactions. The reaction is less corrosive and it is environment friendly, which can be operated in continuous processes. In addition the catalyst can be regenerated and reused [1].

In the use of an alkali catalyst it is mandatory to remove the catalyst as it comes with soaps as by-product, thus it requires conditions to manage waste streams with a high pH. Due to the sensitivity of alkali catalysts to the fatty acids and water contents, a superior quality of raw materials is always desired. In addition, alkaline transesterification is low in selectivity leading to undesirable side reactions. Equipment corrosion and the need of vigorous stirring required for the mixing of the two-phase mixture of oil and alcohol are some of the technical problems encountered in this approach [6]. However, the alkali-catalysed (i.e. NaOH, KOH) process is relatively fast but is affected by water content and FFAs of oils or fats. FFAs can react with alkali catalysts to form soap and water. Formation of soap not only lowers the yield of alkyl esters but also increases the difficulty in the separation of biodiesel and in the catalyst water washing step due to the presence of emulsions. From the literature it is observed that, mostly methoxide catalysts give higher yields than hydroxide catalysts and potassium-based catalysts give better biodiesel yield than sodium-based catalysts [1]. The alkaline catalysed transesterification is carried out in a multiphase reactor where the oil reacts with an alcohol, in the presence of a catalyst, to form fatty acid esters and glycerol. The glycerol obtained is separated from the oil phase at the outlet of the reactor, where two liquid phases co-exist; one of them rich in glycerol and the other in fatty acid esters. The unreacted alcohol is distributed between these two liquid phases [7].

Acid-catalysed reactions (i.e. H_2SO_4, H_3PO_4) are used to convert FFAs to esters, or soaps to esters as a pre-treatment step for high FFA feedstocks and these are characterized by slow reaction rate and high ratio of alcohol. A high conversion efficiency with acid-catalysed transesterification can be achieved by increasing the molar ratio of alcohol to oil, reaction temperature, catalyst loading and the reaction time [1].

Alcohol is the main source in the production of biodiesel and based on the type of alcohol used, the method can be further sub-categorised. In general, the production is carried out using methanol, owing to its low cost and physical and chemical advantages. Nevertheless, ethanol has the potential to become prevalent in the production process, especially in regions where it is easily produced. It is less toxic and comes with a superior dissolving capacity. The use of biodiesel, which is composed of fatty acid ethyl esters, is also more environment friendly due to lower emissions of nitrogen oxides and carbon monoxide. Due to the extra carbon added, fatty acid ethyl esters have a higher heat content and cetane number and improved storage properties. In addition, biodiesel produced from methanol cannot be classified as entirely carbon-neutral as it is derived from natural gas or coal via synthesis gas, while ethyl ester biodiesel can be totally derived from agricultural sources [7]. The conventional processes for the production of biodiesel are now briefly presented.

2.1.1. Homogenous alkali catalysed transesterification

Homogenous alkali catalysed transesterification reaction commonly uses alkali catalysts such as NaOH, CH_3ONa and KOH. The major advantages of using alkali catalysts in the industries include their wide availability, economical factors and competency to catalyse the reaction at low temperature, and atmospheric pressure, leading to high conversion in a minimal amount of time. The limitation of this catalyst is that it can be applied only for refined vegetable oil with less than 1 wt% FFAs. Thus, it is not suitable for a feedstock with an average FFAs content higher than 1 wt% as it very sensitive to the purity of the reactant. Under identical experimental conditions, it has been found that the virgin oil yields higher ester conversion (97%) compared to waste frying oils (92%). If the FFAs content in the oil reaches higher value, for example 3 wt%, it has been found that the alkaline-catalysed transesterification process is not suitable to produce esters. In order to prevent the saponification reaction, the FFAs and water content of feed must be below 1

and 0.1 wt%, respectively. Due to these reasons, only pure vegetable oil feeds are appropriate for alkali-catalysed transesterification without extensive pre-treatment [1].

2.1.2. Homogenous acid catalysed transesterification

This transesterification process is usually catalysed by H_2SO_4, HCl, BF_3, H_3PO_4, or organic sulfonic acids. The main advantage of acid-catalysed transesterification process is the direct biodiesel production from low-cost lipid feedstocks, such as used cooking oils and greases, which are known for higher FFAs contents, as acid catalysed transesterification is insensitive to the FFAs content in the feedstock. Since alkali catalysed transesterification process poses limitations especially for oil or fat with high FFAs concentration, liquid acid catalysts are proposed in order to overcome the limitations. Acid-catalysed transesterification is a one step process, thereby more economical than the alkali catalysed process which requires an extra step to convert FFAs to methyl esters. These reactions are performed at high alcohol to oil molar ratios, low-to-moderate temperatures and pressures, high acid catalyst concentrations. Although it is insensitive to FFAs in the feedstock, homogeneous acid-catalysed transesterification has been largely ignored mainly because of its relatively slower reaction rate compared to alkali catalysed transesterification reaction [1].

2.1.3. Heterogeneous alkali catalysed transesterification

The heterogeneous catalyst process is anticipated to be an effective biodiesel production process with low cost and minimal environmental impact, because of the possibility of simplifying the production and purification processes under mild conditions. The commonly used catalysts include zeolites, alkaline earth metal oxides and hydro-talcites. The solid base catalysts are easily regenerated and have a less corrosive nature, leading to safer, cheaper and more environment friendly operations, and can also be used directly as a catalyst to prepare biodiesel when the FFAs content is lower than 1 wt% [1].

2.1.4. Heterogeneous acid catalysed transesterification

Heterogeneous acid-catalysed transesterification reactions have the required potential to replace liquid acid catalysts. The solid acid catalysts are insensitive to FFAs content, as esterification and

transesterification occur simultaneously, which avoids the washing step of biodiesel, easier separation of the catalyst from the reaction medium, low product contamination, easier regeneration and recycling of catalyst and reduction in the corrosion problems even in the presence of acid species. In spite of these advantages, it has the limitations of slow reaction rate, and possible undesirable side reactions. The ideal characteristics of a solid acid catalyst are its interconnected system of large pores, moderate to high concentration of strong acid sites and hydrophobic surface [1].

2.2 Supercritical

In the conventional transesterification process, high FFAs and water contents result in soap formation, which reduces catalyst efficiency with high catalyst consumption, altogether resulting in low conversion [1]. As an alternative to conventional methods of bio-diesel production, a catalyst-free method for transesterification, uses supercritical methanol/ethanol, at very high temperatures and pressures in a continuous process. Alcohol fulfil dual roles, one as a reactant and the other, it can be used as an acid catalyst in supercritical process. In the supercritical state, the oil and methanol are in a single phase and reaction occurs spontaneously. A set of recent works addressing the supercritical synthesis of biodiesel suggests that, this process have several advantages over the catalysed approaches, and could successfully overcome a number of problems associated with conventional processes [6]. Supercritical transesterification is designed to overcome the reaction initiation lag time caused by extremely low solubility of the alcohol in the triglyceride phase. With a very high molar ratio of methanol to oil (42:1), the reaction is completed in a short time. The absence of catalyst makes the glycerol recovery and biodiesel purification much easier, trouble-free and more environment friendly [1]. The issues related to catalyst removal, replacement and sensibility to fatty acids and water content are not of concern as no catalyst is used. Very good quality of glycerol is produced and only a simple evaporation process, of the excess amount of ethanol is necessary to get fatty acid methyl esters (FAMEs) within the specified characteristics [6]. The supercritical transesterification method can give nearly complete conversions under appropriate conditions, in a short processing times (minutes instead of hours), and the process can tolerate feedstocks with a high concentration of FFAs and water [5]. The free fatty acids in the oil are esterified simultaneously with the triglycerides, and therefore, the duration of the reaction is significantly shorter, even with low-quality raw

materials. Hence, it requires a smaller reactor size to achieve the same production output of the conventional biodiesel production process [6].

Although the supercritical process requires high pressures and temperatures, the advantages of a non-catalysed process may make it competitive with the existing alkali catalysed processes, especially for the conversion of inferior quality raw resources, rich in free fatty acids and water, such as waste cooking oils. In addition, to the elimination of catalyst removal step, the process can tolerate water in the feedstock and free fatty acids are converted to ethyl esters instead of soap, so a wide variety of feedstocks can be used [6]. Depending upon the type of oil used in the supercritical transesterification, the temperature can range in between 473 K to 673 K and the pressure can range from 2 Mpa to 65 Mpa. Nonetheless, at industrial level, the synthesis of biodiesel by supercritical ethanol is not a viable option due to its severe reaction conditions and high operational costs. Therefore, intense research is dedicated to decrease the severity of the reaction conditions of temperature and pressure using co-solvents, such as carbon dioxide, hexane, propane, or subcritical conditions with small amount of catalyst are some of the options currently under attention [1].

2.3 Separation Issues

Traditionally, in a conventional process when using an alkali catalyst, it is mandatory to remove the catalyst and the soaps (by-product) from the biodiesel [6]. The separation issue with the catalyst is more predominantly seen in homogenous catalyst than heterogeneous catalyst, as the separation of catalyst from the reaction mixture requires huge quantities of wastewater to separate and clean the catalyst and the by-products. The separation of catalyst from the reaction mixture is automatically achieved when using a plug flow reactor with heterogeneous catalyst [1]. The separation of the catalyst after the transesterification is achieved using water as the separating agent, within an un-economically wet-washing process. Contrary to the conventional separation techniques, dry-washing of biodiesel with naturally available adsorbent was performed at a pilot scale in the work developed by Pandey et al. [9]. The adsorbent is ash, and it is usually obtained from the combustion of the left-over oil extract materials, such as seeds or husks. In heterogeneous catalysis, the catalyst can be regenerated and reused adding advantages from the point of view of cost and efficiency. As no catalyst is used in the supercritical

transesterification, the problems associated with catalyst separation are not encountered as it makes the glycerol recovery and biodiesel purification trouble free and environment friendly [1].

In the transesterification of ethanol with oils, globally the stoichiometry for the reaction is set at 3:1 ethanol to oil ratio. However, this ratio is much increased in order to promote the reaction rate by adding a catalyst, especially because of the possibility of the reversibility of the transesterification reaction. Depending upon the type of catalyst, the ratio of ethanol to oil is 6:1 for alkali catalyst and 30:1 for acid catalyst. At the end of the transesterification under the given temperature and pressure conditions, esters and glycerol are produced forming two immiscible phases; the top ester rich phase and the bottom glycerol rich phase.

Ethanol has higher solvent properties than methanol, implying difficulty in its recovery. Under such circumstances the separation between the liquid phases is accomplished by evaporating the ethanol, under heterogeneous catalyst or supercritical conditions. Whereas, under conditions of alkaline homogenous catalyst, the ratio of ethanol to oil is approximately set at 6:1, the quantity of ethanol is quite less, therefore an excess of glycerol is added to the mixture for the phase separation.

Chapter 3. Phase Equilibrium

Regardless of the approach undertaken to produce biodiesel, knowledge of the phase diagram for the multicomponent system is essential to design an adequate, suitable and reliable process. Obtaining the phase diagrams of the reaction medium through the use of thermodynamic data is the basis for developing models, which are crucial for the optimization of the purification process. In this context, the main objective of this work is to enhance the experimental databank by providing information on the VLE related to binary and ternary systems that are involved in biodiesel production and purification processes. Phase equilibrium data are also essential for better understanding the processes and improve the reaction rate, the selectivity of the desired product, and the separation process for the product mixture. Moreover, simulations for developing new processes for such systems require an activity coefficient or equation of state based model that can adequately describe these multiphase systems. For a rational design and operation of biodiesel production processes, with supercritical alcohols or by the other conventional route, it is compulsory to have quantitative and reliable information about the phase equilibria of mixtures containing alcohols, fatty acid esters and glycerol, near or above the critical temperature of the alcohol.

3.1 Methods for VLE

The purpose of this work is the experimental and theoretical study of vapour-liquid equilibria of a binary system. Accurate measurement of high- and low-pressure multi-component (VLE) has presented one of the most compelling experimental challenges to chemical engineers and physical chemists for a considerable time. In general terms, the separation of VLE system is carried out by:

3.1.1 Static Method

In this method a thoroughly degassed liquid mixture is filled into an equilibrium cell immersed in an isothermal environment. When equilibrium is attained, the pressure is measured and the equilibrium liquid composition is calculated from the charge composition. The commonly used static apparatus is shown in the **Figure 2**. In the static method the vapour and liquid compositions are not measured, but are obtained by calculation indicating a requirement of

considerable amount of effort because the P-x isotherm must be of the highest accuracy and even a small change in curve shape can cause large errors [11]. Therefore this method is well adapted for study of mixtures constituted by compounds presenting very different volatalities.

There are two types of static methods: The first is the “classic” TPx which works at different sequential constant temperatures, for a given composition of the liquid phase, the composition of the vapour phase being calculated by thermodynamic relations. This method is relatively fast and very accurate in a large pressure range by using a combination of pressure sensors. The most delicate step prior to the pressure measurements is the degassing of the liquid mixture to remove air and volatile impurities without changing the composition of the sample. Ebullition under vacuum with flowing back of the condensed vapour is an effective method for liquid degassing. This static method is well suited to the development of thermodynamic models. The second type is the static-analytical method TPxy in which both vapour and liquid phases are analysed, making it quite suitable to study multicomponent systems, and also for the validation of thermodynamic models [2].

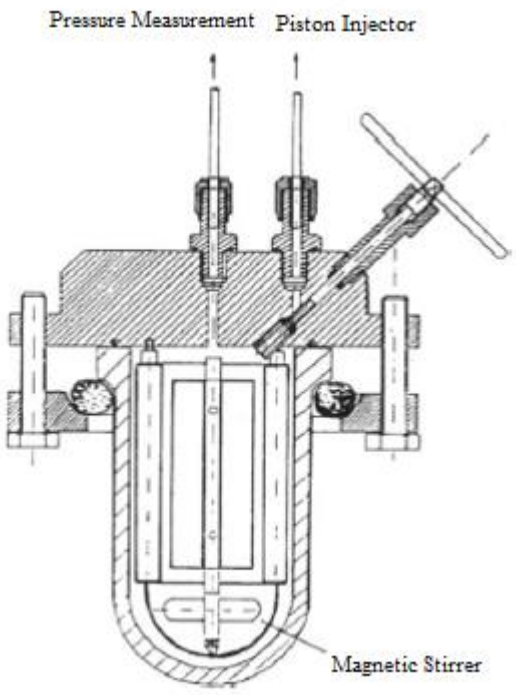

Figure 2. Static equilibrium cell of (adapted from Fischer and Gmehling [11]).

3.1.2 Dynamic Method

In dynamic methods, both the liquid and vapour phases are circulated. Recirculating equilibrium stills have accounted for most of the low pressure VLE data. In spite of their popularity, the various equilibrium stills present a number of problems especially when accurate data is desired for non-ideal systems.

Some of the problems include:

- Failure to attain true equilibrium.
- Partial condensation of equilibrium vapour.
- At a given temperature and pressure, the attainment of smooth boiling and a steady state with minimum fluctuations is hard to find.
- Errors in composition measurement.

There are various apparatus employed within the dynamic method (**Figure 3**), the problems associated with them also include failure to accurately measure the temperature. Searching for better efficiency to attain an equilibrium state, a Cottrell vapour lift pump is used to circulate both the vapour and liquid. The most successful version of the apparatus achieves dynamic equilibrium by forcing the vapour and liquid downward co-currently through a short packed adiabatic chamber.

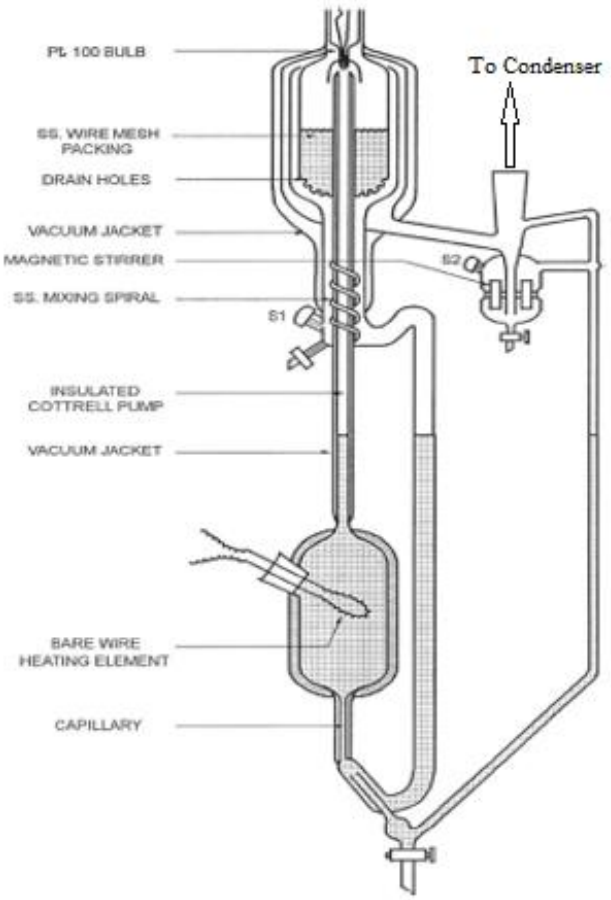

Figure 3. Dynamic VLE equilibrium still (adapted from [11]).

In order to achieve isobaric, or isothermal mode, the apparatus is controlled with the help of computer. The apparatus is compact, robust and the equilibrium chamber is symmetric and the temperature is measured at the bottom of the packing ensuring, usually, the measurement of thermodynamically consistent data. The sample can be analysed with the help of flame ionization detector (FID) equipped in gas chromatograph or other analytical techniques such as refractive index, densimetry or TCD.

3.1.3 Ebulliometric Method

An ebulliometer is designed to accurately measure the boiling point of liquids by measuring the temperature of the vapor-liquid equilibrium either isobarically or isothermally.

A Swietoslawski ebulliometer is one such kind which operates isobarically, the primary components are: the boiler, the Cottrell pumps, the thermowell, and the condenser. Such an ebulliometer can be used for extremely accurate measurements of boiling temperature, molecular weights, mutual solubilities, and solvent purities by using a resistance thermometer (RTD) to measure the near-equilibrium conditions of the thermowell. This ebulliometer is widely used for measuring the alcohol content of dry wines.

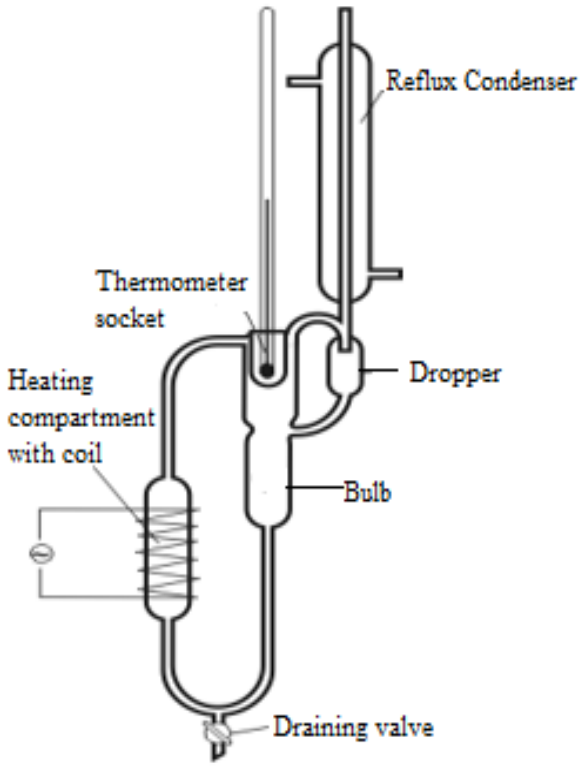

Figure 4. Swietoslawski ebulliometer still (adapted from [11]).

3.2 Database

After reviewing several papers devoted to the production of bio-diesel, information about the data pertaining to the VLE and LLE equilibrium for systems containing ethanol and /or various ethyl esters is compiled in **Table 1**.

Table 1. Information related to experiments and modelling of phase equilibrium for systems involved in ethyl biodiesel production.

System	Type of the phase equilibrium	T range (K)	P range (MPa)	Experimental information [a]	Modeling information	Reference
Ethyl palmitate + Ethyl stearate Ethyl palmitate + Ethyl linoleate Ethyl palmitate + Ethyl oleate Ethyl myristate + Ethyl palmitate	**VLE**	**502-519** **517-537** **503-536** **420-472**	**0.0053329** **0.0093326** **0.005332 - 0.009332** **0.0005-0.0015**	**No**	**CPA EoS**	[12]
Ethyl myristate + Ethyl palmitate	**VLE**	**421-469**	**0.0005-0.0015**	**Yes**	**NRTL, UNIFAC, Dortmund**	[13]
Ethanol + Ethyl hexanoate	**VLE**	**329-440**	**0.04-0.1013**	**Yes**	**Wilson, NRTL**	[14]
Ethanol + Ethyl laurate Ethanol + Ethyl myristate	**VLE**	**493 -543**	**2.23 – 7.09** **2.11 – 6.93**	**Yes**	**None**	[15]
Ethanol + Ethyl laurate, Ethanol + Ethyl myristate	**VLE**	**493 – 543**	**2.11 – 8.49**	**No**	**SRK/WS/COSMO-SAC**	[16]
Ethanol + Ethyl stearate Ethanol + Ethyl palmitate	**VLE**	**313 -419** **309 – 422**	**0.017 – 0.098** **0.015 – 9.3**	**Yes**	**NRTL, UNIQUAC and UNIFAC**	[17]
Jatropha FAEE + Ethanol + Water Jatropha FAEE + Ethanol Jatropha FAEE + Ethanol + Glycerol	**VLE**	**296 – 342** **295 – 382** **296 – 343**	**0.0067 – 0.0667**	**Yes**	**UNIQUAC**	[18]
CO2 + Methanol CO2 + Soybean oil FAME CO2 + Methanol + Soybean oil FAME	**VLE** **VLE + LLE** **VLE**	**303 – 343**	**3.2 – 11.2** **1.9 – 17.3** **4.2 – 13.6**	**Yes**	**PR-vdW2 and PR-WS (better)**	[19]
CO2 + Soybean oil CO2 + Castor oil CO2 + Soybean oil FAEE CO2 + Castor oil FAEE CO2 + Ethanol + Castor oil	**VLE**	**313 – 343**	**3.76 – 26.44** **2.12 – 25.50** **1.35 – 6.01** **1.77 – 25.45** **2.13 – 26.27**	**Yes**	**SAFT (better) and PR**	[20]

CO_2 + Ethanol	**VLE**	**291 – 313**	**N.A.** [b]	**No**	**CPA-EOS**	[21]
Glycerol + Water Glycerol + Ethanol	**VLE**	**384 – 481** **363 – 454**	**0.101**	**Yes**	**CPA-EOS**	[22]
Ethanol + Ethyl laurate Ethanol + Ethyl myristate Ethanol + Glycerol	**VLE**	**493 – 523** **493 – 573**	**2.0 – 7.00** **2.0 – 8.00** **2.0 – 8.00**	**No**	**CPA-EOS**	[6]
Ethyl palmitate + Ethyl stearate Ethyl palmitate + Ethyl oleate Ethyl palmitate + Ethyl linoleate	**VLE**	**502 – 520** **502 – 537** **514 – 537**	**0.0053** **0.0053 , 0.0093** **0.0093**	**Yes**	**Wilson, NRTL (better), UNIQUAC**	[23]
Glycerol + Water	**VLE**	**353 – 473**	**0.0062 – 0.8363**	**Yes**	**NRTL**	[24]
Ethyl laurate Ethyl myristate Ethyl palmitate Ethyl stearate Ethyl oleate Ethyl linoleate	**VLE**	**420 – 464** **446 – 492** **464 – 515** **491 – 534** **486 – 537** **486 – 537**	**0.00133 – 0.00933**	**Yes**	**Antoine equation**	[25]
Ethyl laurate Ethyl myristate	**VLE**	**313 – 462** **333 – 462**	**0.1810^{-5} – 0.0085** **0.1510^{-5} – 0.0032**	**Yes**	**Antoine equation**	[26]
Ethanol + Sunflower oil Azeotropic ethanol (96°) + Sunflower oil	**Phase transition (VLL-VL-V)**	**400 – 650**	**1.0 – 35.0**	**Yes**	**GCA – EOS**	[27]
CO2 + Soybean oil + Ethanol	**VLE**	**303-343**	**4.3-16.72**	**Yes**	**PR-vdW2 and PR-WS**	[28]

[a] *Here "Yes" denotes that the experimental information is provided by the reference mentioned in the table, whereas "No" denotes that the experimental information was obtained from another source.*

[b] *N.A implies information not available in the reference.*

3.3 Modelling

This section describes the models that are most frequently used for the description of VLE phase diagrams for the types of substances studied in this work.

3.3.1 NRTL Model

The non-random two-liquid model (NRTL) is a correlative excess Gibbs energy based model. The driving principle for NRTL model is based on the Wilson's hypothesis; that the local concentration around a molecule is different from the bulk concentration due to the difference in the interaction energy thus creating a non-random behaviour at local molecular level. The NRTL equation for the excess Gibbs energy (g^E) of a binary systems is given by [29]:

$$\frac{g^E}{RT} = x_1 x_2 \left(\frac{\tau_{21} G_{21}}{x_1 + x_2 G_{21}} + \frac{\tau_{12} G_{12}}{x_2 + x_1 G_{12}} \right) \quad (1)$$

where,

$$\tau_{12} = \frac{g_{12} - g_{22}}{RT} \quad (2)$$

$$\tau_{21} = \frac{g_{21} - g_{11}}{RT} \quad (3)$$

$$G_{12} = \exp(-\alpha_{12} \tau_{12}) \quad (4)$$

$$G_{21} = \exp(-\alpha_{12} \tau_{21}) \quad (5)$$

Here R is the ideal gas constant, T is the absolute temperature, x_i is the mole fraction of component i, and g_{ij} is a measure of the interaction energies between species i and j.

NRTL equation has three parameters per binary systems; two interaction parameters (τ_{12}, τ_{21}) and one non-randomness parameter (α_{12}), which is an energy parameter characteristic of the 1-2 interactions. For a large number of binary systems, the value varies from about 0.20 to 0.47, and when the value equals to zero it signifies that the mixture is completely random.

From the above equation (**1**), the activity coefficients of species 1 (γ_1) and 2 (γ_2) are:

$$\ln\gamma_1 = \; x_2^2\left[\tau_{21}\left(\frac{G_{21}}{x_1 + x_2 G_{21}}\right)^2 + + \frac{\tau_{12}G_{12}}{(x_2 + x_1 G_{12})^2}\right] \tag{6}$$

$$\ln\gamma_2 = \; x_1^2\left[\tau_{12}\left(\frac{G_{12}}{x_2 + x_1 G_{12}}\right)^2 + + \frac{\tau_{21}G_{21}}{(x_1 + x_2 G_{21})^2}\right] \tag{7}$$

The NRTL equation offers usually a good representation of experimental data for partially miscible systems and strongly non-ideal mixtures [29].

3.3.2 UNIFAC Based Models

The UNIFAC (UNIQUAC Functional Group Activity Coefficients) method uses the functional groups present in the molecules of a liquid mixture to calculate the activity coefficients. The group contribution (GC) methods, presenting a high predictive character, are most successful for the calculation of activity coefficients in the liquid phase, where the liquid phase is considered to be a mixture of structural groups, instead of a mixture of compounds, providing a significant advantage for the calculation of any systems, needing a relatively small number of parameters. The essential idea of a solution-of-groups model is to utilize existing phase equilibrium data for predicting phase equilibria of systems for which no experimental data are available. In concept, the UNIFAC method follows the ASOG (Analytical Solution of Groups) method, wherein activity coefficients in mixtures are related to interactions between structural groups [30]. The essential features are:

1. Suitable reduction of experimentally obtained activity-coefficient data to yield parameters characterizing interactions between pairs of structural groups.

2. Use of those parameters to predict activity coefficients for other systems that have not been studied experimentally but that contain the same functional groups.

The UNIFAC model splits up the activity coefficient for each species in the system into two components; a combinatorial (γ_i^c) and a residual (γ_i^R) component i.e for each compound, the activity coefficients are broken down.

In UNIQUAC, the two adjustable binary parameters τ_{ji} and τ_{ij} appearing in eq.10 must be evaluated from experimental phase equilibrium data. No ternary (or higher) parameters are

required for systems containing three or more components. In the UNIFAC method the combinatorial part of the UNIQUAC activity coefficients, eq.9, is used directly. Only pure component properties enter into this equation.

$$\ln\gamma_i = \ln\gamma_i^C + \ln\gamma_i^R \tag{8}$$

$$\ln\gamma_i^C = \ln\frac{\varphi_i}{x_i} + \frac{z}{2}q_i\ln\frac{\theta_i}{\varphi_i} + l_i - \frac{\varphi_i}{x_i}\sum_j x_j l_j \tag{9}$$

$$\ln\gamma_i^R = q_i\left[1 - \ln\left(\sum_j \theta_j\tau_{ji}\right) - \sum_j \frac{\theta_j\tau_{ij}}{\sum_k \theta_k\tau_{kj}}\right] \tag{10}$$

$$\ln\gamma_i^C = \ln\frac{\varphi_i}{x_i} + \frac{z}{2}q_i\ln\frac{\theta_i}{\varphi_i} + l_i - \frac{\varphi_i}{x_i}\sum_j x_j l_j$$

$$\ln\gamma_i^R = q_i\left[1 - \ln\left(\sum_j \theta_j\tau_{ji}\right) - \sum_j \frac{\theta_j\tau_{ij}}{\sum_k \theta_k\tau_{kj}}\right]$$

$$l_i = \frac{z}{2}(r_i - q_i) - (r_i - 1), generally\ z = 10 \tag{11}$$

where,

$$\theta_i = \frac{q_i x_i}{\sum_j q_j x_j} \tag{12}$$

$$\varphi_i = \frac{r_i x_i}{\sum_j r_j x_j} \tag{13}$$

$$\tau_{ji} = \exp\left(-\frac{u_{ji} - u_{ii}}{RT}\right) \tag{14}$$

In these equations, the summations are over all components, θ_i is the area fraction, φ_i is the segment fraction, which is similar to the volume fraction. Pure-component parameters r_i and q_i are, respectively measures of molecular van der Waals volumes and molecular surface areas and are calculated as the sum of the respective parameters of each constituting groups [30]. UNIFAC presents different parameter tables for VLE, LLE, infinite dilution activity coefficients, and also some variants. The most well-known are the modified UNIFAC from Lyngby and Dortmund.

Although the UNIFAC model is a successful model for VLE calculations extrapolations above 425 K should be avoided. Excess enthalpies and LLE are poorly predicted as well as

representation of dilute systems and phase equilibria for mixtures containing certain complex compounds like water as well as multifunctional chemicals. The latter represent an inherent limitation of 'first-order' GC methods, which do not account for the effects of several polar groups close to each other (proximity effects). The modified UNIFAC versions of Lyngby and Dortmund correct both the combinatorial and residual terms compared to the original UNIFAC. The former is accomplished by using an exponent-type term as described in the equations below and the latter by adding a temperature dependency in the interaction parameters. Due to this temperature dependency, these modified UNIFAC versions are quite successful for both VLE and to some extent excess enthalpies and infinite dilution activity coefficients, especially the Dortmund version, which is based on larger experimental database. Modified UNIFAC models can extrapolate VLE at higher temperatures better than the original UNIFAC. Moreover, these temperature-dependent UNIFAC versions employ more than just VLE data in the parameter estimation, typically H^E and γ^∞ as well. The UNIFAC variants adds strength, flexibility to the GC model approach [31].

The primary difference in the Lyngby variant is the presence of different combinatorial terms as can be seen in the following equations.

$$\ln\gamma_i^c = \ln\frac{\varphi_i}{x_i} + 1 - \frac{\varphi_i}{x_i} \tag{15}$$

$$\varphi_i = \frac{{r_i}^{2/3} x_i}{\sum_j {r_j}^{2/3} x_j} \tag{16}$$

The temperature dependency of Lynby modified UNIFAC is logarithmic in nature given by the expression $a_{mn} = a_{mn,0} + a_{mn,1}(T - T_0) + a_{mn,2}(T \ln\frac{T}{T_0} + T - T_0)$, where a_{mn} are interaction parameters between the groups *m,n*. Lyngby UNIFAC model is applied also beyond its ordinary VLE and LLE calculations. Some of its applications include calculation of surface tension, solubility of antibiotics in mixed solvents, flashpoint of flammable liquid mixtures, flavour sorption in packaging polymer, solvents selection for extractions [31].

The Dortmund modified UNIFAC considers the group surface area parameters marking an important difference between the Lyngby version. In addition, the Dortmund version has the most extensive parameter tables within the various UNIFAC versions.

$$\ln\gamma_i = \ln\frac{\acute{\varphi}_\iota}{x_i} + 1 - \frac{\acute{\varphi}_\iota}{x_i} - \frac{Z}{2}q_i\left(\ln\frac{\varphi_i}{\vartheta_i} + 1 - \frac{\varphi_i}{\vartheta_i}\right) \quad (17)$$

$$\acute{\varphi}_i = \frac{{r_i}^{3/4}x_i}{\sum_j {r_j}^{3/4}x_j} \quad (18)$$

$$\varphi_i = \frac{r_i x_i}{\sum_j r_j x_j} \quad (19)$$

Where ϑ_i (also represented as θ_i) is similar to **eq.12.** The temperature dependency term is exponential in nature given by the expression $a_{mn} = a_{mn,0} + a_{mn,1}T + a_{mn,2}T^2$. The wider applications of the Dormund modified version includes in the determination of Henry's law constant [31].

3.4 Consistency Tests for VLE

Consistency tests are applied to check the standard of error present in a VLE data, thus gauging the generated results in the development of high fidelity models used in the chemical process design. The enormous difficulty in carrying out precise VLE measurements which can interfere in the quality of the models developed for chemical process simulation, leads to the developments of a big set of VLE consistency tests. One of the most important approach is the algorithm proposed by Kang et al. [32] which is under development and applied at National Insitute of Standards and Technology (NIST, Boulder Colorado, USA). The algorithm in question exercise the use of Gibbs-Duhem equation in checking the consistency between the VLE binary data and pure component vapour pressures and these procedures are shown to be valuable in regression analysis of thermodynamic model parameters and detection of anomalies.

Consistency tests for vapor-liquid equilibrium data must conform the constraints given by the Gibbs-Duhem equation

$$\sum_i x_i \mathrm{d}\bar{M}_i - \left(\frac{\mathrm{d}M}{\mathrm{d}P}\right)_{x,T}\mathrm{d}P - \left(\frac{\mathrm{d}M}{\mathrm{d}T}\right)_{x,P}\mathrm{d}T = 0 \quad (20)$$

where M is a molar thermodynamic property, $\bar{M}_i$ is a partial molar property; and T, p, and x are temperature, pressure, and liquid composition, respectively; i is the summation over the

components in the chemical system. If the molar thermodynamic property is written in terms of excess Gibbs energy, it yields

$$M \equiv \frac{G^{\mathrm{E}}}{RT} = \sum_i x_i \ln\gamma_i \tag{21}$$

$$\sum_i x_i \mathrm{d}\ln\gamma_i - \frac{V^{\mathrm{E}}}{RT} + \frac{H^{\mathrm{E}}}{RT^2}\mathrm{d}T = 0 \tag{22}$$

where V^{E} is the excess volume and H^{E} is the excess enthalpy.

The results of each test correspond to a quality factor ranging from 0.025 to 0.25. The maximum sum of the three quality factors is 0.75 if all tests are passed. The detailed algorithm is presented in the paper by Kang et al.[32] and therefore only the important results pertaining to each test are presented.

3.4.1 Herington Test (Area Test)

Herington test is one of the oldest tests used for VLE consistence studies. It can be applied to both isothermal and isobaric data and it is based on the integration of Gibbs-Duhem equation. Due to the difficulty to evaluate the excess enthalpy for the test, it has been observing constant changes. In this work, the approach by Kang et al.[32] is used which involves the calculation of the following parameters

$$D = 100\left|\frac{(A-B)}{(A+B)}\right|, J = 150\left|\frac{\Delta T_{\max}}{T_{\min}}\right|$$

where A is the area above the zero line on the plot of $\ln(\gamma_1/\gamma_2)$ against x_1, and B is the area below the line. For isobaric data sets, the condition for passing the test is $|D - J| < 10$. The Herington test indicates compliance with the Gibbs-Duhem equation over the whole composition range. It has the advantage of simple implementation, and a single plot of $\ln(\gamma_1/\gamma_2)$ against x_1 shows the overall quality of a VLE data set. The quality factor for the Herington test F_{test1} can be calculated using of the values D and J obtained during the test.

For isobaric data sets.

$$F_{\text{test1}} = 0.25\,\frac{10}{|D-J|}, 10 \le |D-J| \le 100 \tag{23}$$

3.4.2 Van Ness Test

The Van Ness test is regarded as a modeling capability test. In the approach given here NRTL model is selected, estimating five-parameters, the non-randomness parameters and for isobaric sets temperature dependent interactions are introduced in accordance to:

$$\frac{g_{ji} - g_{ii}}{RT} = A_{ji}^{A} + A_{ji}^{B}/T \tag{24}$$

The five-parameters namely A^{A}_{12}, A^{B}_{12}, A^{A}_{21}, A^{B}_{21}, α_{12} are estimated for the complete *T-p-x-y* data set, and after bubble pressure calculations the following parameters are obtained:

$$\Delta P = \frac{1}{N}\sum_{i=1}^{N}\Delta P_i = \frac{1}{N}\sum_{i=1}^{N} 100\left|\frac{P_i^{\exp} - P_i^{\mathrm{cal}}}{P_i^{\exp}}\right| \tag{25}$$

$$\Delta y = \frac{1}{N}\sum_{i=1}^{N}\Delta y_i = \frac{1}{N}\sum_{i=1}^{N} 100\left|y_i^{\exp} - y_i^{\mathrm{cal}}\right| \tag{26}$$

where *N* is the number of properties values, the superscript *exp* indicates experimental data and the superscript *cal* indicates values calculated with the NRTL equation. If Δp and Δy are less than 1, the data set passes the test. The quality factor for the Van Ness test is calculated as follows:

$$F_{\mathrm{test2}} = 0.25\frac{2}{\Delta P + \Delta y}, 1 \le \Delta P \le 10, 1 \le \Delta y \le 10 \tag{27}$$

3.4.3 Infinite Dilution Test

The infinite dilution test consists in the correlation of the experimental data either to represent $G^{\mathrm{E}}/(x_1 x_2 RT)$ or $\ln(\gamma_2/\gamma_1)$. The model should be the same, and as a matter of consistency the NRTL model is also implemented here. Using the parameters estimated the limits at the infinite dilution are calculated, which theoretically must be the same. The percent deviations in both limits are calculated by:

$$I_1 = 100\left|\frac{G^{\mathrm{E}}/(x_1 x_2 RT) - \ln(\gamma_2/\gamma_1)}{\ln(\gamma_1/\gamma_2)}\right|_{x_{1=0}} \tag{28}$$

$$I_2 = 100 \left| \frac{G^{\mathrm{E}}/(x_1 x_2 RT) - \ln(\gamma_1/\gamma_2)}{\ln(\gamma_1/\gamma_2)} \right|_{x_{2=0}} \tag{29}$$

The quality factors for the infinite dilution test are calculated by use of the relative differences in the estimated activity coefficients at infinite dilution.

$$F_{\mathrm{test3}} = 0.25 \frac{60}{I_1 + I_2}, 30 \leq I_1, I_2 \leq 300 \tag{30}$$

The three consistency tests taken into account measures the quality of a VLE data set on a pass/fail basis. When the test results differ with one another, it creates a problem to arrive at a decision whether to accept or reject a data set. Therefore a more adequate approach to counter the inconsistencies of test results is taken by creating a global quality factor from the individual test results and later normalising it to 1.

$$(F_{\mathrm{test1}} + F_{\mathrm{test2}} + F_{\mathrm{test3}})/.75 = 1 \tag{31}$$

The pure component test was not considered in this work since for most substances studied, the amount of information available in the open literature is not enough for definite answers.

Chapter 4. Experimental VLE Measurements

4.1 Chemicals used

The list of chemicals used in this work is mentioned in **Table 2** along with the name of supplier and their purity. Most of these chemicals are of the highest available purity and therefore they were used without any further purification.

Table 2. Source and purity of compounds used in this study.

Chemical name	Synonym	CAS no.	Source	Purity/mol %
Ethanol	Ethyl alcohol	**64-17-5**	Sigma Aldrich	**≥ 99.8**
Ethyl hexanoate	Ethyl Caproate	**123-66-0**	Sigma Aldrich	**≥ 99**
1-Pentanol	Pentyl alcohol	**71-41-0**	Sigma Aldrich	**≥ 99**
Ethyl Octanoate	Ethyl Caprylate	**106-32-1**	Sigma Aldrich	**≥ 99**
1-Octanol	Octyl alcohol	**111-87-5**	Sigma Aldrich	**≥ 99**
1-Dodecanol	Lauryl alcohol	**112-53-8**	Sigma Aldrich	**≥ 98**
Butanol	Butyl alcohol	**71-36-3**	Fluka	**≥ 99.5**
1-Decanol	n-Decyl alcohol	**112-30-1**	Fluka	**≥ 99.5**
Methy heptadecanoate	Methyl margarate	**1731-92-6**	Fluka	**≥ 99**
Potassium hydroxide	Potassium hydrate	**1710-58-3**	Fluka	**≥ 85**

4.2 Production of BAEE

Within the scope of this thesis it is also interesting to have equilibium data of real multicomponent mixtures. In this way, a NEVO is produced, for which the following experimental scheme was carried out. Balanites aegyptica oil was obtained by extraction, i.e. simultaneous cold pressing and filtration of the seed kernels collected from trees growing in arid and semi-arid regions of Burkina Faso [34]. The presence of FFA's and other impurities especially water limit the use of NEVO in large scale biodiesel production. The widely used methods for industrial biodiesel production employ homogenous catalyst (alkali catalysts) despite their high amount of water consumption and catalyst loss in aqueous effluents during the purification stage. The BA ethyl esters (BAEEs) were synthesized via alkali catalysis

(KOH), under a two-stage procedure based on intermediate addition of glycerol. Alkali catalysis was operated at 35 °C, with an ethanol to oil molar ratio equal to 8:1, a catalyst concentration of 1 wt% based on the initial mass of oil, and a reaction time of 50 min, while the addition of glycerol marking the start of the second step was carried out after 30 min of reaction. The ester content of the BAEEs yielded 97% on weight basis. The resulting ethyl esters are later purified to cleanse off its impurities. There are two purification methods, the wet purification method (classical) and the dry purification. The esters used in this study were purified via the dry purification method. At laboratory scale, adsorptive treatments with Magnesol or rice husk ash (RHA) are efficiently applied to substitute the wet-purification stage of biodiesel. The dry-purification method offers benefits such as using local agricultural solid waste rendering the process more environment friendly, while reducing substantially the total production time, as water-washing requires two treatment cycles and one centrifugation stage [34].

Dry purification method is conducted in batch mode by using 4 wt% of RHA, which was mixed and stirred continuously for 20 min and heated at 65 ºC. A vacum distillation (180-200 °C; 10 mbar) was finally carried out in order to insure a high grade level of the BAEE mixture used afterwards for VLE study. The BAEE final composition is later evaluated via analytical method [34].

Fatty acid composition is an important property for any biodiesel feedstock as it determines the efficiency process to produce biodiesel. The percentage and type of fatty acids composition relies mainly on the plant species and their growth conditions. The fatty acid composition and distribution of some non-edible oils are generally aliphatic compounds with a carboxyl group at the end of a straight-chain. The most common fatty acids are C16 and C18 acids and the same is the case with Balanites Aegyptiaca, therefore its variations in fatty acid chain lengths are not substantial and thus its effects on fuel properties is trivial. However, some feedstocks contain significant amounts of fatty acids other than the typical C16 and C18 acids. A study has shown that the total unsaturated fatty acids in balanites are less than soy and rapeseed oil. The oil quality parameters are known to be quite similar with the soy oil which is the most common oil used for biodiesel production, signifying that balanites can be can be an attractive alternative for sustainable biodiesel production. The results of fatty acid composition in terms of molar fractions% were analysed using the Gas chromatography and they are presented in **Table 3**.

Table 3. **Composition in terms of fatty acids (molar fractions %) for the investigated NEVO: *Balanites aegyptica ethyl esters* (BAEE).**

Fatty acids *(name)*	NEVO BAEE
Ethyl palmitate	**13.29**
Ethyl palmitoleate	**0.12**
Ethyl heptadecanoate	**0.11**
Ethyl Stearate	**10.81**
Ethyl Oleate	**28.97**
Ethyl Cis-Vaccenate	**0.68**
Ethyl Linoleate	**41.44**
Ethyl Linolenate (bis)	**0.22**
Ethyl Arachidate	**0.31**
Ethyl Docasapentaenoate	**0.23**
Unidentified Ester	**0.18**
Unobservable esters[a]	**3.58**
Total	**100.00[b]**

a : Due to dilution of the BAEE with alcohols, the ethyl esters with mole fraction less than 0.10 is not observable which account to 3.58.

b : Experimental uncertainty in composition is found to be 0.01.

4.3 VLE Measurements

The ebulliometric method for VLE measurements was employed in this work. The schematic diagram is shown in **Figure 5** and the experimental setup is provided in **Figure 6**. **Table 4** describes the main components and its features in-line with the figure.

4.3.1 VLE Apparatus

The VLE experiments were performed by using an all-glass dynamic recirculating ebulliometer, model EEA 3000 manufactured by Pignat (France). The ebulliometer's operating conditions for the study of VLE mixtures was from 10 mbar (1 kPa/7.5 mmHg) to 1 bar (100 kPa/750.06 mmHg) in pressure and from 30 °C to 250 °C in temperature. The

minimum and maximum allowable volumes of liquid in the ebulliometer are 75 and 100 mL, respectively. The operating principle of the ebulliometer is based on the dynamic recirculation of vapour and liquid phases to achieve faster thermodynamic equilibrium at a fixed pressure, temperature or composition in static configuration. In addition, the ebulliometer is equipped with a Cottrell pump that ensures optimum contact of phases in equilibrium. Finally, the mixing cell is equipped with a magnetic stirrer which helps in proper mixing of both the vapour and liquid phases condensed before recirculation, thereby avoiding the appearance of concentration and temperature gradients, and contributing to the rapid establishment of thermodynamic equilibrium [35].

The ebulliometer which is depicted in **Figure 5** and **Figure 6** is very well adapted to volatile mixtures. The circulation of the liquid resulting from the condensation of the vapour phase allows reaching the equilibrium quickly. This method is not suitable for low-volatile mixtures because the mass transfer becomes too weak and also for studying mixtures with components of very different volatility (e.g. water-glycerol, glycerol-ethanol).

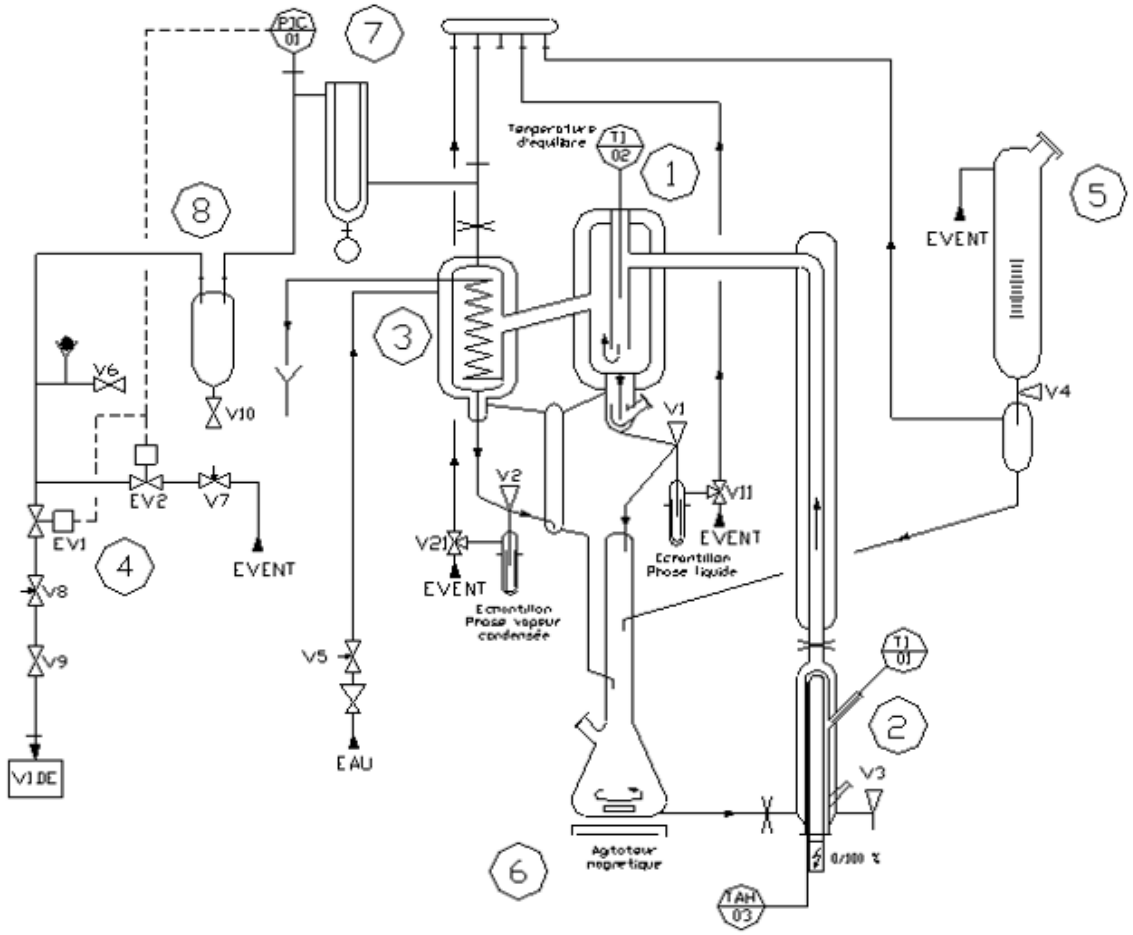

Figure 5. Schematic diagram of the dynamic ebulliometer (Pignat Company, France, ACS model 3000) [35].

Table 4. Description of various components of Pignat Ebulliometer.

Number	Description
1	**A double envelope adiabatic equilibrium chamber, equipped with cottrell pump – also provided is an optional plug sample for the liquid phase**
2	**Electrical resistance (maximum power 500 Watt)**
3	**Glass condenser (coiled in a jacket with cooling by circulating tap water) - also provided is a plug for sampling the condensed vapour**
4	**Vacuum circuit (comprising pump valves, vent valves, control valves)**
5	**Funnel for loading the mixture to be studied (maximum volume 150 mL)**
6	**Magnetic stirrer**
7	**Dry ice trap**
8	**Reserve capacity glass buffer (8 L) for balancing the vacuum (for stabilization of the pressure of the device after sampling)**

Figure 6. A dynamic recirculation ebulliometer (Societe Pignat, France, modele EEA 3000) [35].

4.3.2 VLE Procedure

The liquid mixture to be studied is introduced into the boiler (2) via the funnel (5). A portion of the liquid mixture is evaporated in the boiler by means of an electrical resistance of 500 W. The vapour and liquid phases are rigorously mixed within the Cottrell pump. The adiabaticity of the equilibrium chamber (1) is performed by vacuum with a silver wall having an outlet temperature (TI / 02) from the vapour-liquid outlet of the Cottrell pump. The vapour phase is condensed (3) and sent by gravity into the buffer cell equipped with a magnetic stirrer (6), while the liquid phase is fed directly by gravity in the same buffer cell (6). The two mixed phases are then recycled to the boiler (2). The samples are collected from the two sampling outlets by taking them in a test tubes fitted on the return circuits of condensed vapour and liquid phases, upstream of the buffer cell. The vacuum circuit (4) for performing VLE measurements under reduced pressure is connected at the bottom of the condenser (3). It consists of a solenoid pressure control system (EV1 and EV2). A dry ice trap (7) is also provided at the top of the equipment to protect the pressure sensor (PIC/01) from contact with the fluids being studied. It should be noted that the dry ice trap is also used for the precise measurements under atmospheric pressure. A control box allows the display of the temperature of the balance chamber (TI/02) of the boiler temperature (TI/01), the regulation of the pressure device (PIC/01) and the heating power of the boiler ranges from (0-100%). The control unit also has an automatic cut-off device adjustable on high temperature of the electrical resistance of the boiler (TAH/03).

The experimental VLE measurement with the ebulliometer can be carried out in two ways:

(a) Sequential method
(b) Semi-continuous method

(a) Sequential method: 'N' number of solutions are prepared for the less volatile component with the molar compositions varying between 0 and 1. The VLE is carried out by sequentially introducing each of the prepared solutions (starting from i) into the ebulliometer, then heating and reaching the equilibrium, and later collecting the samples of each vapour and liquid phase. The ebulliometer is drained and then filled with the solution with the following molar composition (i + 1). The process is continued until all the 'N' number of solutions are studied. Temperature variations between two solutions are induced by their compositional variation. This method involves high consumption of products, but its implementation is quite

simple and more importantly the analysis is more precise when compared with the semi-continuous method.

(b) Semi-continuous method: Various solutions of increasing molar compositions constituting the less volatile component are prepared in-situ successively within the ebulliometer so as to sweep the whole composition range [0-1]. Thus, the first solution corresponds to the most volatile component (pure), which is filled in the ebulliometer. After reaching the VLE, the samples of liquid and vapour phases are collected (2x1 mL), changes in the composition of the solution is accomplished by introducing a fixed volume (2 mL) of the less volatile component placed in the dropping funnel. This provides a new i + 1 solution which can be used to study the VLE. Again, the compositional change of the mixture being studied induces a new equilibrium temperature. Measuring the VLE of the less volatile (pure) component must be studied separately, after cleaning of the ebulliometer. This method allows to save on the amount of pure products being utilized, but on the other hand it requires careful monitoring of volumes collected and volumes added.

As part of this work, the semi-continuous method was applied for the VLE studies. The procedure is described in the next section for an intermediate solution between the composition of pure component 1 (the most volatile) and the pure component 2 (least volatile) [35].

4.3.3 Experimental VLE Method

4.3.3.1 Calibration

Temperature Calibration: Calibration is performed, to assure that the temperature of the sensor in the ebulliometer is in agreement with the used temperature thermometer (reference thermometer). Hot water (100 °C) is taken and poured in a flask which can accommodate the two thermometers. The temperature reflected on both the thermocouples is noted down simultaneously and this process is continued for varying temperatures by cooling the water with the help of addition of ice. Calibration is established once the plot of the temperature of the reference versus temperature of the sensor gives the slope and the intercept which will be used in all the work.

Pressure Calibration: The purpose of the pressure calibration is same as that of temperature. The calibration of the equipment also helps to extend considerably the available vapour

pressure data for the studied compounds. Pure component vapour pressures are calculated and compared with the values available in the literature or database given by DIPPR (Design Institute for Physical Properties). The reference component taken in our pressure calibration is ethanol.

The data obtained from the calibration of temperature and pressure sensor, their calibration parameters with their respective diagrams are all shown in **Appendix A**.

4.3.3.2 VLE Determination

The vapour pressures of all the pure compounds used in the binary system which are to be studied are determined using the dynamic ebulliometer. The measurement of vapour pressure serves two guiding purposes. Firstly, it serves to check the calibration of the equipment and, secondly, to verify the attained vapour pressure temperatures for a particular component to that given by DIPPR database.

The experimental work entails two steps. In the first step, Isobaric VLE measurements are carried out using the ebulliometer with a dynamic recirculation of liquid and vapour phases over two different set-point pressures for each binary system. The initial solution introduced involves more volatile component (alcohols), the equilibrium temperature is noted down and samples are collected simultaneously from the liquid and vapour phases for quantification. The less volatile component (esters) are introduced in fractions equivalent to the amount removed from the ebulliometer in the form of vapour and liquid samples. This procedure is continued until the samples in both the liquid and vapour phase finally results in pure ester, signifying the end of the equilibrium diagram. This is apparent when the temperature of the ebulliometer reaches a constant value and the addition of more esters has an insignificant effect on the equilibrium temperature.

The samples collected from the VLE studies are quantified by gas chromatography equipped with flame ionization detector for fine precision to determine the composition of alcohol and esters in both the vapour and liquid phases defined in terms of mole fractions. The phase diagram is thus generated by plotting the VLE measurements on the entire composition range.

4.3.3.3 Compositional Analysis

The samples collected from the ebulliometer are subjected to compositional analysis via Gas Chromatography equipped with flame ionization detector. Flame-Ionization helps in the composition analysis with a wide dynamic response range enhancing accuracy and minimizing sample preparation requirements especially for samples that contain very high or very low compound concentrations.

The model of GC equipment used in this work was GC-FID 7820 Agilent Technology (USA), with an HP-INNOWax column (30 m × 320 μm id × 0.25 μm film of polyethylene glycol. The composition of the investigated mixtures is performed at a set flowrate and pressure of carrier gas. The GC uses hydrogen (Air Liquide, France) as a carrier gas with a flowrate of 1.5 mL/min operating at a pressure of 27.5 kPa. The GC operating conditions are: Column temperature: 60 °C for 2 min (initial), 10 °C/min to 200 °C (rate 1), 5 °C/min to 240 °C (rate 2), hold time 7 min. Injector: split/splitless at 250 °C with a split flow of 100 mL/min; detector parameters: 250 °C, hydrogen flow 40 mL/min, air flow 400 mL/min; make up (nitrogen) 40 mL/min; Injection: automatic liquid sampler/injector system (ALSI) with a volume of 1μL.

While for the BAEEs a single internal standard (IS) was used, an additional IS was introduced for mixtures [Alcohol(s) + FAEE(s)] in order to capture matrix effects (solution non-ideality) involved by component interactions (hydrogen bonds between alcohol and ester groups, steric effects between long chain and short-chain molecules). The GC-FID calibration was adapted accordingly. Selection of the internal standard(s) and response factor value(s) obtained for each studied system are given in **Appendix B**.

Chapter 5. Results & Discussion

As the ebulliometer in question is a dynamic equipment, some traces of compounds used in the prior measurement, or during the cleaning process, may still exist in minute traces. In order to compensate for the accurate measurement of vapour pressure of pure components or the VLE data of binary systems, the runs were performed multiple times and averages were considered.

5.1 Pure Component Vapour Pressures

Vapour pressure data is needed for a variety of chemical engineering and thermodynamic calculations. The data collected represents a physicochemical property of fuels and they are highly essential for the biodiesel production as it reflects the volatility, stability, and security of the fuel, besides being important in the development of separation processes.

Pure component vapour pressures of three alcohols namely, 1-pentanol, 1-octanol, 1-dodecanol and two saturated fatty acid ethyl esters (FAEEs) that are ethyl hexanoate and ethyl octanoate were measured using a dynamic ebulliometer with a pressure ranging from 7.1 kPa to 97.1 kPa, and temperature ranging from 303K to 473K. It must be mentioned that for some of the substances the number of data available in the open literature is very low, like for ethyl octanoate for each only 29 data-points are registered in the Dortmund databank.

The experimental T and P^{sat} values of the different components are reported in **Table 5**. The data were fitted using the Antoine equation given below. The coefficients of Antoine's equation are normally given in mmHg, although SI units(Pa) is widely preferred.

$$\log_{10} P^{sat}/\text{mmHg} = A + \frac{B}{C + T/^{\circ}\text{C}} \tag{32}$$

where *A*, *B*, and *C* are the Antoine equation constants estimating from least-squares fitting, as in **Table 5**. The minimized objective function (*S*) is:

$$S = \sum_{i=1}^{n} \left(\frac{P_{\text{exp}} - P_{\text{cal}}}{P_{\text{exp}}} \right)^2 \tag{33}$$

The experimental uncertainty in composition is different for each binary system. For each individual point the uncertainties are mentioned **%Δ*P*/Pa**, whereas the average uncertainty marked

with (*) for each binary system is specified at the footnotes of each table. The experimental uncertainty on the vapour pressure is estimated to be 0.11 Pa, whereas the uncertainty in system temperature is estimated to be 0.02 K. The calculated pressure values (P_{cal}) were obtained from the correlated Antoine equation regressed from the experimental data.

Table 5. Experimental pure component vapour pressures of different components obtained in this study.

Ethyl hexanoate			Ethyl octanoate			1-pentanol		
T (K)	P_{exp} (Pa)	% $\Delta P/P$	T (K)	P_{exp} (Pa)	% $\Delta P/P$	T (K)	P_{exp} (Pa)	% $\Delta P/P$
359.49	**6597.01**	**0.08**	**406.46**	**10473.80**	**-0.07**	**354.82**	**10473.80**	**0.41**
361.29	**7131.68**	**0.14**	**413.97**	**13810.74**	**-0.11**	**360.63**	**13810.74**	**-0.21**
370.59	**10473.37**	**0.08**	**419.97**	**17147.67**	**0.31**	**365.23**	**17147.67**	**-0.08**
377.70	**13815.07**	**-0.11**	**425.28**	**20484.61**	**-0.05**	**369.24**	**20484.61**	**-0.39**
379.90	**15004.71**	**-0.23**	**429.88**	**23845.02**	**-0.12**	**372.64**	**23845.02**	**-0.14**
383.50	**17156.76**	**-0.28**	**433.88**	**27195.65**	**0.10**	**375.74**	**27195.65**	**-0.29**
396.40	**27181.84**	**-0.10**	**437.59**	**30546.29**	**-0.01**	**378.44**	**30546.29**	**0.00**
399.80	**30523.54**	**0.00**	**440.89**	**33896.92**	**0.18**	**380.94**	**33896.92**	**0.13**
402.91	**33865.23**	**0.08**	**444.09**	**37247.55**	**-0.12**	**383.25**	**37247.55**	**0.25**
405.81	**37206.93**	**0.04**	**446.89**	**40598.18**	**0.12**	**385.45**	**40598.18**	**0.12**
408.51	**40548.62**	**-0.01**	**449.6**	**43889.40**	**-0.06**	**387.45**	**43890.35**	**0.08**
411.00	**43890.32**	**0.05**	**452.1**	**47209.67**	**-0.02**	**389.35**	**47210.55**	**0.04**
415.61	**50586.90**	**-0.01**	**454.5**	**50529.94**	**-0.09**	**391.15**	**50530.75**	**-0.03**
417.71	**53932.93**	**0.02**	**456.8**	**53850.21**	**-0.22**	**392.85**	**53850.95**	**-0.06**
419.71	**57278.96**	**0.04**	**458.9**	**57170.48**	**-0.09**	**394.45**	**57171.14**	**-0.03**
421.61	**60624.99**	**0.08**	**460.91**	**60490.75**	**0.00**	**395.96**	**60491.34**	**0.09**
423.41	**63971.02**	**0.17**	**462.81**	**63811.01**	**0.16**	**397.46**	**63811.54**	**-0.03**
426.81	**70663.08**	**0.28**	**464.81**	**67131.28**	**-0.17**	**398.76**	**67131.73**	**0.36**
430.02	**77355.14**	**0.20**	**466.51**	**70451.55**	**0.11**	**400.16**	**70451.93**	**0.18**
431.52	**80701.16**	**0.23**	**468.31**	**73771.82**	**-0.06**	**401.46**	**73772.13**	**0.19**
433.02	**84047.19**	**0.12**	**469.91**	**77092.09**	**0.15**	**402.66**	**77092.32**	**0.38**
434.42	**87393.22**	**0.15**	**471.61**	**80412.36**	**-0.06**	**404.06**	**80412.52**	**-0.28**
435.82	**90739.25**	**0.07**	**473.11**	**83732.63**	**0.11**	**405.16**	**83732.72**	**-0.03**
437.22	**93689.39**	**-0.54**			**0.11***	**406.36**	**87052.92**	**-0.24**
438.52	**97011.96**	**-0.56**				**407.46**	**90373.11**	**-0.24**
		0.15*				**408.47**	**93693.31**	**0.00**
						409.57	**97013.51**	**-0.20**
								0.17*

Table 5. (continued)

1-Octanol			1-Dodecanol		
T (K)	P_{exp} (Pa)	% $\Delta P/P$	T (K)	P_{exp} (Pa)	% $\Delta P/P$
393.05	**7128.08**	**0.20**	**448.30**	**7128.08**	**0.22**
401.76	**10464.31**	**-0.08**	**450.60**	**7795.33**	**0.12**
408.37	**13800.55**	**-0.12**	**452.80**	**8462.57**	**-0.14**
413.77	**17147.67**	**-0.10**	**454.80**	**9129.82**	**-0.11**
418.37	**20484.61**	**-0.16**	**456.70**	**9797.07**	**-0.10**
422.38	**23845.02**	**-0.03**	**458.60**	**10464.31**	**-0.44**
425.98	**27195.65**	**-0.08**	**460.21**	**11131.56**	**0.00**
429.18	**30546.29**	**0.08**	**461.81**	**11798.81**	**0.16**
432.18	**33896.92**	**-0.03**	**463.41**	**12466.05**	**0.09**
434.89	**37247.55**	**0.10**	**464.91**	**13133.30**	**0.15**
437.49	**40598.18**	**-0.08**	**466.41**	**13800.55**	**0.01**
439.79	**43889.40**	**0.06**			**0.14***
441.99	**47209.67**	**0.14**			
444.09	**50529.94**	**0.16**			
446.09	**53850.21**	**0.13**			
448.00	**57170.48**	**0.12**			
449.90	**60490.75**	**-0.15**			
451.60	**63811.01**	**-0.04**			
453.20	**67131.28**	**0.16**			
454.80	**70451.55**	**0.16**			
456.40	**73771.82**	**-0.02**			
457.90	**77092.09**	**-0.05**			
459.30	**80412.36**	**0.06**			
460.71	**83732.63**	**0.03**			
462.11	**87052.89**	**-0.11**			
463.51	**90373.16**	**-0.37**			
464.61	**93693.43**	**0.12**			
465.91	**97013.70**	**-0.06**			
		0.11*			

[a] *% ΔP/P = 100*(P_{exp}-P_{cal})/P_{exp}*

A graphical method was used for checking the consistency, and also for screening the vapour pressures of pure compounds. The diagrams representing the vapour pressure (P_S) vs.

temperature (T) clearly show the linear dependency of $\ln(P_S)$ vs. $1/T$, as can be seen in **Appendix C**. Nevertheless, for vapour pressures ranging in a large temperature range, it is difficult to show precisely the differences that may occur between experimental data sets from various literature sources. Therefore, we proposed to use the method similar to Wilsak and Thodos's [36], which gives the deviation from linearity of $\ln(P_S)$ vs. $1/T$ as described in the following section.

Graphically, it is possible to represent the deviations δ between the experimental value of $\ln(P_r)$ and the value obtained by linear interpolation, selecting a reduced coordinate system, i.e. $P_r = P_S/P_{max}$ and $T_r = T/T_{max}$, for the whole data set by taking into account the extreme temperatures T_m □ and T_{max}. The deviations δ are calculated by:

$$\delta = \ln(P_r) - A\,(1/T_r - 1) \tag{34}$$

with $A = \ln(P_{min}/P_{max})\,/(T_{max}/T_{min} - 1)$ which equals zero for the data points selected as reference, i.e. (P_{min}, T_{min}) and (P_{max}, T_{max}).

Hence, without using an intermediary equation for regression, it is possible to observe graphically, the relative deviation between two vapour pressure data points measured at the same temperature via this method. By introducing the data points $(P_{S,1}, T_0)$ and $(P_{S,2}, T_0)$ in eq. (34) for considering δ_1 and δ_2, the equation becomes:

$$\delta_1 - \delta_2 = \ln(P_{S,1}/P_{S,2}) \tag{35}$$

$$P_{S,1}/P_{S,2} = \exp(\delta_1 - \delta_2) \tag{36}$$

The difference $(\delta_1 - \delta_2)$ being usually very small, eq. (36) can be rewritten as:

$$P_{S,1}/P_{S,2} = 1 + (\delta_1 - \delta_2) \tag{37}$$

Or

$$\delta_1 - \delta_2 = (P_{S,1} - P_{S,2})/P_{S,2} \quad (38)$$

Vapor pressures of ethyl hexanoate, ethyl octanoate, 1-pentanol, 1-octanol and 1-dodecanol measured by various authors were plotted according to this method (Figures 7, 9, 11, 13 and 15 respectively). The traditional graphs giving the relative deviations between the values obtained by Antoine equation with parameters fitted on the experimental values generated in this work and the measured data found in the literature were also plotted (Figures 8, 10, 12, 14 and 16 for ethyl hexanoate, ethyl octanoate, 1-pentanol, 1-octanol and 1-dodecanol, respectively).

Regarding ethyl hexanoate, the disagreement observed between the measurements from this work and measurements from Benziane et al. [26] and Matsuda et al. [14] are likely due to *(i)* the different basis methods of the equipments used (dynamic method in this work, static method for the other two sources) and *(ii)* the difference in purity of the sample used (>99 mol% in this work; 98 mol% for Benziane et al. [26], although the provider Sigma Aldrich is the same; 99 wt% for Matsuda et al. [14] with a different provider, Kanto Chemical Co). These arguments are also valid to explain the disagreement between the measurements from this work and measurements from the literature observed for the other compounds investigated (ethyl octanoate, 1-pentanol, 1-octanol, and 1-dodecanol). Furthermore, it should be worthy to mention that the data by Plyasunov et al. [37] derives from a correlation with parameters fitted by the authors on available experimental information (similarly to DIPPR data [38]).

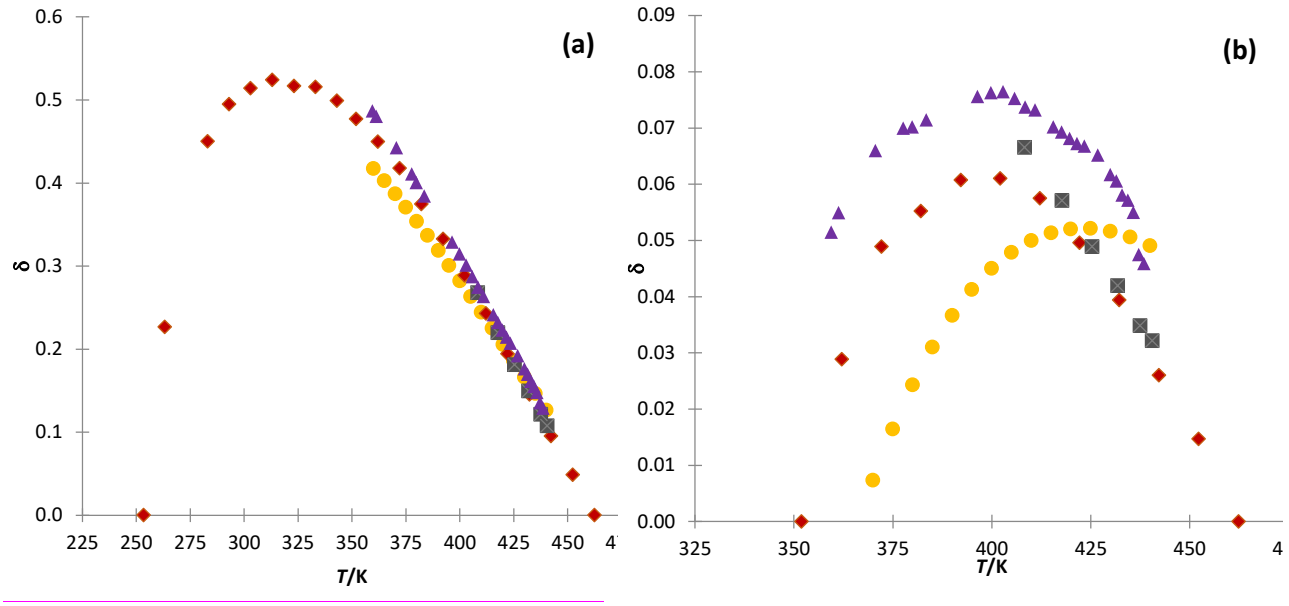

Figure 7. Graphical method to check the agreement between experimental vapor pressures from various literature sources. (a) over the entire temperature range of the experimental data; (b) over the temperature range common to the experimental data - Case study of ethyl hexanoate: ▲, this work; ● Plyasunov et al. [37]; ◆, Benziane et al. [26]; ■, Matsuda et al. [14].

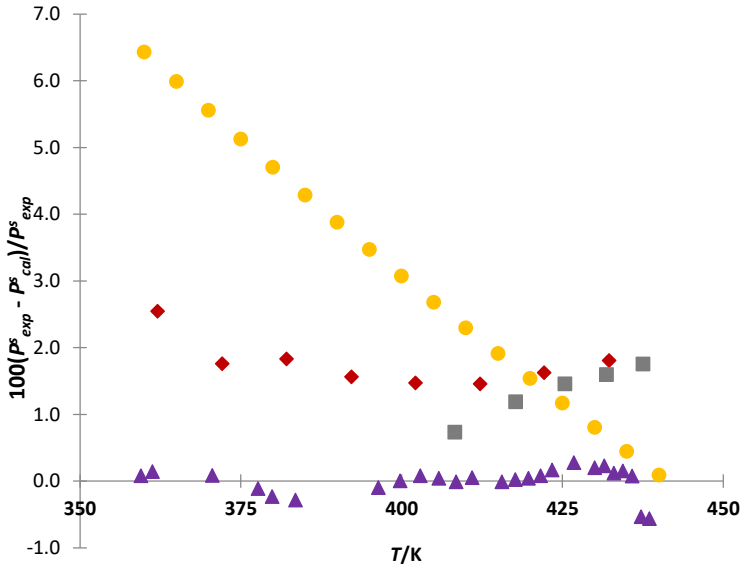

Figure 8. Percent relative deviations between experimental vapor pressures of ethyl hexanoate from various literature sources and values obtained from Antoine equation with parameters fitted on measurements made in this work. P^s_{cal} is Antoine equation value at the temperature of the corresponding experimental data P^s_{exp}. This work (Antoine equation) vs. ▲, this work (measurements); vs. ●, Plyasunov et al. [37]; vs. ◆, Benziane et al. [26]; vs. ■, Matsuda et al. [14].

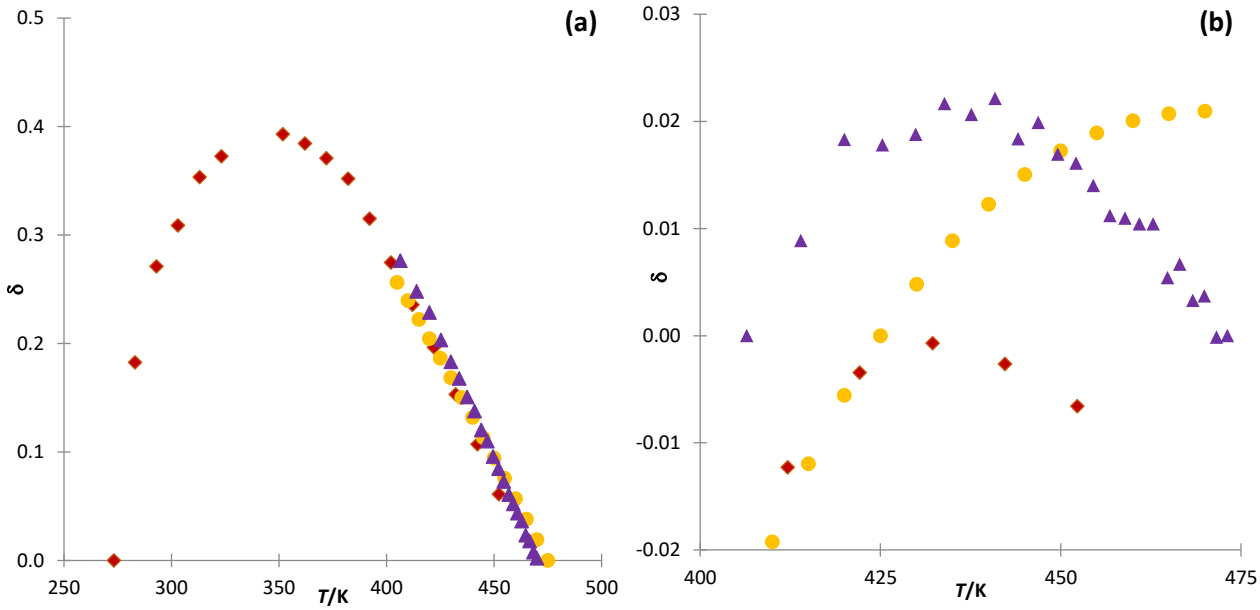

Figure 9. Graphical method to check the agreement between experimental vapor pressures from various literature sources. (a) over the entire temperature range of the experimental data; (b) over the temperature range common to the experimental data - Case study of ethyl octanoate: ▲, this work; ● Plyasunov et al. [37]; ◆, Benziane et al. [26].

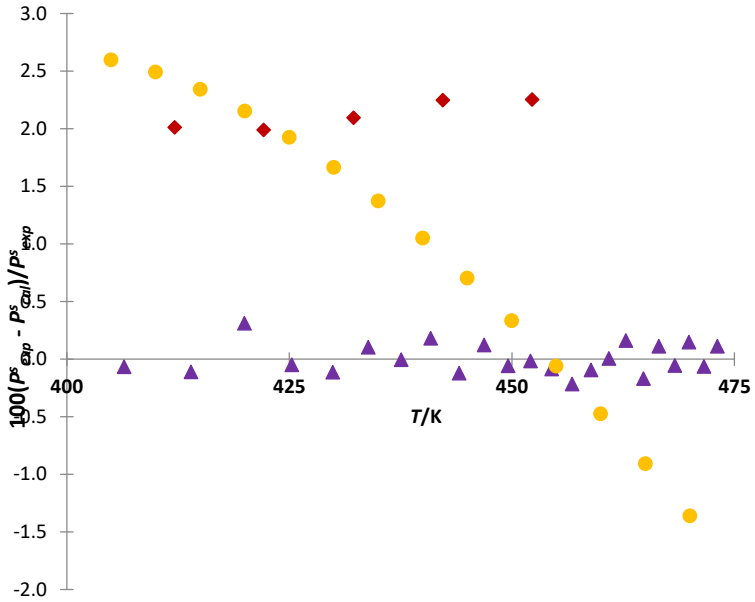

Figure 10. Percent relative deviations between experimental vapor pressures of ethyl octanoate from various literature sources and values obtained from Antoine equation with parameters fitted on measurements made in this work. P^s_{cal} is Antoine equation value at the temperature of the corresponding experimental data P^s_{exp}. This work (Antoine equation) vs. ▲, this work (measurements); vs. ●, Plyasunov et al. [37]; vs. ◆, Benziane et al. [26].

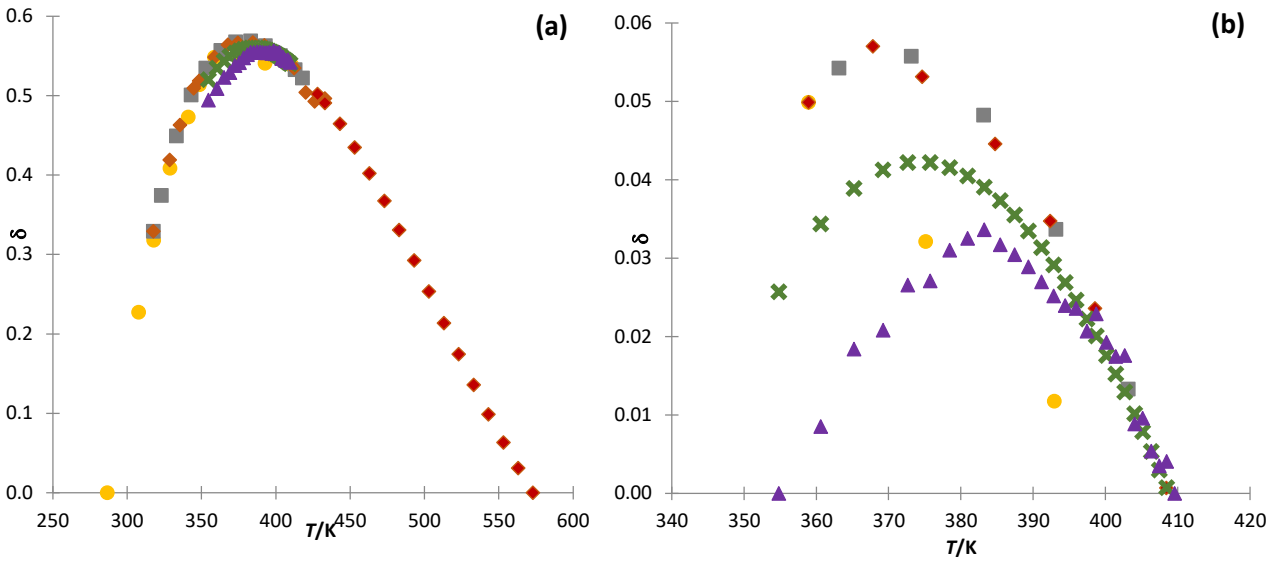

Figure 11. Graphical method to check the agreement between experimental vapor pressures from various literature sources. (a) over the entire temperature range of the experimental data; (b) over the temperature range common to the experimental data - Case study of 1-pentanol: ▲, this work; ✖, DIPPR [38]; ◆, TRC [39]; ■, Wilhoit et al. [40]; ● Stull et al. [41].

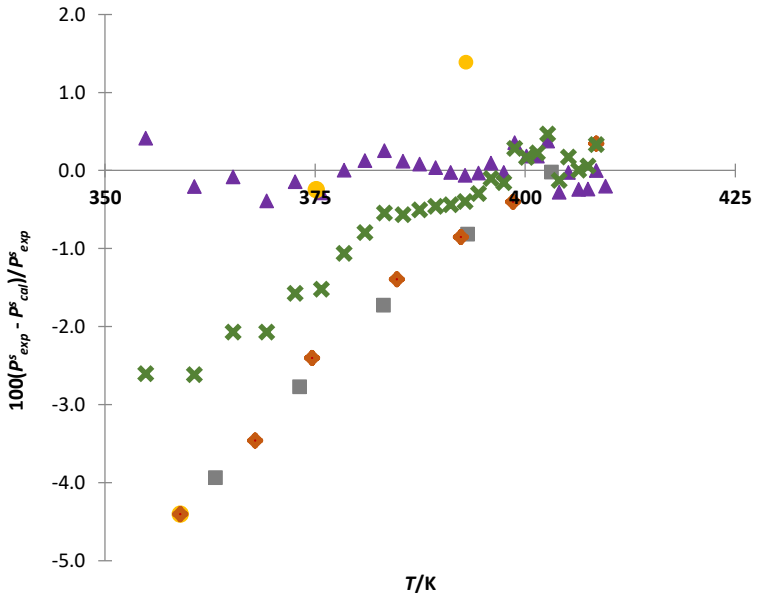

Figure 12. Percent relative deviations between experimental vapor pressures of 1-pentanol from various literature sources and values obtained from Antoine equation with parameters fitted on measurements made in this work. P^s_{cal} is Antoine equation value at the temperature of the corresponding experimental data P^s_{exp}. This work (Antoine equation) vs. ▲, this work (measurements); vs. ✖, DIPPR [38]; vs. ◆, TRC [39]; vs. ■, Wilhoit et al. [40]; vs. ●, Stull et al. [41].

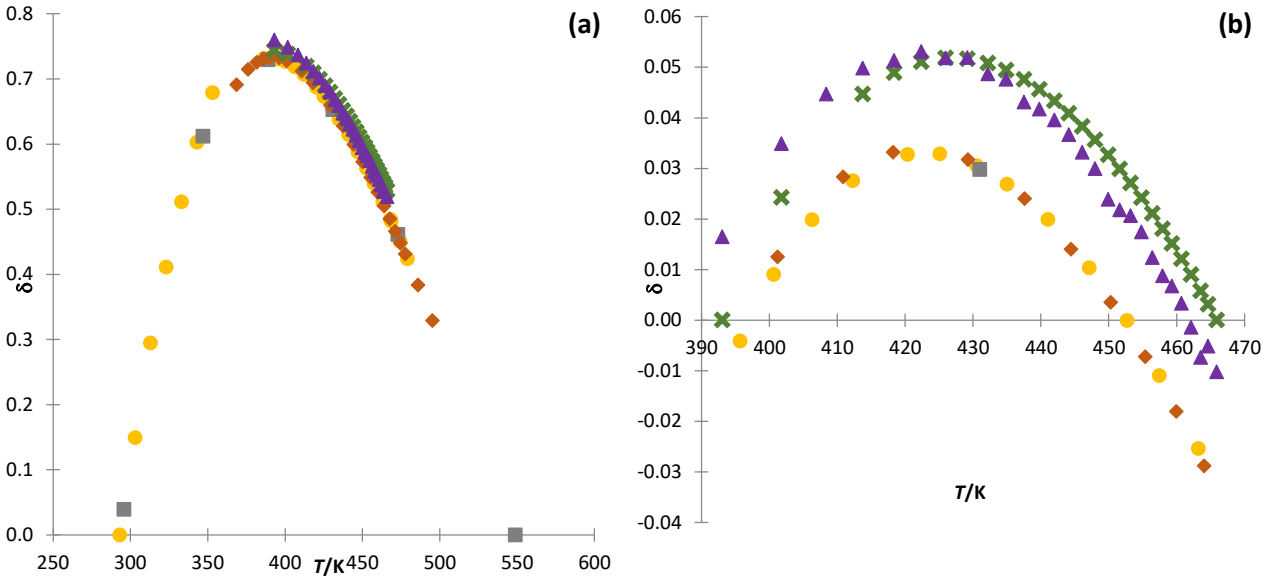

Figure 13. Graphical method to check the agreement between experimental vapor pressures from various literature sources. (a) over the entire temperature range of the experimental data; (b) over the temperature range common to the experimental data - Case study of 1-octanol: ▲, this work; ✖, DIPPR [38]; ◆, TRC [39]; ■, Smith et al. [42]; ● Boublik et al. [43].

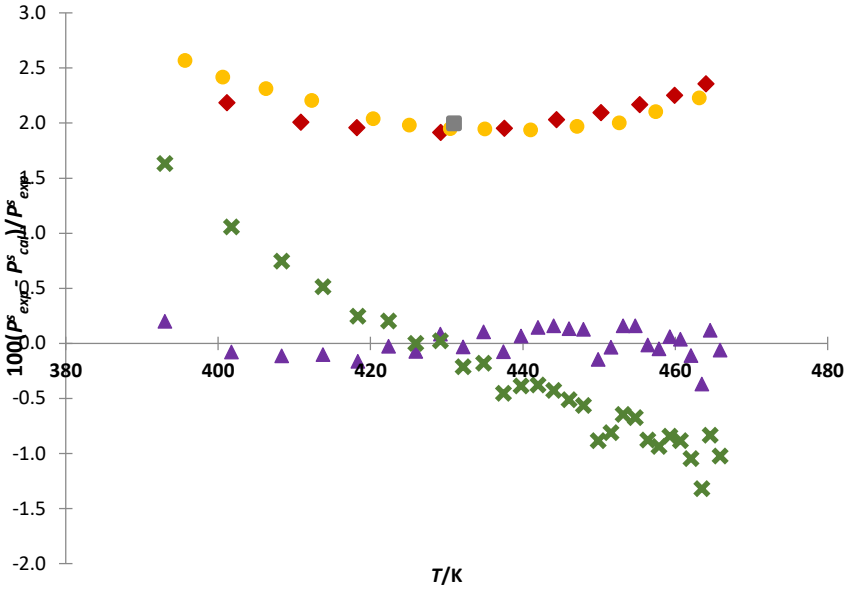

Figure 14. Percent relative deviations between experimental vapor pressures of 1-octanol from various literature sources and values obtained from Antoine equation with parameters fitted on measurements made in this work. P^s_{cal} is Antoine equation value at the temperature of the corresponding experimental data P^s_{exp}. This work (Antoine equation) vs. ▲, this work (measurements); vs. ✖, DIPPR [38]; vs. ◆, TRC [39]; vs. ■, Smith et al. [42]; vs. ● Boublik et al. [43].

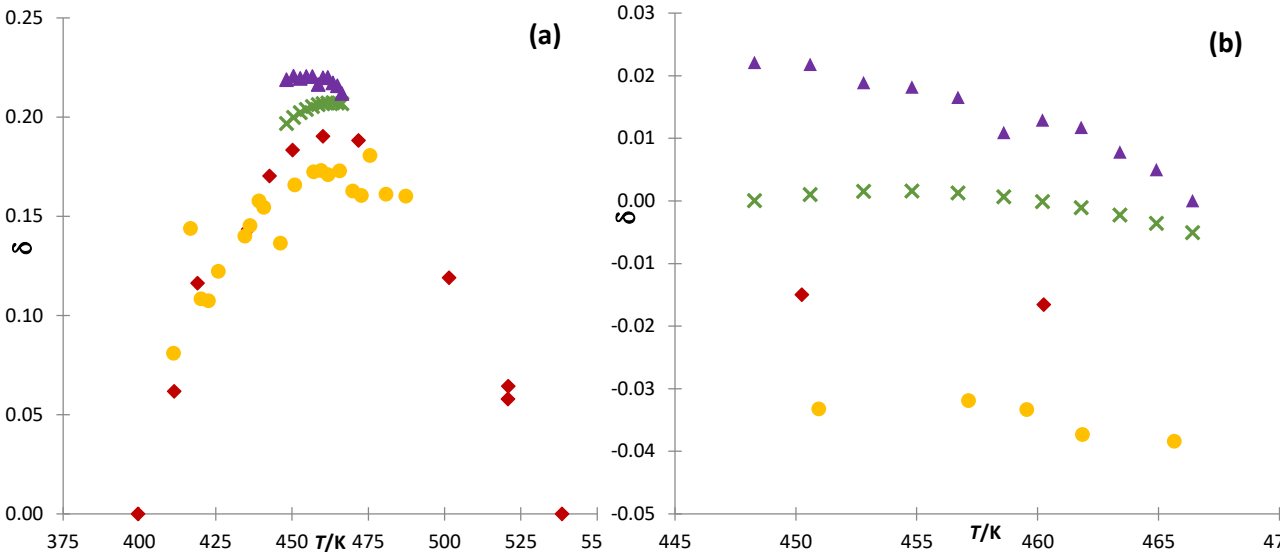

Figure 15. Graphical method to check the agreement between experimental vapor pressures from various literature sources. (a) over the entire temperature range of the experimental data; (b) over the temperature range common to the experimental data - Case study of 1-dodecanol: ▲, this work; ✖, DIPPR [38]; ◆, Kemme and Kreps [44]; ● Rose et al. [45].

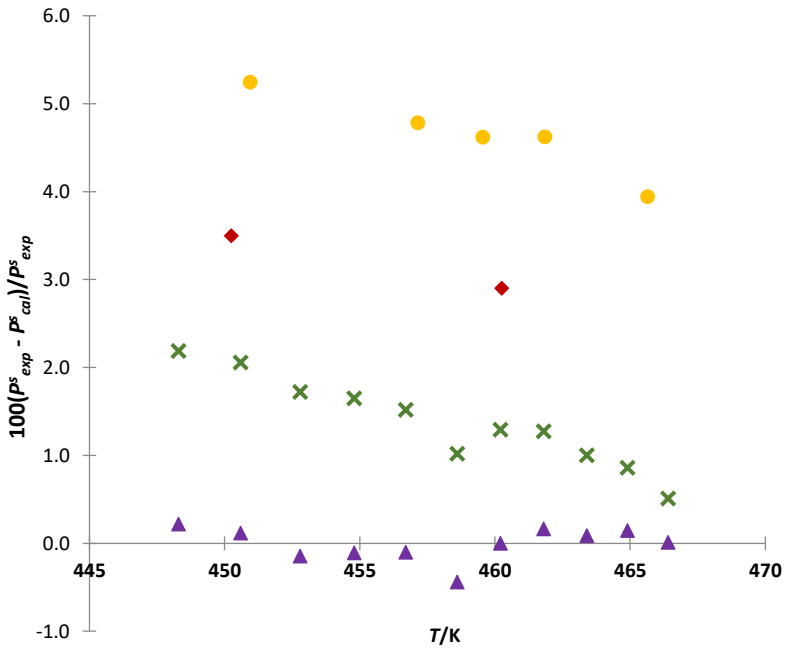

Figure 16. Percent relative deviations between experimental vapor pressures of 1-dodecanol from various literature sources and values obtained from Antoine equation with parameters fitted on measurements made in this work. P^s_{cal} is Antoine equation value at the temperature of the corresponding experimental data P^s_{exp}. This work (Antoine equation) vs. ▲, this work (measurements); vs. ✖, DIPPR [38]; vs. ◆, Kemme and Kreps [44]; vs. ●, Rose et al. [45].

The regressed Antoine parameters (**eq. 32**) *A, B,* and *C* and average deviations are given in **Table 6**.

Table 6. Antoine equation parameters and percent relative deviation [a,b].

Compound	A	B	C	Temperature range/K	$\delta_r(P)\%$
Ethyl hexanoate	**21.5791**	**-3783.95**	**-63.5348**	**359.49 - 438.52**	**0.15**
Ethyl octanoate	**21.1369**	**-3736.88**	**-91.8964**	**406.46 - 473.11**	**0.11**
1-Pentanol	**21.4903**	**-3002.93**	**-109.443**	**354.82 - 409.57**	**0.17**
1-Octanol	**20.8292**	**-3115.91**	**-132.512**	**393.05 - 465.91**	**0.11**
1-Dodecanol	**17.2005**	**-1746.06**	**-238.707**	**448.30 - 466.41**	**0.14**

[a] *Antoine equation written as: ln(P/Pa) = A + B/(C + T/K).*

[b] $\delta_r(P)\% = 100/N_P \cdot \sum_{k=1}^{N_P} \left|P^s_{exp,k}(T) - P^s_{cal,k}(T)\right| / P^s_{exp,k}(T)$ *where* N_P *is the number of vapor pressures measured in this work for the considered compound of which* $P^s_{exp,k}(T)$ *is the* k^{th} *value at temperature T and* $P^s_{cal,k}(T)$ *the corresponding value calculated via the given Antoine equation parameters.*

By inspecting all the above **Figures 7-16**, we can clearly notice that the data acquired for the pure component vapour pressures is very much in agreement with the available literature including the prediction from DIPPR for the three alcohols conforms to the experimental data. In addition, the percent relative deviations regressed to the relative Antoine equation as depicted in **Table 6** shows low errors for all the components.

5.2 VLE for Binary System

Three different binary systems were selected for the generation of VLE data, namely (a) ethanol + ethyl hexanoate (b) 1-pentanol + ethyl hexanoate (c) 1-pentanol + ethyl octanoate and for ach binary system two pressures were selected. The VLE study for the first binary system ethanol + ethyl hexanoate was precisely conducted at the same initial pressures as that available in the work done by Matsuda *et.al* in order to compare the obtained values for its quality. The two substances present very different boiling points, which turns VLE measurements pretty demanding. On the contrary, 1-pentanol and ethyl hexanoate have very close boiling points, and the VLE behavior for this system was studied at 14.65 and 40 kPa. The VLE data for the system 1-pentanol + ethyl octanoate was studied at 15 and 40 kPa in order to comply with the limitations

imposed by Ebulliometer in line with the normal boiling points. All mixtures studied do not present azeotropic behavior.

5.2.1 Experimental Data

Ethanol and ethyl hexanoate present a very different normal boiling point, which turns VLE binary measurements pretty hard to attain. VLE studies for this binary system were carried out at two different pressures i.e. 40 and 53.33 kPa. The data is compiled in **Table 7.**

Table 7. Experimental boiling points, liquid-phase mole fraction (x_1), vapour-phase mole fraction (y_1) and temperature (T), for ethanol (1) + ethyl hexanoate (2)

40 kPa			53.33 kPa		
T (K)	x_1	y_1	T (K)	x_1	y_1
329.58	**1.0000**	**1.0000**	**335.98**	**1.0000**	**1.0000**
331.08	**0.9091**	**0.9892**	**337.68**	**0.9014**	**0.9889**
332.48	**0.8115**	**0.9819**	**338.88**	**0.8217**	**0.9823**
334.18	**0.6874**	**0.9743**	**340.58**	**0.7144**	**0.9755**
336.58	**0.5223**	**0.9663**	**343.08**	**0.5653**	**0.9669**
338.98	**0.4317**	**0.9588**	**346.48**	**0.4283**	**0.9553**
341.68	**0.3439**	**0.9486**	**350.19**	**0.3130**	**0.9408**
348.29	**0.2284**	**0.9210**	**356.49**	**0.2421**	**0.9164**
357.49	**0.1423**	**0.8722**	**362.79**	**0.1624**	**0.8816**
373.29	**0.0710**	**0.7334**	**369.39**	**0.1179**	**0.8408**
384.60	**0.0402**	**0.5740**	**388.70**	**0.0586**	**0.6535**
400.10	**0.0166**	**0.2011**	**402.81**	**0.0323**	**0.3806**
408.02	**0.0000**	**0.0000**	**417.31**	**0.0000**	**0.0000**

The uncertainty in mole fraction composition for the binary system, ethanol + ethyl hexanoate was estimated to be 0.004.

At both the experimental pressures, the mixture ethanol/ethylhexanoate does not behave azeotropically and this is indicated in the Figures 17 and 18. By visual analysis, the two phase region was also not found like shown by Matsuda *et.al* [14]. It must be noted that the vapour phase representing the dew point curve was not measured by Matsuda *et.al*, thus this data will add much needed information for both the phases. Further comparison between the experimental

pressures and those obtained by Matsuda *et.al* are given in the modelling section 5.2.2, where the experimental values are close to the predicted values than the data obtained by Matsuda *et.al*.

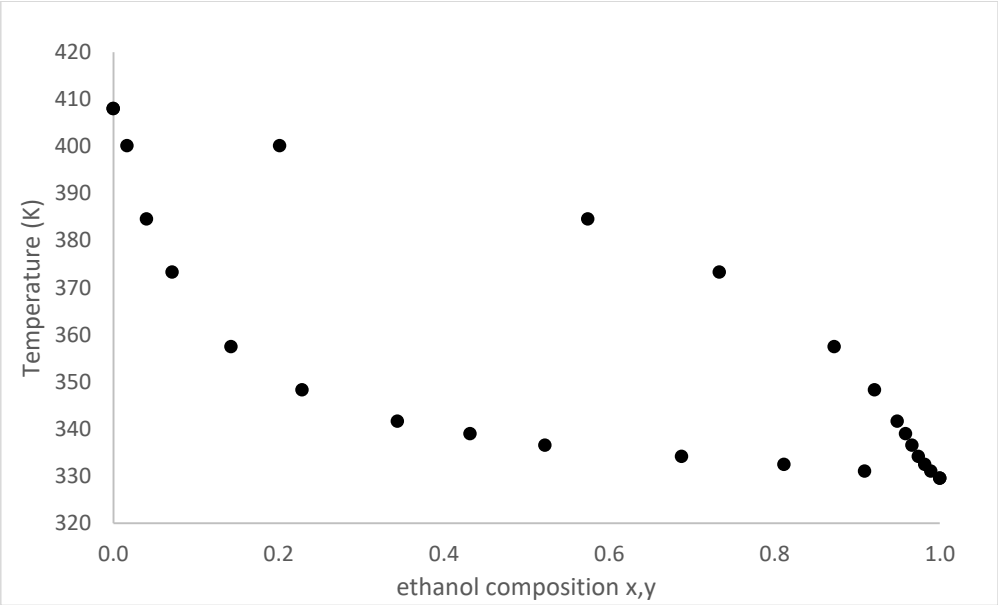

Figure 17. Temperature composition VLE phase diagram for ethanol-ethyl hexanoate at 40 kPa.

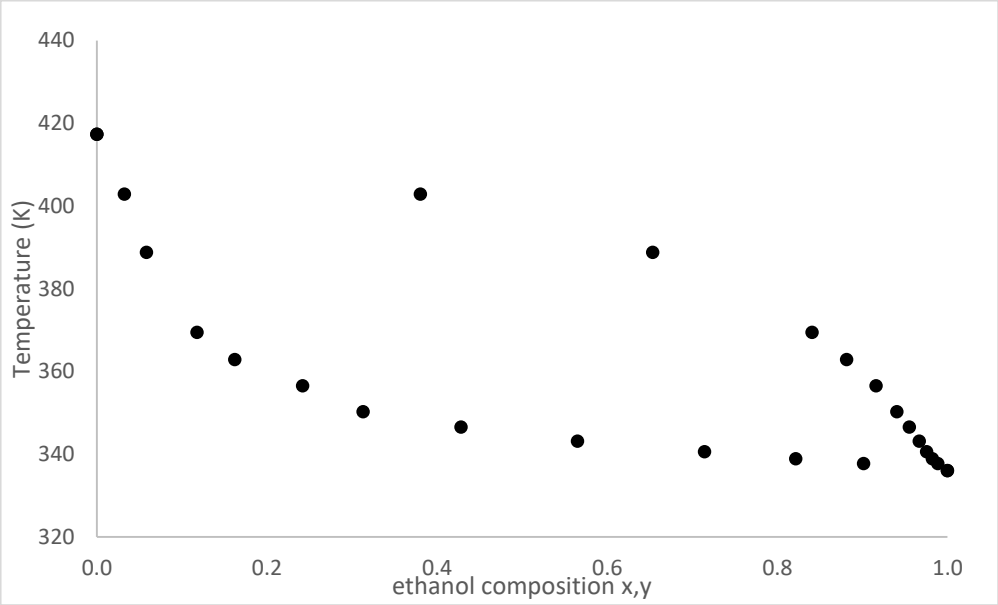

Figure 18. Temperature composition VLE phase diagram for ethanol-ethyl hexanoate at 53.33 kPa.

The binary system of 1-pentanol and ethyl hexanoate has a very narrow normal boiling points and the VLE data for this system was studied at two different pressures i.e. 14.65 and 40 kPa. The data is presented in **Table 8.** The uncertainty in mole fraction composition for the binary system, 1-pentanol + ethyl hexanoate was estimated to be 0.002.

Table 8. Experimental boiling points, liquid-phase mole fraction (x_1), vapour-phase mole fraction (y_1) and temperature (T), for 1-pentanol (1) + ethyl hexanoate (2)

14.65 kPa			40 kPa		
(K)	x_1	y_1	(K)	x_1	y_1
361.830	**1.000**	**1.000**	**385.147**	**1.000**	**1.000**
362.230	**0.883**	**0.906**	**386.048**	**0.862**	**0.912**
362.830	**0.802**	**0.850**	**386.949**	**0.784**	**0.855**
363.531	**0.683**	**0.779**	**388.050**	**0.684**	**0.795**
364.432	**0.587**	**0.724**	**389.551**	**0.578**	**0.731**
365.432	**0.492**	**0.667**	**390.652**	**0.499**	**0.685**
366.533	**0.412**	**0.612**	**393.354**	**0.392**	**0.589**
368.234	**0.312**	**0.533**	**395.555**	**0.304**	**0.504**
371.137	**0.196**	**0.400**	**397.857**	**0.239**	**0.416**
374.639	**0.103**	**0.243**	**401.060**	**0.146**	**0.297**
379.143	**0.000**	**0.000**	**403.261**	**0.094**	**0.207**
			404.362	**0.071**	**0.158**
			408.065	**0.000**	**0.000**

The temperature composition relationship or the VLE phase diagram for the binary system 1-pentanol + ethyl hexanoate is given in **Figure 19** conducted at vapour pressure of 14.65 kPa, whereas the **Figure 20** shows the experiment conducted at vapour pressure of 40 kPa. From both the figures we can conclude that the obtained data is found to be consistent as the curves are linear.

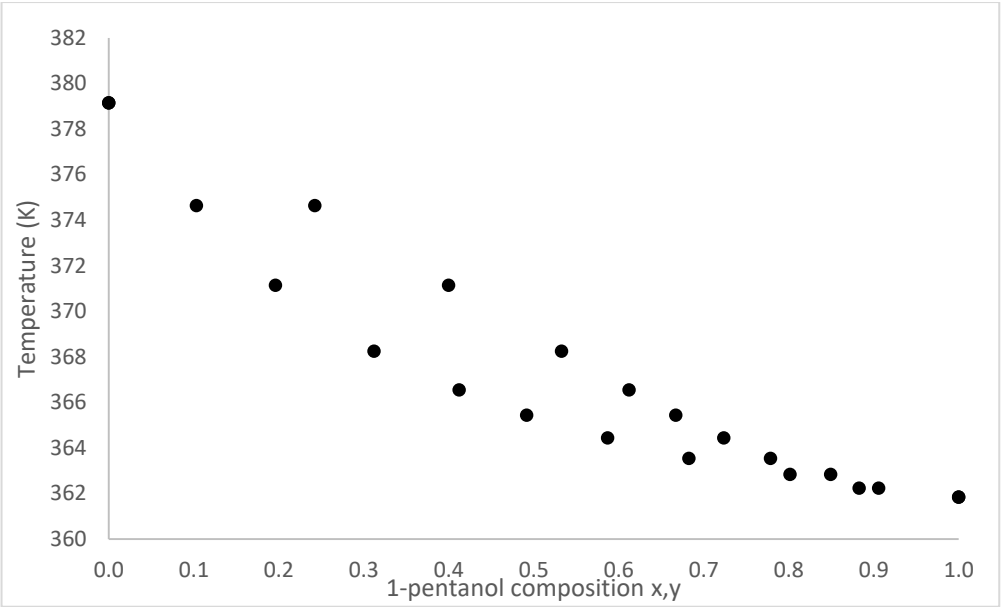

Figure 19. Temperature composition VLE phase diagram for 1-pentanol-ethyl hexanoate at 14.65 kPa.

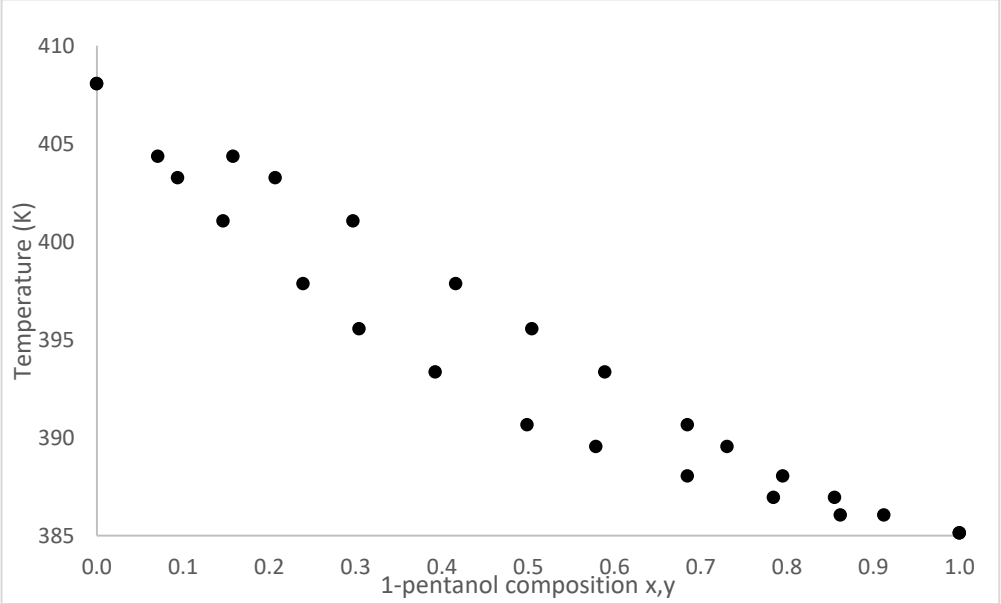

Figure 20. Temperature composition VLE phase diagram for 1-pentanol-ethyl hexanoate at 40 kPa

The binary system of 1-pentanol and ethyl octanoate was studied and the VLE data for this system was measured at two different pressures i.e. 15 and 40 kPa. The uncertainty in mole fraction composition for the binary system, 1-pentanol + ethyl octanoate was estimated to be 0.002. The data is represented in **Table 9.**

Table 9. Experimental boiling points, liquid-phase mole fraction (x_1), vapour-phase mole fraction (y_1) and temperature (T), for 1-pentanol (1) + ethyl octanoate (2)

15 kPa			40 kPa		
(K)	x_1	y_1	(K)	x_1	y_1
362.330	**1.000**	**1.000**	**385.047**	**1.000**	**1.000**
364.131	**0.893**	**0.982**	**386.849**	**0.863**	**0.979**
365.632	**0.820**	**0.968**	**389.751**	**0.784**	**0.961**
367.634	**0.713**	**0.950**	**392.153**	**0.686**	**0.944**
369.736	**0.612**	**0.933**	**394.455**	**0.600**	**0.926**
373.138	**0.483**	**0.903**	**397.057**	**0.495**	**0.900**
376.841	**0.374**	**0.870**	**401.160**	**0.412**	**0.870**
380.444	**0.295**	**0.830**	**407.565**	**0.297**	**0.814**
384.947	**0.223**	**0.778**	**415.281**	**0.204**	**0.723**
397.257	**0.106**	**0.574**	**426.679**	**0.112**	**0.555**
405.963	**0.051**	**0.359**	**438.689**	**0.040**	**0.250**
416.271	**0.000**	**0.000**	**446.394**	**0.000**	**0.000**

The temperature composition relationship or the VLE phase diagram for the binary system 1-pentanol + ethyl octanoate is given in **Figure 21** conducted at vapour pressure of 15 kPa, whereas the **Figure 22** shows the experiment conducted at vapour pressure of 40 kPa. From both the figures we can conclude that the obtained data is found to be consistent as the curves are linear.

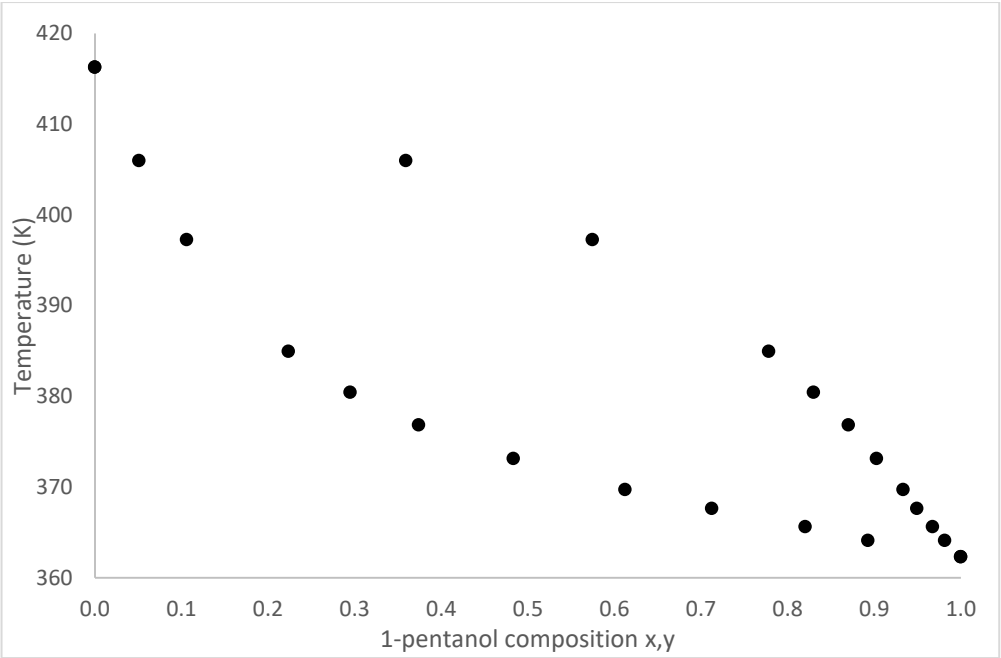

Figure 21. Temperature composition VLE phase diagram for pentanol-ethyl octanoate at 15 kPa

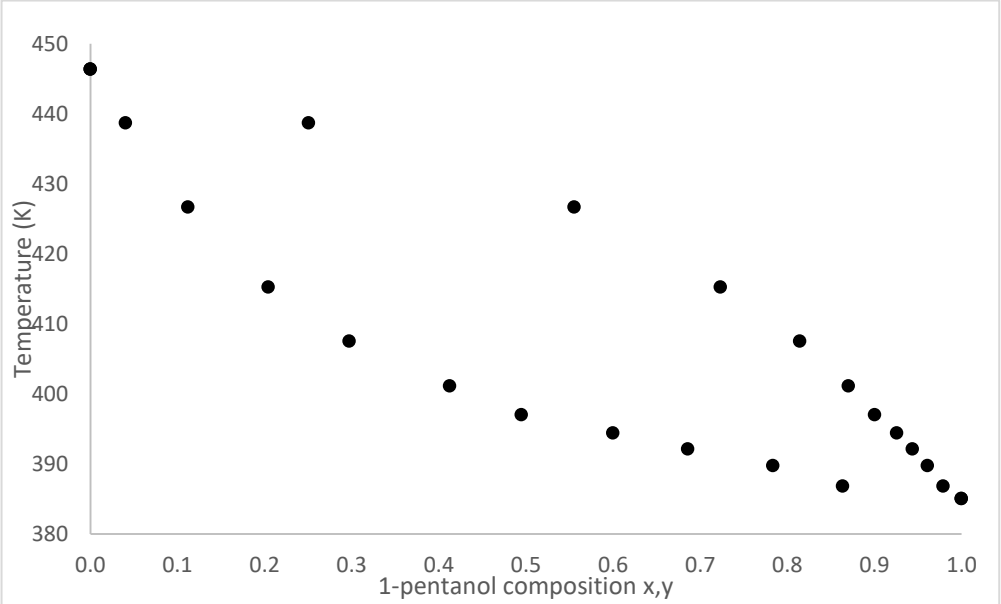

Figure 22. Temperature composition VLE phase diagram for pentanol-ethyl octanoate at 40 kPa

5.2.2 Thermodynamic Modelling

The performance of NRTL model [46] with 5 parameters (given previously in **eqs. 6-7**), together with Lyngby Modified UNIFAC [47] and Dortmund Modified UNIFAC ([48], [49], [50], [51], [52]) models, are gathered in Tables 10, 11 and 12 for the whole of the binary systems investigated, and shown separately in Figures 23, 24 and 25 for the systems: [ethanol + ethyl hexanoate], [1-pentanol + ethyl hexanoate], and [1-pentanol + ethyl octanoate], respectively. From Table 10, 11 and 12 and Figures 23-25, a better agreement between experimental data acquired in this work and correlation via NRTL (5 parameters) is most often observed when parameter estimation is carried out by using PTx information (and thus eq. (39) as objective function) than by using PTxy information (and thus eq. (40) as objective function). The plots of parameter estimation generated for all the binary systems based on PTxy information is shown in **Appendix D**. Furthermore, Dortmund Modified UNIFAC model performs quite accurately VLE predictions (almost with the same degree of accuracy as NRTL model with parameters fitted on PTx information). Note that, although NRTL parameters were fitted for each binary system by considering the whole experimental data generated at the two selected pressures, model performance is evaluated in terms of average deviations in temperature and vapor phase composition (of the alcohol) for each isobaric VLE data set.

$$F_{ob} = \sum_{k=1}^{N_P} \left(1 - \frac{P_k^{cal}}{P_k^{exp}}\right)^2 \tag{39}$$

$$F_{ob} = \sum_{k=1}^{N_P} \left(\sum_{i=1}^{2} \left(1 - \frac{y_{ik}^{cal}}{y_{ik}^{exp}}\right)^2 + \left(1 - \frac{P_k^{cal}}{P_k^{exp}}\right)^2 \right) \tag{40}$$

NRTL (5 parameters) for a binary system [1 + 2].

$$\tau_{12} = a_{12} + \frac{b_{12}}{T}, \tau_{21} = a_{21} + \frac{b_{21}}{T} \text{ with } T \text{ in K} \tag{41}$$

Table 10. Comparative performance of several selected thermodynamic models (correlative approach: NRTL 5 parameters; predictive approach: Lyngby and Dortmund Modified UNIFAC) [a,b] - binary system: [ethanol (1) + ethyl hexanoate (2)].

Model	$\delta_r(P)\%$	Δy_{av}	From VLE calculations at given P and x			
			$\Delta T_{av}(isoP)/K$		$\Delta y_{av}(isoP)$	
			40 kPa	53.33 kPa	40 kPa	53.33 kPa
NRTL 5 parameters fitted on the *PTxy* exp. data from this work (a_{12} = 9.74057; b_{12} / K = -2937.76; a_{21} = -5.96358; b_{21} /K = 2122.24; $\alpha_{12} = \alpha_{21}$ = 0.5) [c]	**0.92**	**0.0009**	**0.92**	**1.30**	**0.010**	**0.010**
NRTL 5 parameters fitted on the *PTx* exp. data from this work (a_{12} =-9.60829; b_{12} /K = 3603.15; a_{21} = 4.74859; b_{21} /K = -1493.84; $\alpha_{12} = \alpha_{21}$ = 0.5) [d]	**0.38**	–	**0.37**	**0.45**	**0.007**	**0.006**
Lyngby Modified UNIFAC	–	–	**2.20**	**2.50**	**0.020**	**0.020**
Dortmund Modified UNIFAC	–	–	**0.39**	**0.94**	**0.010**	**0.010**

$\delta_r(P)\% = 100 \cdot \sum_{k=1}^{N_P} \left|1 - \frac{P_k^{cal}}{P_k^{exp}}\right| / N_P$ *with* N_P *the number of data points for the two sets of isobaric measurements;*

$\Delta y_{av} = \sum_{k=1}^{N_P} |y_{ik}^{exp} - y_{ik}^{cal}| / N_P$ *where i stands for ethanol;*

[b] $\Delta T_{av}(isoP)/K = \sum_{k=1}^{N_{isoP}} |T_k^{exp} - T_k^{cal}| / N_{isoP}$ *with* N_{isoP} *the number of data points for each set of isobaric measurements;* $\Delta y_{av}(isoP) = \sum_{k=1}^{N_{isoP}} |y_{ik}^{exp} - y_{ik}^{cal}| / N_{isoP}$ *(where i stands for ethanol);*

[c] $F_{ob} = \sum_{k=1}^{N_P} \left(\sum_{i=1}^{2} \left(1 - \frac{y_{ik}^{cal}}{y_{ik}^{exp}}\right)^2 + \left(1 - \frac{P_k^{cal}}{P_k^{exp}}\right)^2 \right)$;

[d] $F_{ob} = \sum_{k=1}^{N_P} \left(1 - \frac{P_k^{cal}}{P_k^{exp}}\right)^2$

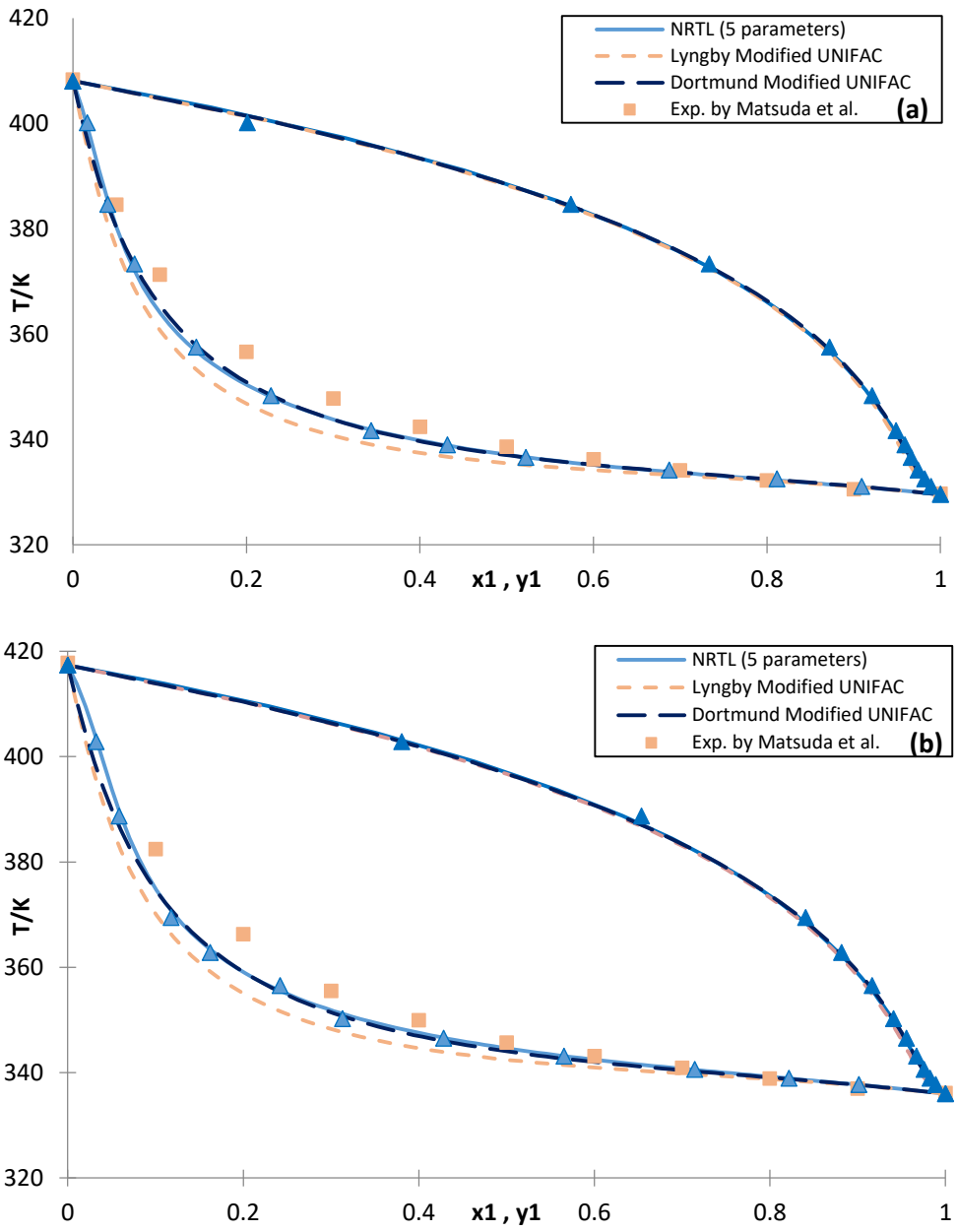

Figure 23. PTxy diagram for [ethanol (1) + ethyl hexanoate (2)] at (a) 40 kPa and (b) 53.33 kPa (NRTL parameters were fitted on PTx data measured in this work at 40 and 53.33 kPa: a_{12} = -9.60829; b_{12} /K = 3603.15; a_{21} = 4.74859; b_{21} /K = -1493.84; α_{12} = α_{21} = 0.5)

The above figures clearly show a better agreement between the experimental data together with the NRTL and Dortmund modified UNIFAC model, whereas the Lyngby modified UNIFAC shows a slight deviation and the deviation is quite apparent when compared with values obtained by Matsuda *et.al*.

Table 11. Comparative performance of several selected thermodynamic models (correlative approach: NRTL 5 parameters; predictive approach: Lyngby and Dortmund Modified UNIFAC) [a] - Binary system: [1-pentanol (1) + ethyl hexanoate (2)].

Model	$\delta_r(P)\%$	Δy_{av}	From VLE calculations at given P and x			
			$\Delta T_{av}(isoP)/K$		$\Delta y_{av}(isoP)$	
			14.65 kPa	40 kPa	14.65 kPa	40 kPa
NRTL 5 parameters fitted on the *PTxy* exp. data from this work (a_{12} = -5.09210; b_{12} /K = 2030.19; a_{21} = 1.10083; b_{21} /K = -345.249; $\alpha_{12} = \alpha_{21} = 0.5$)	**1.2**	**0.002**	**0.25**	**0.38**	**0.004**	**0.01**
NRTL 5 parameters fitted on the *PTx* exp. data from this work (a_{12} = 4.08558; b_{12} = -1289.77; a_{21} = -4.20085; b_{21} = 1539.95; $\alpha_{12} = \alpha_{21} = 0.5$)	**0.23**	**-**	**0.09**	**0.10**	**0.005**	**0.02**
Lyngby Modified UNIFAC	**-**	**-**	**0.59**	**0.58**	**0.008**	**0.02**
Dortmund Modified UNIFAC	**-**	**-**	**0.40**	**0.65**	**0.006**	**0.02**

[a] *All footnotes are the same as in Table 10.*

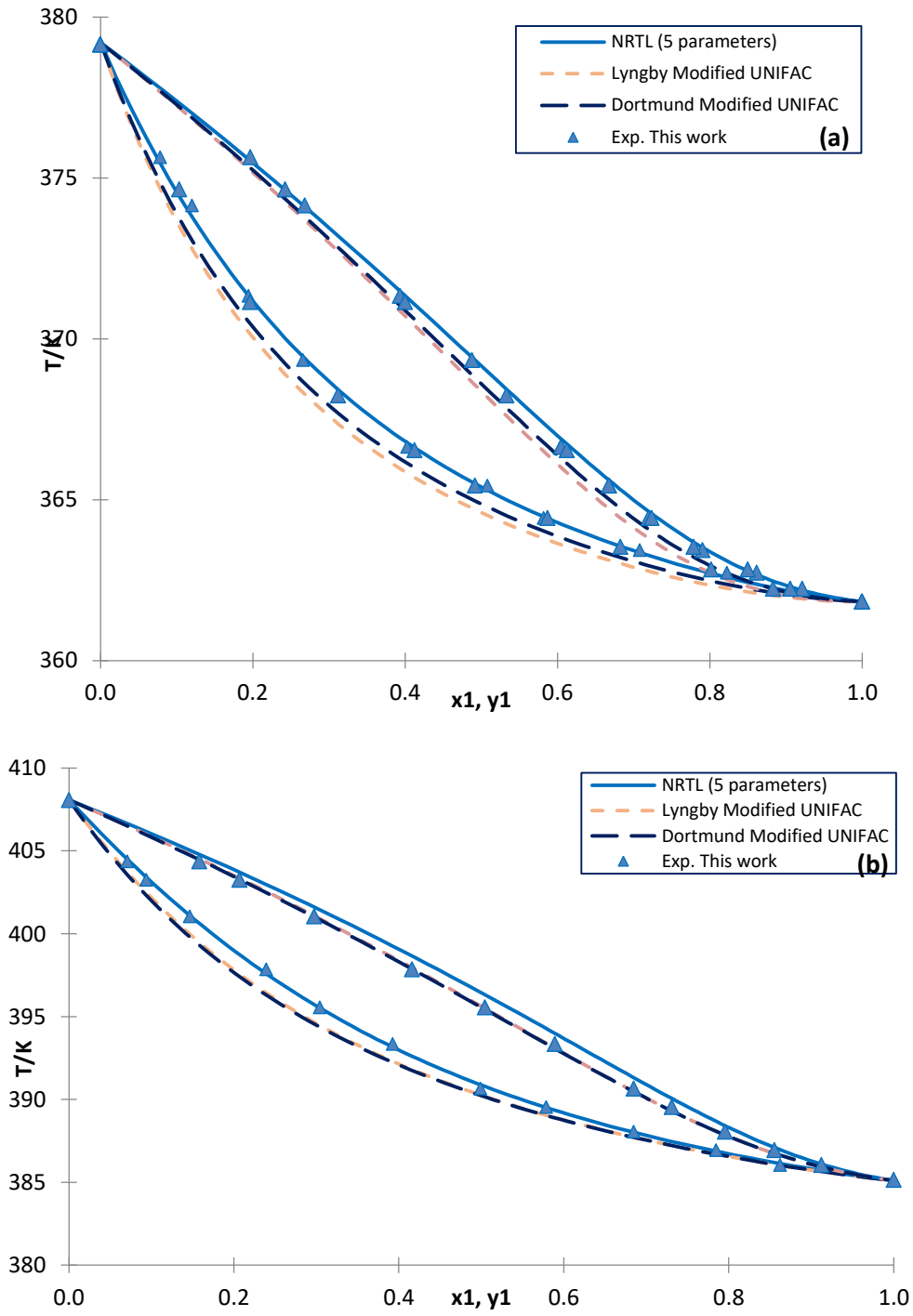

Figure 24. PTxy diagram for [1-pentanol (1) + ethyl hexanoate (2)] at (a) 14.65 kPa and (b) 40 kPa (NRTL parameters were fitted on PTx data measured in this work at 14.65 and 40 kPa: a_{12} = 4.08558; b_{12} /K = -1289.78; a_{21} = -4.20085; b_{21} /K = 1539.95; α_{12} = α_{21} = 0.5).

The above figures show a better agreement between the experimental data and the NRTL model with a slight deviation from the Dortmund model and Lyngby modified UNIFAC.

Table 12. Comparative performance of several selected thermodynamic models (correlative approach: NRTL 5 parameters; predictive approach: Lyngby and Dortmund Modified UNIFAC) [a,b] - Binary system: [1-pentanol (1) + ethyl octanoate (2)].

Model	$\delta_r(P)\%$	Δy_{av}	From VLE calculations at given P and x			
			$\Delta T_{av}(isoP)/K$		$\Delta y_{av}(isoP)$	
			15 kPa	40 kPa	15 kPa	40 kPa
NRTL 5 parameters fitted on the *PTxy* exp. data from this work (a_{12} = 3.42889; b_{12} = -1035.93270; a_{21} = -3.25291; b_{21} = 1191.12747; $\alpha_{12} = \alpha_{21}$ = 0.5) [c]	**1.20**	**0.001**	**0.14**	**0.35**	**0.004**	**0.005**
NRTL 5 parameters fitted on the *PTx* exp. data from this work (a_{12} = 5.295755; b_{12} = -1792.0045; a_{21} = -4.418990; b_{21} = 1656.7028; $\alpha_{12} = \alpha_{21}$ = 0.5) [d]	**0.23**	**-**	**0.21**	**0.30**	**0.003**	**0.006**
Modified UNIFAC (Lyngby, Larsen *et al.*)	**-**	**-**	**1.20**	**0.74**	**0.008**	**0.004**
Modified UNIFAC (Dortmund, Gmehling *et al.*)	**-**	**-**	**0.71**	**0.66**	**0.005**	**0.004**

[a] *All footnotes are the same as in Table 10.*

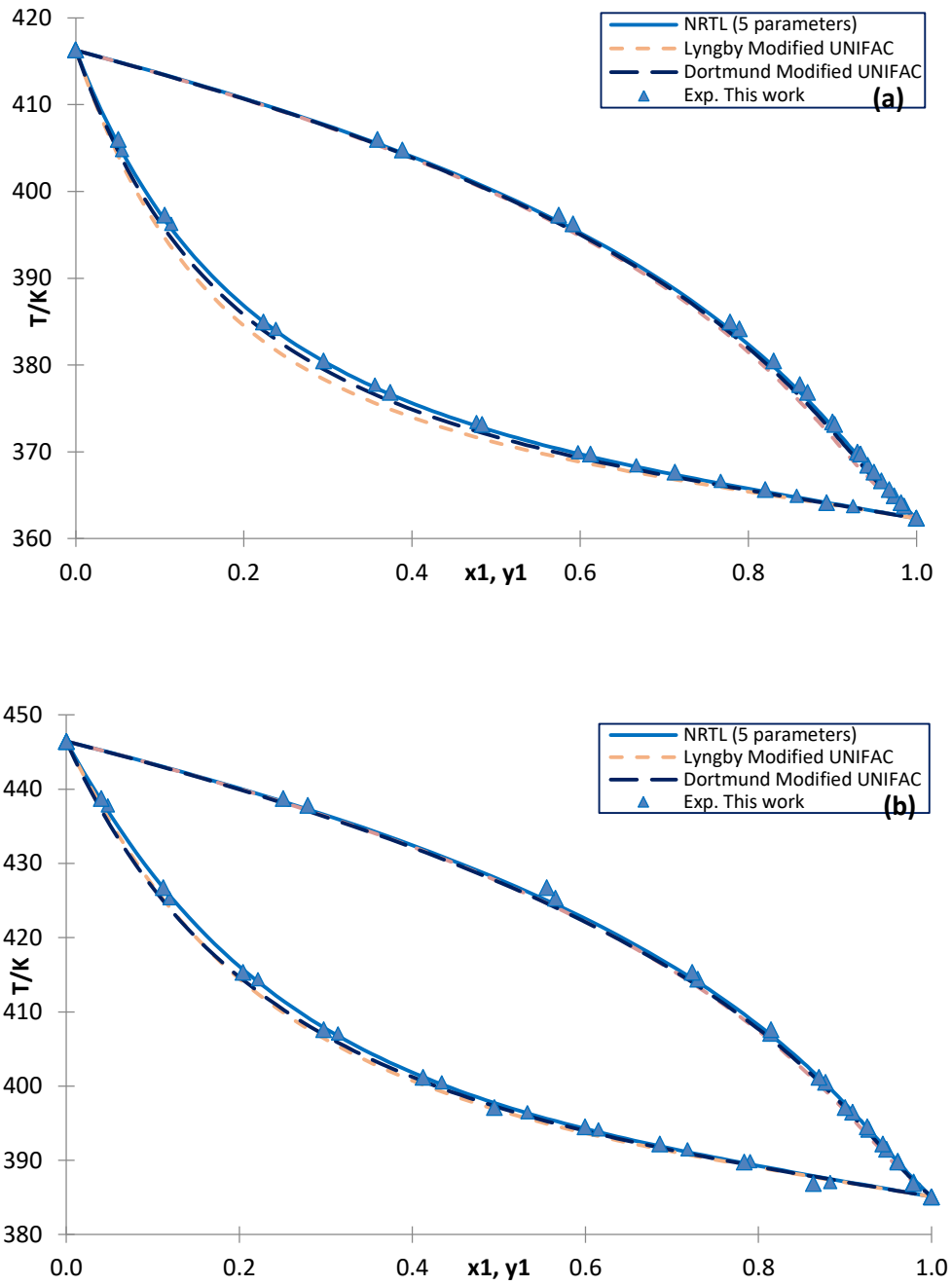

Figure 25. PTxy diagram for [1-pentanol (1) + ethyl octanoate (2)] at (a) 15 kPa and (b) 40 kPa (NRTL parameters were fitted on PTx data measured in this work at 15 and 40 kPa: a_{12} = 5.295755; b_{12} /K = -1792.0045; a_{21} = -4.418990; b_{21} /K = 1656.7028; $\alpha_{12} = \alpha_{21}$ = 0.5).

The above figures clearly indicate the agreement between the experimental data and those predicted by NRTL, Dortmund modified UNIFAC and Lyngby modified UNIFAC models.

5.2.3 Thermodynamic Consistency

The quality of the experimental data was analyzed by applying a quality assessment algorithm for vapor-liquid equilibrium data proposed by Kang *et al.* as mentioned in Chapter 3.

The quality factors are shown in **Table 13**, attaining the maximum value for the 1-pentanol + ethyl hexanoate binary mixture at 14.65 kPa. For the remaining systems, the overall quality factors are between 0.44 and 0.84, which are very satisfactory, as Cunico et al. [53] reports that for systems with fatty esters, fatty acids, among other components relevant in the biofuel industry, only 3% of the data sets presents an overall quality factor higher than 0.5.

Table 13 shows the consistency test results for the three binary system namely (ethanol + ethyl hexanoate), (1-pentanol + ethyl hexanoate), (1-pentanol + ethyl octanoate). Three different tests were performed to check the consistency. Van Ness test gave more precise results for all the binary systems, where the infinite dilution test show much more difficulties. Overall, the test results are found to be positive.

Table 13. Consistency test results for all the binary systems

Pressure	Herington Test	Van Ness Test	Infinite Dilution Test	Overall Test Results
Ethanol-Ethyl hexanoate				
P (40 kPa)	**0.25**	**0.23**	**0.15**	**0.84**
P (53.33 kPa)	**0.21**	**0.17**	**0.10**	**0.63**
1-Pentanol-Ethyl hexanoate				
P (14.65 kPa)	**0.25**	**0.25**	**0.25**	**1.00**
P (40 kPa)	**0.04**	**0.25**	**0.04**	**0.44**
1-Pentanol-Ethyl octanoate				
P (15 kPa)	**0.12**	**0.25**	**0.05**	**0.56**
P (40 kPa)	**0.14**	**0.25**	**0.05**	**0.58**

5.3 Multicomponent VLE

The multicomponent VLE data was extracted for the BAEE by using the alcohol in 1-octanol and 1-dodecanol.

5.3.1 Experimental Data and Prediction

The multicomponent system comprised of BAEE as less volatile component and a mixture of 1-octanol and 1-dodecanol as more volatile component. The multicomponent VLE was conducted at pressures of 8 kPa, 10 kPa and 12 kPa. In total 12 runs were performed at these pressures within a temperature range 446 K – 472 K. The mixture of alcohols was selected in such a proportion in order to effectively reach the equilibrium for BAEE. The limitations imposed by the ebulliometer to attain equilibrium at certain conditions culminated in the selection of pressure and temperature. For each run three samples were collected, one for the liquid composition (x), one for vapour composition (y) and one for the global composition, feed (z) making a total of 36 quantification sets for the determination of esters in GC.

The mass of individual components/esters in the VLE sample from each set is determined with the help of response factor already evaluated during the calibration of the sample. The calibration for attaining the response factor is mentioned in **Appendix B**. Using the Dortmund modified UNIFAC model, by taking into account the average molecular weight of the esters present in BAEE, under identical conditions of temperature and pressure, the mass of each ester is predicted with this model. The obtained results from the prediction are then compared with the experimental results previously obtained from the GC.

The Multicomponent prediction and experimental results are illustrated in **Appendix E**. The prediction results from Dortmund modified UNIFAC model are shown in **Table E.1**, whereas the experimental results from the VLE multicomponent mixture are illustrated in **Table E.2.**

The determination of absolute deviations was calculated by taking into account the following expressions:

- $\Delta xi = xexp(i) - xcal(i)$ with xcal (i) predicted by Dortmund Modified UNIFAC model
- $\Delta yi = yexp(i) - ycal(i)$ with ycal (i) predicted by Dortmund Modified UNIFAC model
- Average Absolute Deviation = $\sum|\Delta xi|/Nc$ ($\sum|\Delta yi|/Nc$) on all liquid (vapor) phase components of the considered data set (the number of components Nc in all considered mixtures is 8 here).
- Average Abs. Dev. (for all x) = $\sum (\sum|\Delta xi|/Nc)/Np$ on all liquid phase components (Nc) of the whole data sets (Np)
- Average Abs. Dev. (for all y) = $\sum (\sum|\Delta yi|/Nc)/Np$ on all vapor phase components (Nc) of the whole data sets (Np).
- Average Abs. Dev. (for all x and y) = $((\sum (\sum|\Delta xi|/Nc)/Np) + (\sum (\sum|\Delta yi|/Nc)/Np))/2$ on all components (Nc) of the two phases for the whole data sets (Np).

The values obtained were:

- Average Abs. Dev. (for all x) = 0.004
- Average Abs. Dev. (for all y) = 0.012
- Average Abs. Dev. (for all x and y) = 0.008

The average deviations for all the components of the multicomponent mixture from all the batches are illustrated in **Table 14.**

Table 14. Average deviations for all the components for all sets

Component	Ave. Dev. (x) for all sets	Ave. Dev. (y) for all sets
1-Octanol	**0.0071**	**0.0492**
1-Dodecanol	**0.0093**	**-0.0368**
Ethyl palmitate	**-0.0024**	**-0.0015**
Ethyl stearate	**-0.0019**	**-0.0012**
Ethyl oleate	**-0.0050**	**-0.0053**
Ethyl cis-Vaccenate	**-0.0001**	**-0.0003**
Ethyl linoleate	**-0.0069**	**-0.0041**
Ethyl arachidate	**0.0000**	**0.0000**

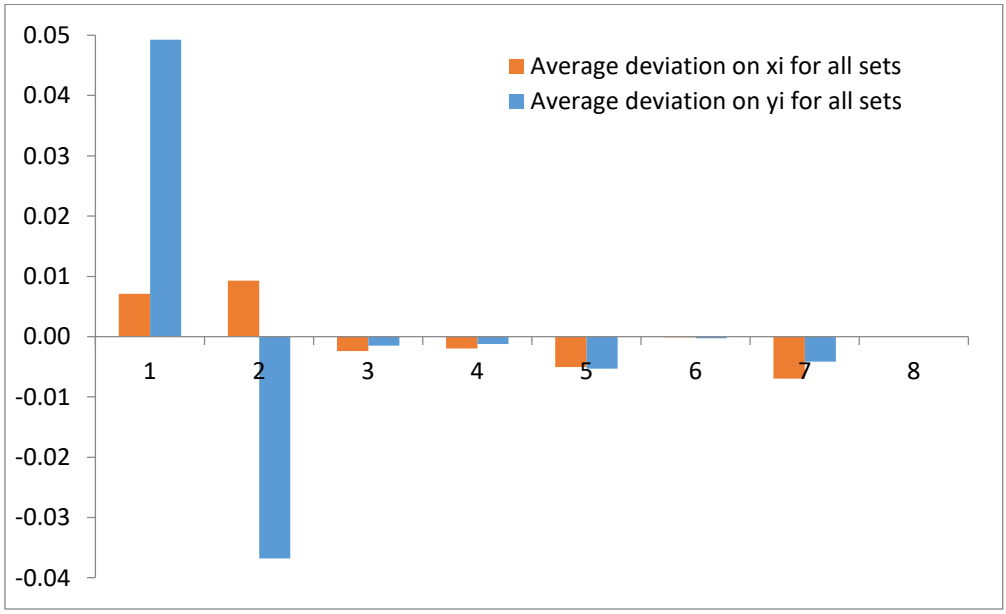

Figure 26. Graphical representation of multicomponent mixture - (1): 1-octanol; (2): 1-dodecanol; (3): ethyl palmitate; (4): ethyl stearate; (5): ethyl oleate; (6): ethyl cis-vaccenate; (7): ethyl linoleate; (8) ethyl arachidate

The graphical representation in bar graph is shown in **Figure 26** for the individual components of the multicomponent mixture. It is interesting to note that the average deviation on yi is considerably high for the first two components i.e 1-octanol and 1-dodecanols is nothing but a mixture of alcohols. We believe that the Dortmund modified UNIFAC model is not able to predict accurately when the most volatile component is a mixture of alcohols, as was shown much better in the binary system, where only one alcohol was used instead of two in the multicomponent system. Also, the average deviation between the alcohols is still quite considerably low, the deviation looks high only when they are compared with the esters.

5.3.2 Thermodynamic Modelling

The vapour pressures of fatty acid ethyl esters of *Balagnites* oil (EEBA) involved in the multicomponent system [1-octanol + 1-dodecanol + EEBA] were evaluated from the DIPPR databank [38] using the modified Riedel expression (**eq. 42**) with parameters shown in **Table 15**. Nevertheless, among the EEBA, ethyl arachidate and ethyl cis-vaccenate were not available in the DIPPR databank [38]. For ethyl arachidate, parameters of the modified Riedel expression

(eq. 42) were fitted in this work by using vapour pressures generated through a semi-theoretical method ([54], [55]) (percent average relative deviation between generated and fitted vapour pressures: 0.01 %). However, this method does not differ among isomers; therefore vapour pressures of ethyl cis-vaccenate were estimated with parameters of its isomer, ethyl oleate.

$$\ln(P/\mathrm{Pa}) = A + (B/(T/\mathrm{K})) + C\ln(T/\mathrm{K}) + D\,(T/\mathrm{K})^2 \qquad (42)$$

Table 15. DIPPR information related to vapour pressures of EEBA pure components [a].

Compound	*A*	*B*	*C*	*D*	*E*	Temperature range/K
Ethyl palmitate	**118.986**	**-15352.6**	**-12.8203**	**1.15929E-18**	**6**	**297.15 - 759.40**
Ethyl stearate	**140.043**	**-17145.2**	**-15.7408**	**2.76295E-18**	**6**	**305.65 - 777.90**
Ethyl oleate	**106.085**	**-14392.3**	**-11.1373**	**2.44407E-18**	**6**	**253.67 - 772.10**
Ethyl cis-vaccenat [b]	**106.085**	**-14392.3**	**-11.1373**	**2.44407E-18**	**6**	**253.67 - 772.10**
Ethyl linoleate	**118.379**	**-15509.5**	**-12.7782**	**2.50162E-18**	**6**	**218.20 - 777.80**
Ethyl arachidate	**122.291**	**-16866.9**	**-13.0981**	**5.15055E-19**	**6**	**393.00 - 582.00**

[a] *Modified Riedel equation:* $ln(P/Pa) = A + (B/(T/K)) + C\,ln(T/K) + D\,(T/K)^2$)

[b] *As ethyl cis-vaccenate is missing in the DIPPR databank [38], the vapor pressures of this compound were considered equal to those of its isomer, ethyl oleate.*

Chapter 6. Concluding Remarks and Future Perspectives

In this work, pure component vapor pressures of two FAEEs and four alcohols at various pressure range satisfying the operating conditions of dynamic Ebulliometer by setting the pressure and measuring the temperature at equilibrium were obtained. The obtained results are consistent and are in good agreement with the available literature data.

VLE data for three different binary mixture were measured at two distinct pressures using a dynamic ebulliometer. All the binary systems showed no azeotropic point at all of the pressures investigated. The experimental VLE data for the three binary mixtures were correlated by the NRTL 5 parameters and reasonable correlation accuracy was obtained with this model. VLE predictions were also performed using the Lyngby modified UNIFAC and Dortmund modified UNIFAC models and they gave qualitative prediction results. The consistency of experimental data was proved on the basis of the Herrington test, Van Ness test and Infinite Dilution test and according to the tests, the quality of measured data can be classified from good to excellent.

Lastly, the VLE data for a multi-component system involving BAEE was measured at 9 different conditions of pressure and temperature. The obtained composition analysis was predicted with Dortmund Modified UNIFAC model and the attained results were found to be positive.

The concept of biodiesel production from renewable resources is still in its infancy and needs a high level of attention. A reality check on the feasibility of agro-based biofuels especially taking into account the environmental aspects and rural development needs to be considered together with the assessment of the quality of alternative and potential energy sources such as solar energy or bio energy from biomass. In conclusion, the quantitative models, which are necessarily based on simplified assumptions, cannot be used to make predictions about future scenarios. The special case of ethanol production from sugar cane in Brazil represents a feasible option, but its desirability in relation to food shortage issues and especially environmental impact is doubtful as there is not much enough evidence to support that the usage of fuel from agro-based sources decreases the pollution level. Indeed, a necessity for change should be considered as an opportunity to remove the lock-ins hampering the technical progress by including the type of discussion related to scientific, political, ethical and socio-economic analyses. The current lack of a feasible and desirable alternative to fossil energy indicates that this is an objective that deserves top priority for the production of fuels from non-edible vegetable oils.

References

[1] Borugadda VB, Goud VV. Biodiesel production from renewable feedstocks: Status and opportunities. Renewable and Sustainable Energy Reviews 2012; 16: 4763–4784.

[2] Coniglio L, Coutinho JAP, Clavier JY, Jolibert F, Jose J, Mokbel I, Pillot D, Pons MN, Sergent M, Tschamber V. Biodiesel via supercritical ethanolysis within a global analysis "Feedstocks-conversion-engine" for a sustainable fuel alternative. Progress in Energy and Combustion Science 2014; 43: 1-35.

[3] Atabani AE, Silitonga AS, Ong HC, Mahlia TMI, Masjuki HH, Badruddin IA, Fayaz H. Non-edible vegetable oils: A critical evaluation of oil extraction, fatty acid compositions, biodiesel production, characteristics, engine performance and emissions production. Renewable and Sustainable Energy Reviews 2013; 18: 211–245.

[4] Bankovic-Ilic IB, Stamenkovic OS, Veljkovic VB. Biodiesel production from non-edible plant oils. Renewable and Sustainable Energy Reviews 2012; 16: 3621– 3647.

[5] Anitescu G, Bruno TJ, Fluid properties needed in supercritical transesterification of triglyceride feedstocks to biodiesel fuels for efficient and clean combustion – A review. J. of Supercritical Fluids 2012; 63: 133–149.

[6] Oliveira MB, Queimada AJ, Countinho JAP. Prediction of near and supercritical fatty acid ester + alcohol systems with the CPA EoS. J. of Supercritical Fluids 2010; 52: 241–248.

[7] Oliveira MB, Barbedo S, Soletti JI, Carvalho SHV, Queimada AJ, Coutinho JP. Liquid - liquid equilibria for the canola oil biodiesel + ethanol + glycerol system. Fuel 2011; 90: 2738-45.

[8] Follegatti-Romero LA, Oliveira MB, Batista EAC, Coutinho JAP, Meirelles AJA. Liquid-liquid equilibria for ethyl esters + ethanol + water systems: experimental measurements and CPA EoS modeling. Fuel 2012; 96: 327-34.

[9] Pandey VC, Singh K, Singh JS, Kumar A, Singh B, Singh RP. Jatropha curcas: a potential biofuel plant for sustainable environmental development. Renew Sustain Energy Rev 2012; 16: 2870-83.

[10] Zhou W, Boocock DGB, Phase distributions of alcohol, glycerol, and catalyst in the transesterification of soybean oil, Journal of American Oil Chemists'Society 2006; 83: 1041-1045.

[11] Ron D. D. Weir. Measurement of the Thermodynamic Properties of Multiple Phases, Elsevier Science; Inc.; 2005, ISBN: 0444519777, ISBN-13: 9780444519771.

[12] Oliveira MB, Follegatti-Romero LA, Lanza M, Batista FRM, Batista EAC, Meirelles AJA. Low pressure vapor–liquid equilibria modeling of biodiesel related systems with the Cubic–Plus–Association (CPA) equation of state. Fuel 2014; 133: 224–231.

[13] Tang G, Ding H, Hou J, Xu S. Isobaric vapor–liquid equilibrium for binary system of ethyl myristate + ethyl palmitate at 0.5, 1.0 and 1.5 kPa. Fluid Phase Equilibria 2013; 347: 8– 14.

[14] Matsuda H, Yamada H, Takahashi R, Koda A, Kurihara K, Tochigi K, Ochi K. Ebulliometric Determination and Prediction of Vapor_Liquid Equilibria for Binary Mixtures of Ethanol and Ethyl Hexanoate. J. Chem. Eng. Data 2011, 56: 5045–5051.

[15] Shimoyama Y, Iwai Y, Abeta T, Arai Y. Measurement and correlation of vapour-liquid equilibria for ethanol + ethyl laurate and ethanol + ethyl myristate systems near critical temperature of ethanol. Fluid Phase Equilib 2008; 264: 228-34.

[16] Shimoyama Y, Abeta T, Iwai Y. Prediction of vapour-liquid equilibria for supercritical alcohol + fatty acid ester systems by SRK equation of state with Wong-Sandler mixing rule based on COSMO theory. J Supercrit Fluids 2008; 46: 4-9.

[17] Coelho R, dos Santos PG, Mafra MR, Cardozo-Filho L, Corazza ML. (Vapor + liquid) equilibrium for the binary systems {water + glycerol} and {ethanol + glycerol, ethyl stearate, and ethyl palmitate} at low pressures. J Chem Thermodyn 2011; 43:1870-6.

[18] Veneral JG, Dirceu Jr LR, Mazutti MA, Voll FAP, Cardozo-Filho L, Corazza ML, et al. Thermophysical properties of biodiesel and related systems: low pressure vapour-liquid equilibrium of methyl/ethyl Jatropha curcas biodiesel. J Chem Thermodyn 2013; 60: 46-51.

[19] Pinto LF, da Silva DIS, da Silva FR, Ramos LP, Ndiaye PM, Corazza ML. Phase equilibrium data and thermodynamic modeling of the system (CO2 þ biodiesel þ methanol) at high pressures. J Chem Thermodyn 2012; 44: 57-65.

[20] Ndiaye PM, Franceschi E, Oliveira D, Dariva C, Tavares FW, Oliveira JV. Phase behavior of soybean oil, castor oil and their fatty acid ethyl esters in carbon dioxide at high pressures. J Supercrit Fluids 2006; 37: 29-37.

[21] Oliveira MB, Queimada AJ, Kontogeorgis GM, Coutinho JAP. Evaluation of the CO_2 behavior in binary mixtures with alkanes, alcohols, acids and esters using the cubic-plus-association equation of state. J Supercrit Fluids 2011; 55: 876-92.

[22] Oliveira MB, Teles ARR, Queimada AJ, Coutinho JAP. Phase equilibria of glycerol containing systems and their description with the cubic-plus association (CPA) equation of state. Fluid Phase Equilib 2009; 280: 22-9.

[23] Akisawa Silva LY, Matricarde Falleiro RM, Meirelles AJA, Krähenbühl MA. Vapor-liquid equilibrium of fatty acid ethyl esters determined using DSC. Thermochim Acta 2011; 512: 178-82

[24] Mokbel I, Sawaya T, Zanota ML, Naccoul RA, Jose J, de Bellefon C. Vapor-liquid equilibria of glycerol, 1,3-propanediol, glycerol þ water, and glycerol + 1,3-propanediol. J Chem Eng Data 2012; 57: 284-9.

[25] Akisawa Silva LY, Matricarde Falleiro RM, Meirelles AJA, Krähenbühl MA. Determination of the vapor pressure of ethyl esters by differential scanning calorimetry. J Chem Thermodyn 2011; 43: 943-7.

[26] Benziane M, Khimeche K, Mokbel I, Sawaya T, Dahmani A, Jose J. Experimental vapor pressures of five saturated fatty acid ethyl ester (FAEE) components of biodiesel. J Chem Eng Data 2011; 56: 4736-40.

[27] Velez A, Pereda S, Brignole EA. Isochoric lines and determination of phase transitions in supercritical reactors. J Supercrit Fluids 2010; 55: 643-7.

[28] Araújo OAS, Silva FR, Ramos LP, Lenzi MK, Ndiaye PM, Corazza ML. Phase behavior measurements for the system (carbon dioxide + biodiesel + ethanol) at high pressures. J Chem Thermodyn 2012; 47: 412–9.

[29] J.M.Prausnitz. Molecular Thermodynamics of Fluid-Phase Equilibria, Prentice-Hall; Inc.; 1999, ISBN: 0-13-977745-8.

[30] B.E.Poling. The Properties of Gases And Liquids, McGraw-Hill; 2001, 0-07-149999-7.

[31] Kontogeorgis GM, Folas GK. Thermodynamic Models for Industrial Applications: From Classical to Advanced Mixing Rules to Association Theories. 2010;ISBN 978-0-470-69726-9.

[32] Kang JW, Diky V, Chirico RD, Magee JW, Muzny CD, Abdulagatov I, Kazakov AF, Frenkel M. Quality Assessment Algorithm for Vapor-Liquid equilibrium Data. J Chem Eng Data 2010, 55: 3631-3640.

[33] Chapagain BP, Yehoshua Y, Wiesman Z. Desert date (Balanites aegyptiaca) as an arid lands sustainable bioresource for biodiesel. Bioresource Technology 2009, 100: 1221-1226.

[34] Yefanova SN, Richard R, Roux ST, Bouyssiere B,Coulibaly YLB, Nébié RHC, Mozet K, Coniglio L. Dry Purification by Natural Adsorbents of Ethyl Biodiesels Derived from Nonedible Oils, Energy & Fuels 2015, 29: 150−159.

[35] http://www.pignat.com/accueil.aspx (PIGNAT SAS - Process Engineering Solutions)

[36] WILSAK, R.A., THODOS, G., Critical Assessment of 4-Vapor Pressure Functions Over the Complete Vapor Liquid Coexistence Region, Ind. Eng. Chem. Fund., 1984, 23, 75-82.

[37] Plyasunov, A. V., Plyasunova, N. V., Shock, E. L., Group Contribution Values for the Thermodynamic Functions of Hydration of Aliphatic Esters at 298.15 K, 0.1 MPa., J. Chem. Eng. Data, 2004, 49, 1152–1167.

[38] http://www.dechema.de/en/dippr801.html (DECHEMA - Gesellschaft für Chemische Technik und Biotechnologie e.V. (Society for Chemical Engineering and Biotechnology)).

[39] Selected Values of Properties of Chemical Compounds, Data Project, Thermodynamic Research Center, Texas A&M University, College Station, Texas (1980-extant).

[40] Wilhoit, R.C., Zwolinski, B.J., Physical and Thermodynamic Properties of Aliphatic Alcohols, J. Phys. Chem. Ref. Data, 1973, 2, Suppl. No. 1.

[41] Stull, D.R., Vapor pressure of Pure Substances, Ind. Eng. Chem., 1947, 39, 517-540.

[42] Smith, B.D., Srivastava, R., Thermodynamic Data for Pure Compounds. Part B. Halogenated Hydrocarbons and Alcohols, Elsevier, Amsterdam (1986).

[43] Boublik, T., Fried, V., Hala, E., The Vapour Pressures of Pure Substances, Elsevier, New York (1973).

[44] Kemme, H.R., Kreps, S.I., Vapor Pressure of Primary n-Alkyl Chlorides and Alcohols, J. Chem. Eng. Data, 1969, 14, 1, 98-102.

[45] Rose, A., Papahronis, B.T., Williams, E.T., Experimental Measurement of Vapor-Liquid Equilibria for Octanol-Decanol and Decanol-Dodecanol Binaries, J. Chem. Eng. Data, 1958, 3, 2, 216.

[46] Renon, H., Prausnitz, J.M., Local compositions in thermodynamic excess functions for liquid mixtures, AIChE J., 1968, 14, 135–144.

[47] Larsen, B.L., Rasmussen, P., Fredenslund, A., A Modified UNIFAC Group-Contribution Model for Prediction of Phase Equilibria and Heats of Mixing, Ind. Eng. Chem. Res., 1987, 26, 2274-2286.

[48] Weidlich, U., Gmehling, J., A Modified UNIFAC Model. 1. Prediction of VLE, h^E, and $\gamma\infty$, Ind. Eng. Chem. Res., 1987, 26, 1372–1381.

[49] Gmehling, J., Li, J., Schiller, M., A modified UNIFAC model. 2. Present Parameter Matrix and Results for Different Thermodynamic Properties., Ind. Eng. Chem. Res., 1993, 32, 178–193.

[50] Gmehling, J., Wittig, R., Lohmann, J., Joh, R., A Modified UNIFAC (Dortmund) Model. 4. Revision and Extension, Ind. Eng. Chem. Res., 2002, 41, 1678–1688.

[51] Gmehling, J., Lohmann, J., Jakob, A., Li, J., Joh, R., A Modified UNIFAC (Dortmund) Model. 3. Revision and Extension., Ind. Eng. Chem. Res., 1998, 37, 4876–4882.

[52] Lohmann, J., Gmehling, J., Modified UNIFAC (Dortmund): Reliable Model for the Development of Thermal Separation Processes, J. Chem. Eng. Jpn., 2001, 34, 43–54.

[53] Cunico LP, Ceriani R, Sarup B, O'Connell JP, Gani R. Data, analysis and modeling of physical properties for process design of systems involving lipids. Fluid Phase Equilibria 2014; 362: 318-327.

[54] Coniglio, L., Knudsen, K., Gani, R., Model prediction of supercritical fluid – liquid equilibria for carbon dioxide and fish oil related compounds., Ind. Eng. Chem. Res., 1995, 34, 2473-84.

[55] Jaubert, J.N., Coniglio, L., Denet, F., From the correlation of binary systems involving supercritical CO_2 and fatty acid esters to the prediction of (CO_2-Fish oils) phase behavior., Ind. Eng. Chem. Res., 1999;38, 3162-71

[EN 14103] EN-14103, Fat and oil derivatives, Fatty Acid Methyl esters (FAME), Determination of ester and linoleic acid methyl ester contents, European Committee for Standardization, Brussels (Belgium), 2003.

Appendix

Appendix A. Calibration of the Ebulliometer for Temperature and Pressure

Temperature Calibration: Initially, the sensors accuracy was analyzed calibrating the temperature sensor in the ebulliometer using a reference thermometer, and measuring the vapor pressure at different temperatures for ethanol selected as reference compound (green species with well-known properties in a large temperature range). Hot water (100 °C) is taken and poured in a flask which can accommodate the two thermometers. The temperature reflected on both the thermocouples is noted down simultaneously and this process is continued for varying temperatures by cooling the water with the help of addition of ice. Calibration is established once the plot of the temperature of the reference versus temperature of the sensor gives the slope and the intercept which will be used in all the experimental work.

Table A.1. Temperature calibration data.

T.Ref(°C)	T.Sensor(°C)
89.2	**89.4**
85.9	**86.0**
83.3	**83.5**
79.4	**79.5**
75.8	**75.9**
73.6	**73.3**
70.9	**70.7**
68.7	**68.8**
66.6	**66.6**
63.9	**64.1**
60.2	**60.2**
57.6	**57.7**
54.8	**55.0**
51.5	**51.5**
48.0	**48.1**
45.3	**45.4**
42.1	**42.1**
40.0	**40.1**
37.1	**37.3**
33.7	**33.8**
30.8	**30.9**
27.8	**28.0**
24.3	**24.3**
22.2	**22.2**
20.4	**20.5**
17.6	**17.7**

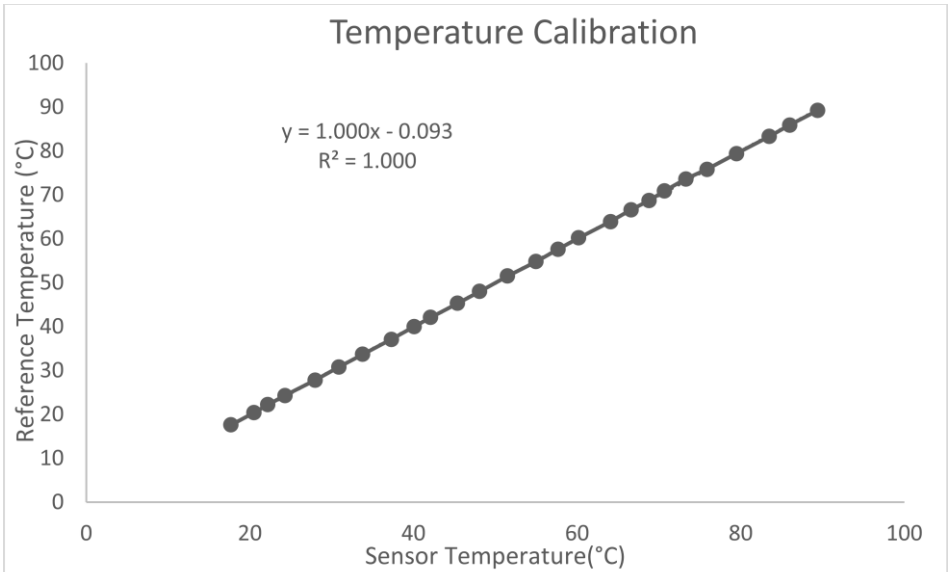

Figure A.1. Calibration of the sensor temperature with respect to the reference temperature.

Table A.2. Temperature calibration parameters

Parameters for Calibration	
Slope	**1.000**
Intercept	**-0.093**

Pressure Calibration: The ebulliometer was equipped with a digital pressure sensor which uses 'mmHg' in its units. The pressure was calibrated into three different ranges in order to attain the most accurate calibration within a defined range of pressures. The calibration was performed from 75 – 725 mmHg.

Table A.3. Vapour pressure data for sensor and literature (DIPPR pressure).

P.Sensor (mmHg)	P.Sensor (Pa)	P.DIPPR (Pa)	P.DIPPR (mmHg)
75	**9999.18**	**10482.54**	**78.63**
100	**13332.24**	**13779.23**	**103.35**
125	**16665.30**	**17201.15**	**129.02**
150	**19998.36**	**20480.91**	**153.62**
175	**23331.41**	**23804.25**	**178.55**
200	**26664.47**	**27177.50**	**203.85**
225	**29997.53**	**30508.83**	**228.84**
250	**33330.59**	**34020.14**	**255.17**
275	**36663.65**	**37173.35**	**278.82**
300	**39996.71**	**40570.16**	**304.30**
325	**43329.77**	**43827.94**	**328.74**
350	**46662.83**	**47092.83**	**353.23**
375	**49995.89**	**50560.10**	**379.23**
400	**53328.95**	**53767.64**	**403.29**
425	**56662.01**	**57144.36**	**428.62**
450	**59995.07**	**60437.43**	**453.32**
475	**63328.13**	**63888.05**	**479.20**
500	**66661.18**	**67218.13**	**504.18**
525	**69994.24**	**70397.01**	**528.02**
550	**73327.30**	**73700.53**	**552.80**
575	**76660.36**	**77132.46**	**578.54**
600	**79993.42**	**80367.05**	**602.80**
625	**83326.48**	**83713.89**	**627.91**
650	**86659.54**	**86824.48**	**651.24**
675	**89992.60**	**90392.88**	**678.00**
700	**93325.66**	**93707.86**	**702.87**
725	**96658.72**	**97123.20**	**728.48**

Table A.4. DIPPR Antoine equation constants obtained for ethanol.

DIPPR Antoine equation constants	
a	**74.475**
b	**-7164.3**
c	**-7.327**
d	**0**
e	**2**

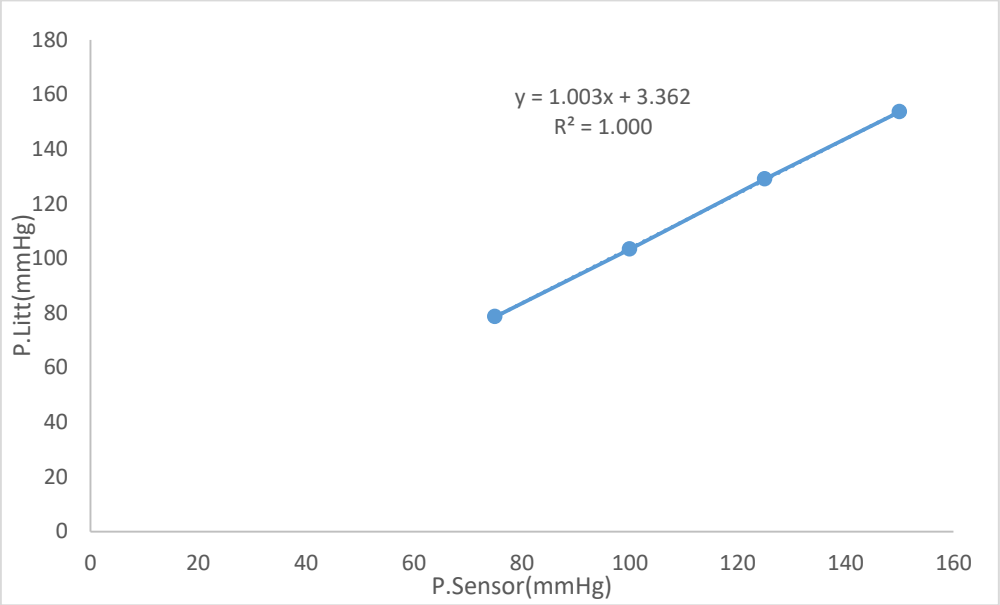

Figure A.2. Calibration of the pressure sensor with literature pressure (range: 75 -150 mmHg).

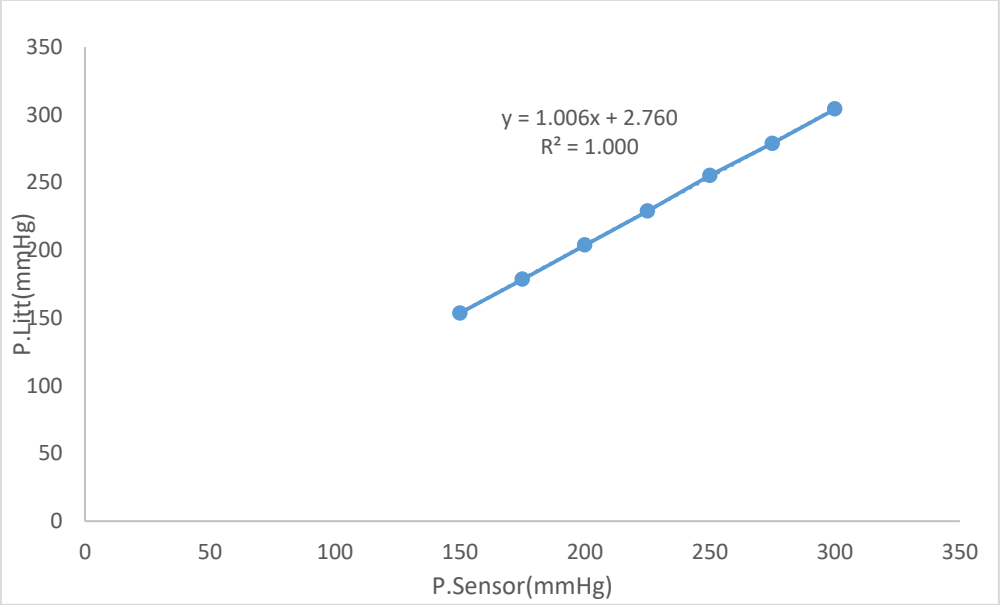

Figure A.3. Calibration of the pressure sensor with literature pressure (range: 150-300 mmHg).

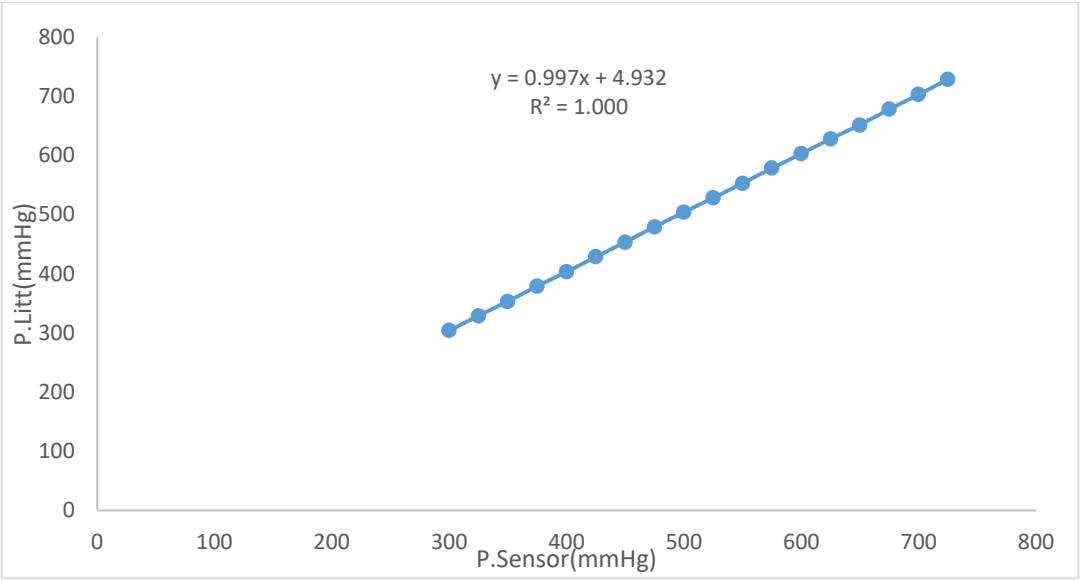

Figure A.4. Calibration of the pressure sensor with literature pressure (range: 300-725 mmHg).

Table A.5. Pressure calibration parameters

Pressure range	Parameters for calibration	
75 -150 mmHg	Slope	1.003
	Intercept	3.362
150-300 mmHg	Slope	1.006
	Intercept	2.760
300-725 mmHg	Slope	0.997
	Intercept	4.932

Appendix B. Evaluation of the Desired Component for Binary Systems and BAEE Content for Multicomponent System (Calibration)

Calibration is the process of determining the response factors used to calculate absolute component concentrations by injecting specially prepared calibration samples. The calibration in our study was taken into account by taking the real mixtures encountered in the VLE samples. The real mixture comprises a solvent, mixture of VLE sample i.e component$_1$ and component$_2$ and two internal standards depending upon the system being studied. In all the calibrations performed for various binary and multicomponent mixtures, the solvent used was toluene. An internal standard is a chemical substance that is added in constant amounts to mother solution for the determination of concentration of other analytes(component$_1$ and component$_2$) by evaluating the response factor. This substance can then be used for calibration by plotting the ratio of the analyte signal(peaks/areas) to the internal standard signal as a function of the analyte concentration. This is done to correct for the loss of analytes during its preparation. An ideal internal standard will have very similar, but not identical retention times to the chemical species of interest in the samples. This ratio for the samples is then used to obtain the analyte concentrations from a calibration curve. The internal standard needs to provide a signal that is similar to the analyte signal in most ways but sufficiently different so that the two signals are readily distinguishable by the instrument.

The calibrations for each binary/multicomponent system was performed by taking the internal standard 1 (IS$_1$/1-butanol) corresponding to the determination of more volatile component (component$_1$) and internal standard 2 (IS$_2$) corresponding to the determination of component$_2$.

A number of calibration samples of various compositions in component$_1$ and component$_2$ were prepared in a stock solution of well-known composition in the internal standards and later accurately weighed. Quantitative GC-analysis of the calibration samples makes possible to draw the calibration curve, i.e. the peak area ratios $A_{component1}/A_{IS1}$ and the corresponding mass ratios $m_{component1}/m_{IS1}$ related to component$_1$ and IS$_1$ (1-butanol) and successively the peak ratios $A_{component2}/A_{IS2,}$ mass ratios $m_{component2}/m_{IS2}$ for component$_2$ and IS$_2$. The slope ($F_{component\ 1/IS1}$) of the resulting curve corresponds to the response factor for component$_1$ and similarly for component$_2$. **Figures B.1-B.6** shows the plot for the binary systems and **Figures B.7-B.10** shows the response factor calibration for the multicomponent system. **Table B.1** shows the response factor with its respective coefficients of determination obtained for the three binary

and multicomponent system. As it can be observed, a very good linearity was obtained for all the binary systems with a R^2 coefficient superior than 0.999, whereas for the multicomponent system the R^2 was found to be 0.899. A detailed scheme is presented in the following paragraphs to utilize the response factor in the determination of composition of each component in the binary and multicomponent system.

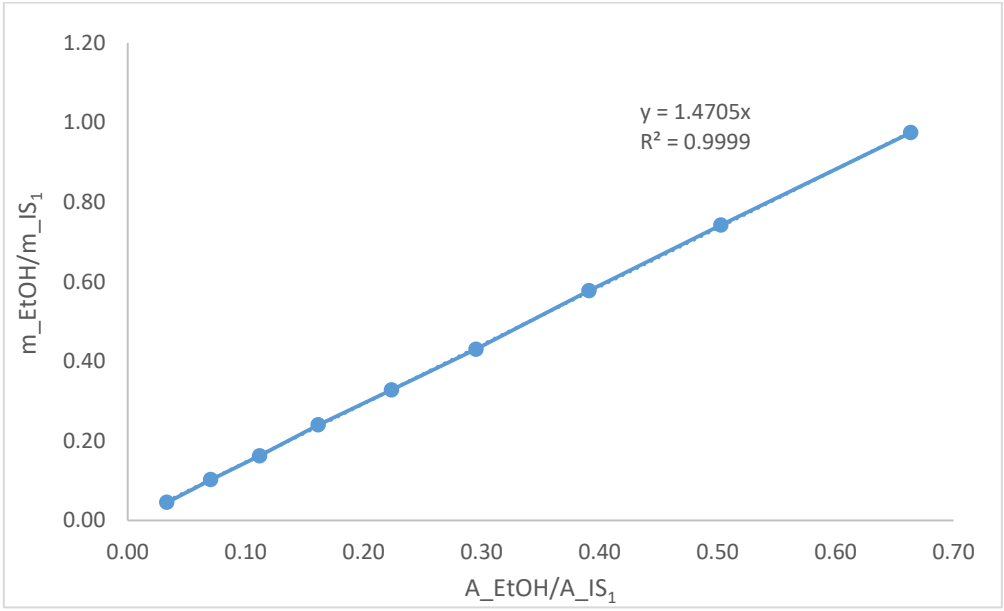

Figure B.1. Calibration for the determination of response factor for ethanol using internal standard (IS) as 1-butanol (binary system – ethanol + ethyl hexanoate).

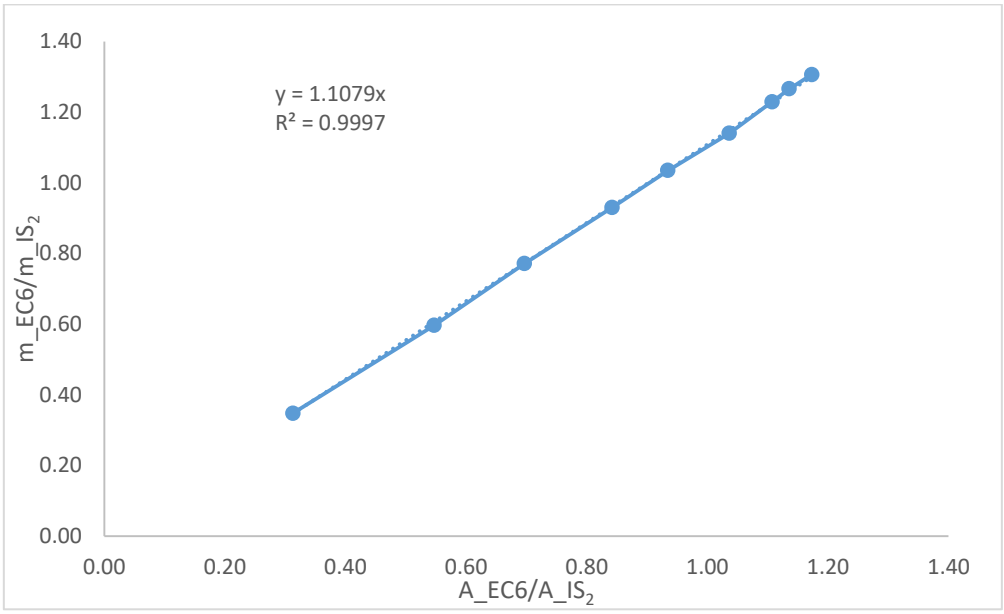

Figure B.2. Calibration for the determination of response factor for ethyl hexanoate using internal standard(IS) as ethyl octanoate (binary system – ethanol + ethyl hexanoate).

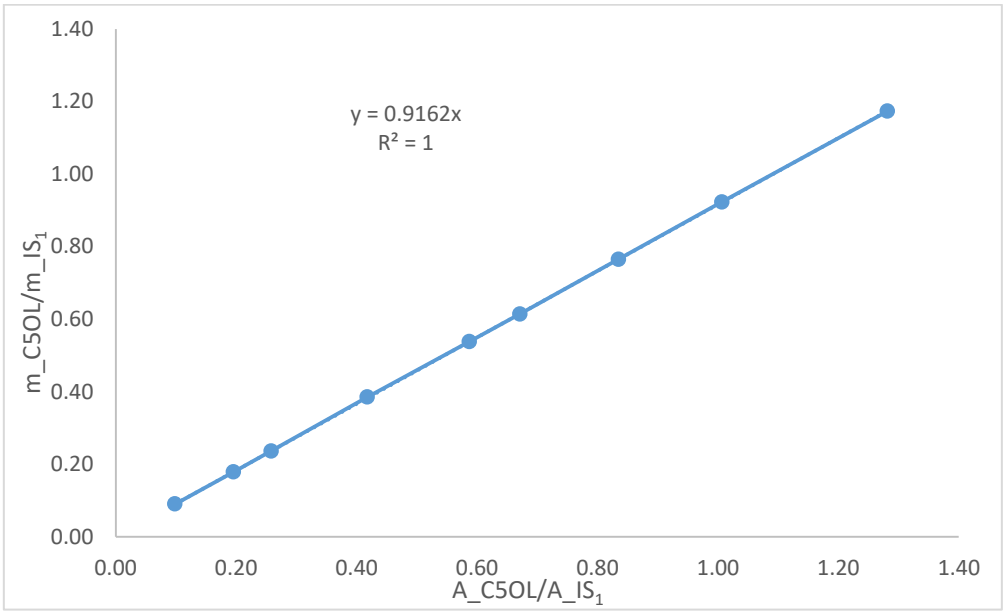

Figure B.3. Calibration for the determination of response factor for 1-pentanol using internal standard (IS) as 1-butanol(binary system – 1-pentanol + ethyl hexanoate).

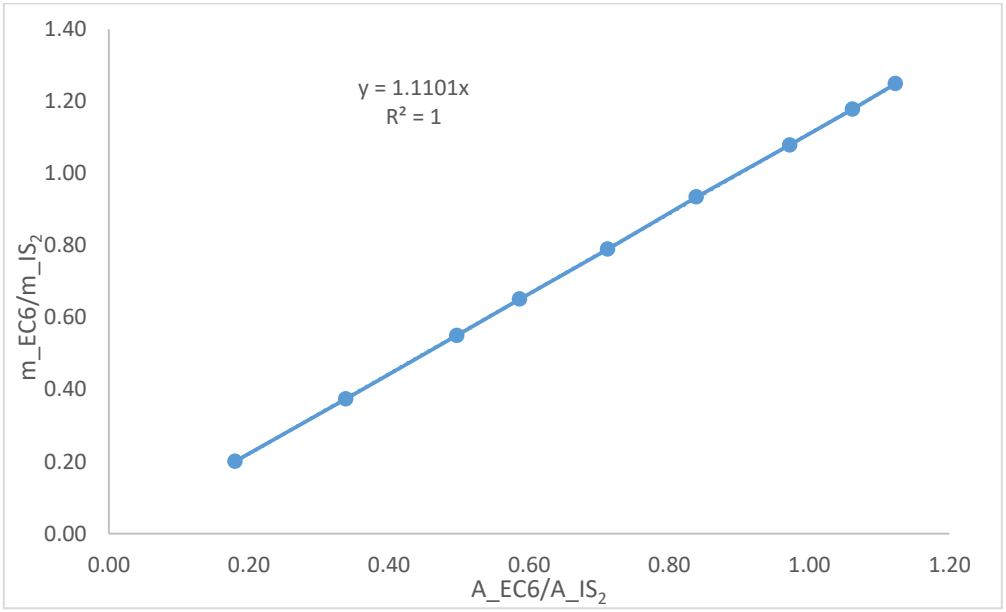

Figure B.4. Calibration for the determination of response factor for ethyl hexanoate using internal standard (IS) as ethyl octanoate (binary system – 1-pentanol + ethyl hexanoate).

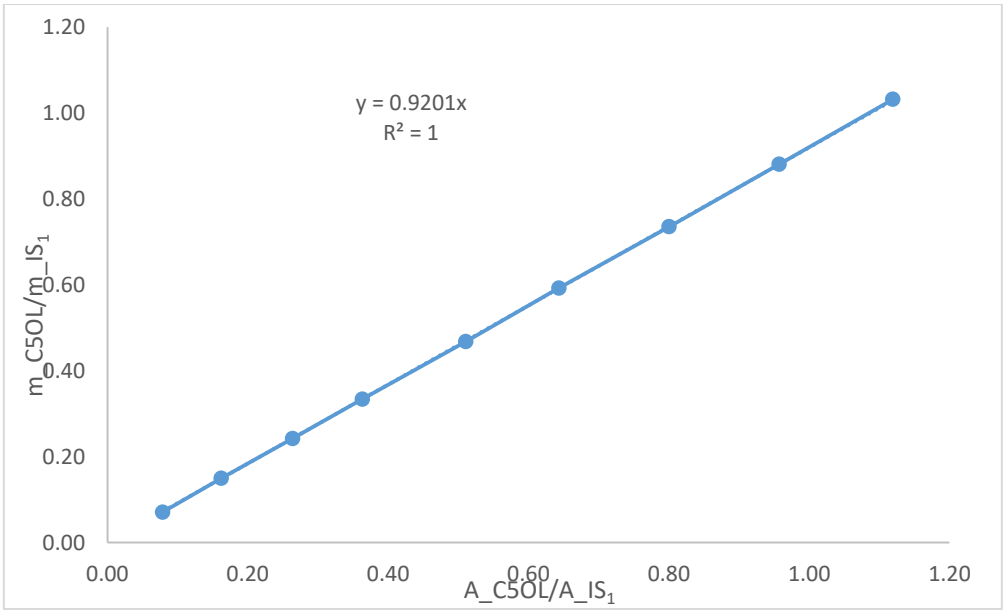

Figure B.5. Calibration for the determination of response factor for 1-pentanol using internal standard (IS) as 1-butanol (binary system – 1-pentanol + ethyl octanoate).

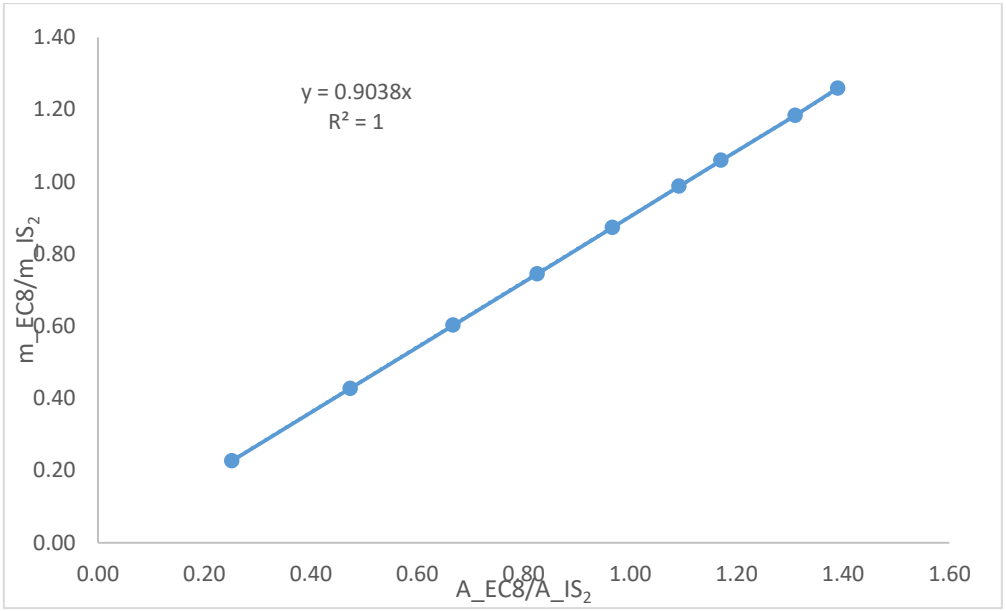

Figure B.6. Calibration for the determination of response factor for ethyl octanoate using internal standard (IS) as ethyl hexanoate (binary system – 1-pentanol + ethyl octanoate).

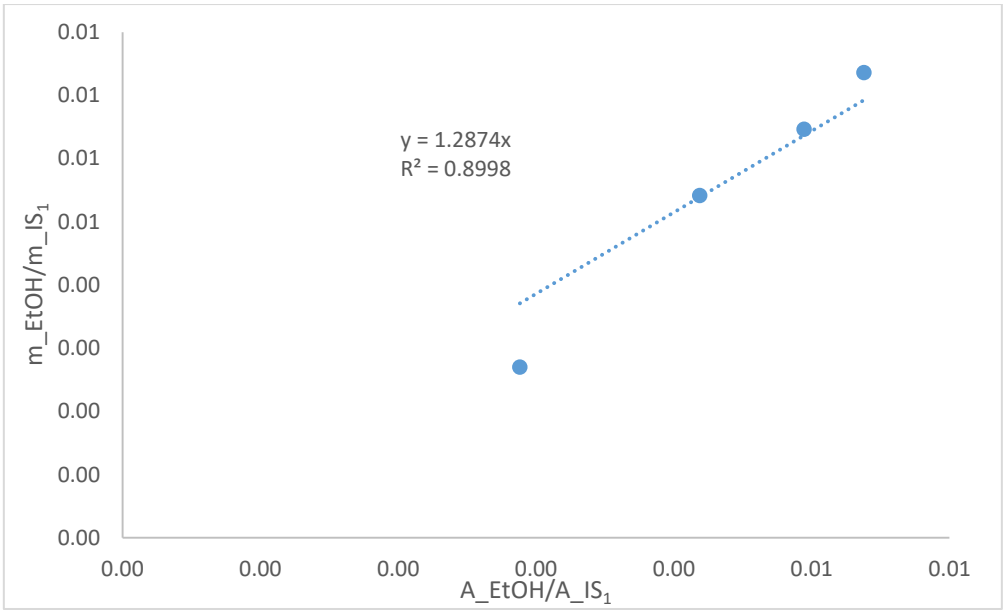

Figure B.7. Calibration for the determination of response factor for ethanol using internal standard (IS) as 1-butanol (multicomponent system – ethanol + 1-octanol + 1-dodecanol + ethyl oleate).

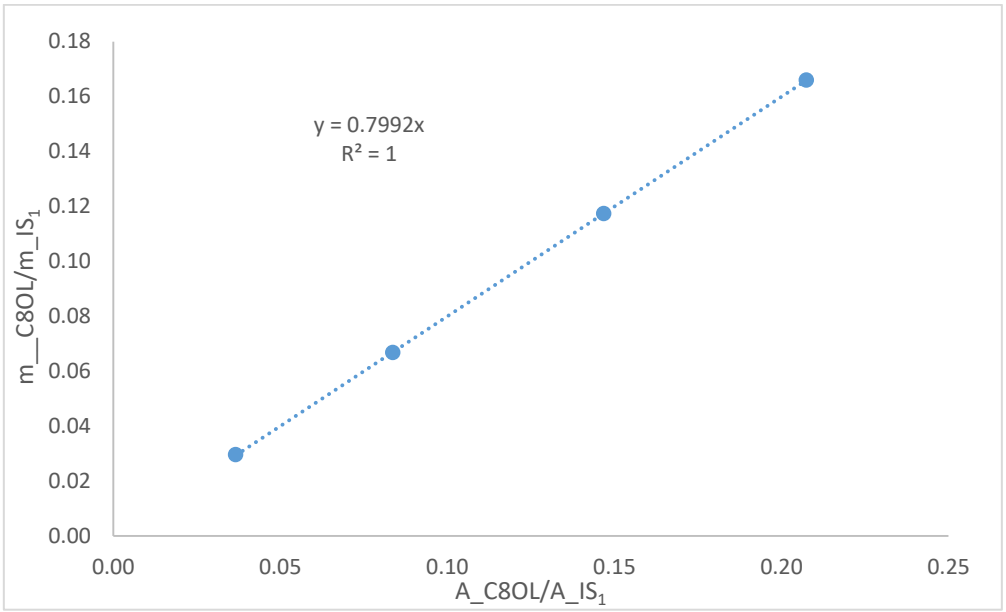

Figure B.8. Calibration for the determination of response factor for 1-octanol using internal standard (IS) as 1-butanol (multicomponent system – ethanol + 1-octanol + 1-dodecanol + ethyl oleate).

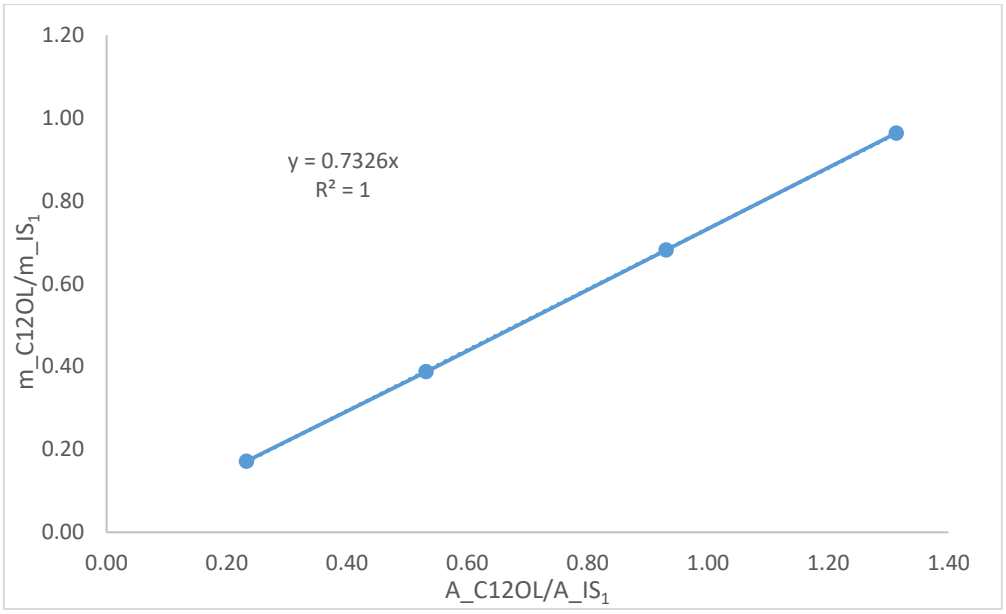

Figure B.9. Calibration for the determination of response factor for 1-dodecanol using internal standard (IS) as 1-butanol (multicomponent system – ethanol + 1-octanol + 1-dodecanol + ethyl oleate).

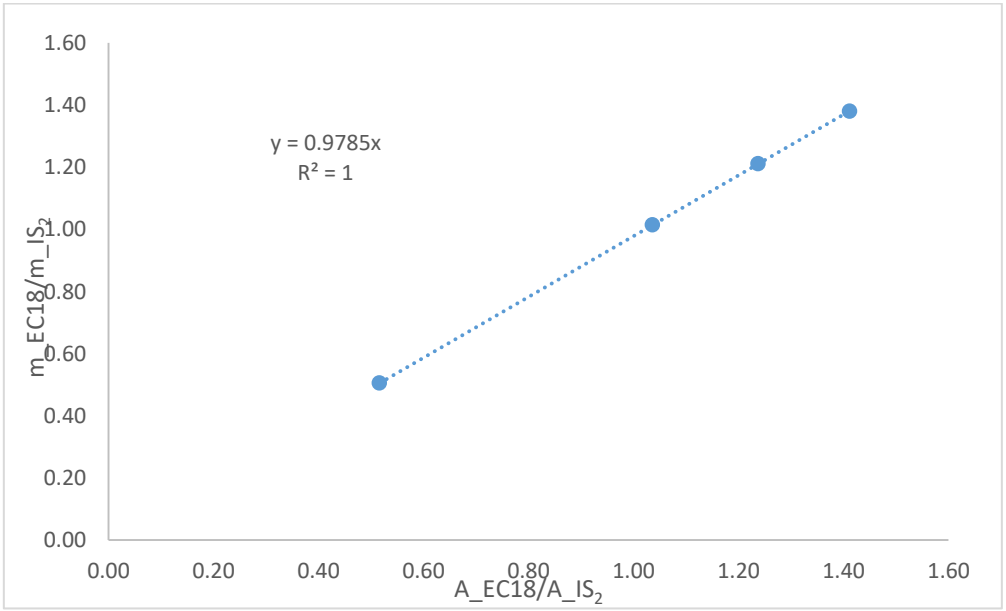

Figure B.10. Calibration for the determination of response factor for ethyl oleate using internal standard (IS) as methyl heptadecanoate (MHD) (multicomponent system – ethanol + 1-octanol + 1-dodecanol + ethyl oleate).

After calibration, the quantification of the desired component is conducted by analyzing within the same operating conditions, a solution prepared by weighing accurately into a GC-ALSI vial, 0.1 mL of the reaction mixture sample and 1 mL of stock solution (prepared for calibration).

The mass of each component is determined by appropriately taking the respective response factors determined in the calibration procedure, the mass from the mixture sample is determined as following:

•*Produced BAEEs*

Standard solutions of well-known composition in ethyl oleate (BAEE model molecule) and methyl heptadecanoate as internal standard (IS) [EN-14103] were prepared in toluene (solvent). After quantitative GC-analysis of the standard solutions, the slope of the calibration curve, peak area ratios A_i/A_{IS} vs. corresponding mass ratios m_i/m_{IS} led to the response factor $F_{i/IS}$ of ethyl oleate i vs. the selected IS. Hence, for an unknown BAEE mixture with N_C identified species, molar fractions in each component (x_j) is determined by:

$$x_j = \frac{n_j}{\sum_{k=1}^{N_C} n_k} \quad \text{with} \quad n_j = \frac{m_j}{M_j} \quad \text{and} \quad m_j = F_{i/IS} \cdot \frac{A_i}{A_{IS}} \cdot m_{IS} \qquad \text{(B.1)}$$

where n_j and M_j are respectively number of moles and molecular weight of component *j*. Thus, eq. B.1 assumes that all BAEEs have similar response factors, taken equal to the one determined previously during GC-FID calibration with ethyl oleate as model molecule.

• *Multicomponent systems [Alcohols + Ethyl oleate] and [Alcohols + BAEEs]*

IS_1: 1-butanol for all alcohols; IS_2: methyl heptadecanoate [EN-14103] for ethyl oleate or all BAEEs. The standard solutions [Alcohols (*i*) + Ethyl oleate (*j*)] are dedicated to determine and check response factor of each component (i or *j*) vs. its related IS (F_i/IS_1 and F_j/IS_2 respectively). These were then used to check the calibration performance for standard solutions [Alcohols + BAEEs].

•*Binary systems [Alcohol(1) + short FAEE (2)]*

IS_1: 1-butanol for all alcohols; IS_2: ethyl octanoate for ethyl hexanoate; ethyl hexanoate for ethyl octanoate. According to eq. B.1, molar fractions in each binary component are thus determined by:

$$x_i = \frac{n_i}{\sum_{j=1}^{2} n_j} \quad \text{with} \quad n_i = \frac{m_i}{M_i} \quad \text{and} \quad m_i = k_{i/IS_i} \cdot \frac{A_i}{A_{IS_i}} \cdot m_{IS_i} \quad \text{for } i\text{=1 to 2,} \qquad \text{(B.2)}$$

where n_i, m_i, and M_i are respectively number of moles, mass and molecular weight of component *i*. while k_{i/IS_i} is response factor of component *i* vs its related internal standard IS_i introduced with a mass m_{IS_i}in the collected sample to quantify.

Table B.1. Internal standards and response factors related to each investigated mixture

Mixture	Alcohol related internal standard (IS_1)	FAEE related internal standard (IS_2)	Response factors
[Ethanol (1) + Ethyl hexanoate (2)]	**1-Butanol**	**Ethyl octanoate**	$\boldsymbol{F_{1/IS_1} = 1.4705,}$ $\boldsymbol{F_{2/IS_2} = 1.1079}$
[1-Pentanol (1) + Ethyl hexanoate (2)]	**1-Butanol**	**Ethyl octanoate**	$\boldsymbol{F_{1/IS_1} = 0.9162,}$ $\boldsymbol{F_{2/IS_2} = 1.1101}$
[1-Pentanol (1) + Ethyl octanoate (2)]	**1-Butanol**	**Ethyl hexanoate**	$\boldsymbol{F_{1/IS_1} = 0.9201,}$ $\boldsymbol{F_{2/IS_2} = 0.9038}$
[Ethanol (1) + 1-Octanol (2) + 1-Dodecanol (3) + Ethyl oleate (4)]]	**1-Butanol**	**Methyl heptadecanoate**	$\boldsymbol{F_{1/IS_1} = 1.2874,}$ $\boldsymbol{F_{2/IS_1} = 0.7992,}$ $\boldsymbol{F_{3/IS_1} = 0.7326,}$ $\boldsymbol{F_{4/IS_2} = 0.9785}$

It must be noted that initially the calibration was performed by taking into account one internal standard for the component$_1$ and the composition of component$_2$ was determined from the overall composition, but the results were not correct based on the consistency test. Hence, we accounted the composition by respectively applying the calibration for the real mixture i.e two internal standards for the two components in the binary mixture which led to more consistent liquid compositions in the experimental results.

Appendix C. A Graphical Representation of Data for the Vapour Pressures of Pure Compounds

As described in section 5.1, for checking the consistency of the vapour pressure of pure components, the diagrams were plotted for the vapour pressure (P_S) vs. temperature (T). As can be seen from the following figures, the data clearly follows a linear dependency of $\ln(P_S)$ vs. $1/T$. The correlation coefficient for each component is mentioned in **Table C.1**.

Table C.1. Correlation coefficient for pure component linear dependency

Component	Slope	Intercept
Ethyl hexanoate	**-5361.2**	**23.725**
Ethyl octanoate	**-5968.8**	**23.960**
1-pentanol	**-5887.7**	**25.874**
1-octanol	**-6504.8**	**25.466**
1-dodecanol	**-7643.8**	**25.925**

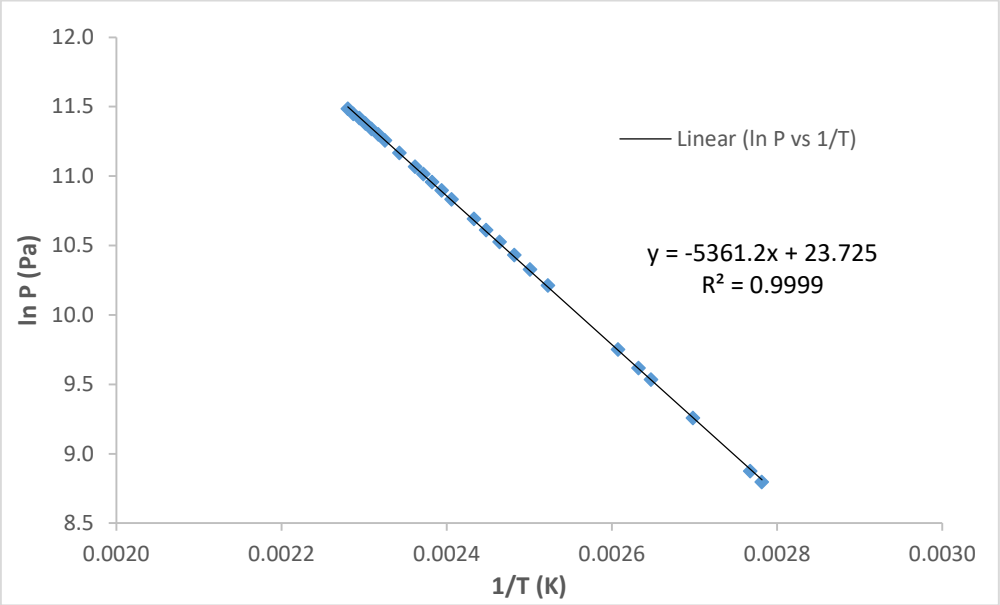

Figure C.1. A graphical representation of vapour pressure vs temperature for ethyl hexanoate.

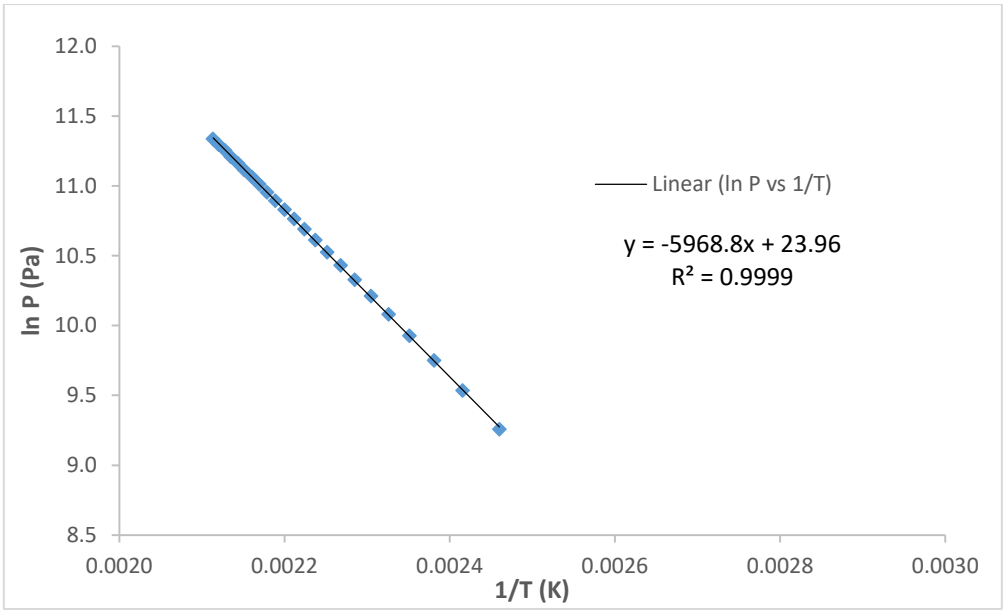

Figure C.2. A graphical representation of vapour pressure vs temperature for ethyl octanoate.

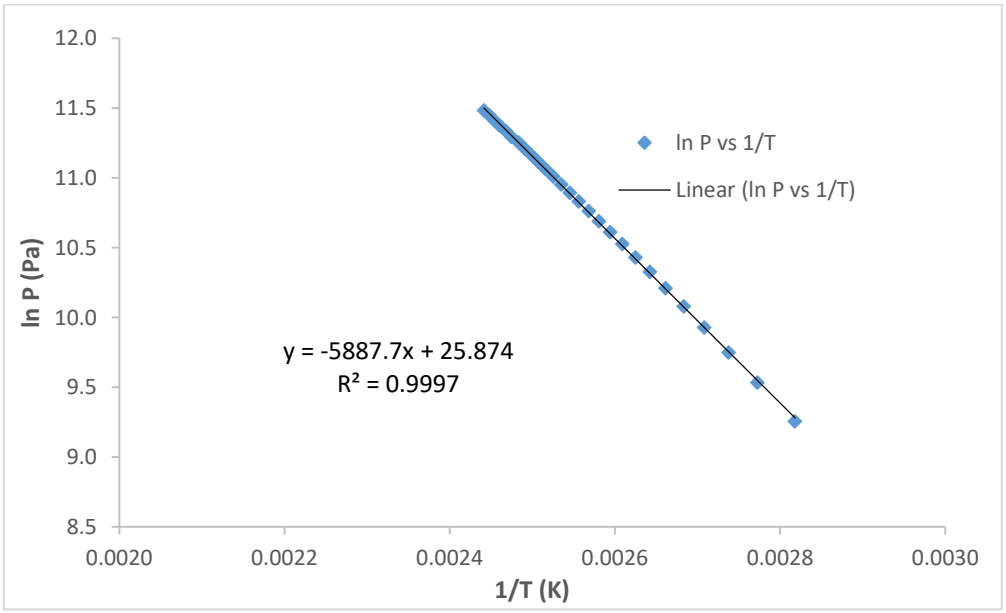

Figure C.3. A graphical representation of vapour pressure vs temperature for 1-pentanol.

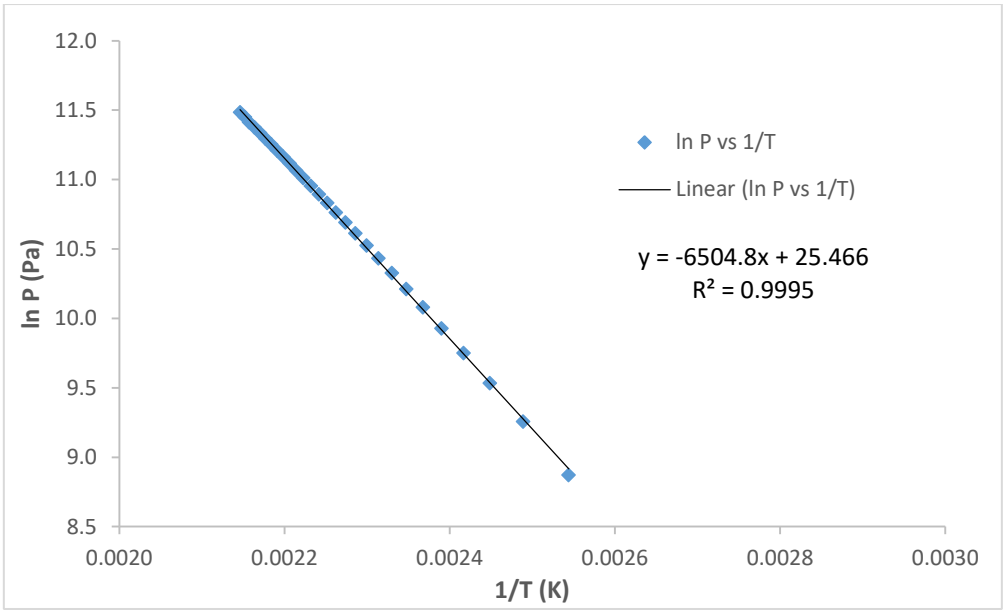

Figure C.4. A graphical representation of vapour pressure vs temperature for 1-octanol.

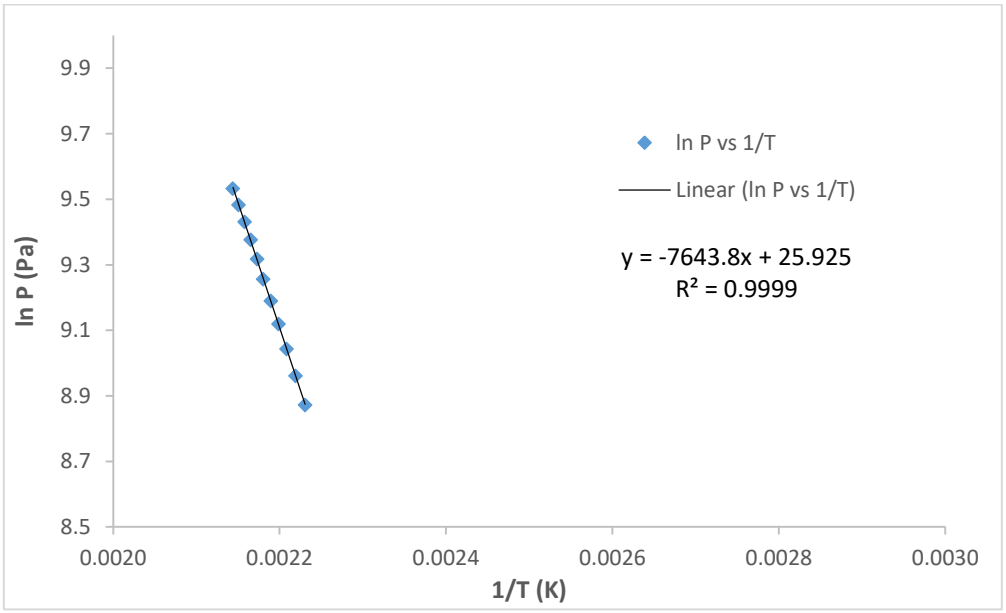

Figure C.5. A graphical representation of vapour pressure vs temperature for 1-dodecanol.

Appendix D. Performance of Various Models for the Investigated Binary Systems

As shown in the section 5.2.2, the performance of NRTL model together with Lyngby Modified UNIFAC and Dortmund Modified UNIFAC models shows a better agreement between experimental data and correlation via NRTL (5 parameters) is most often observed when parameter estimation is carried out by using PTx information. Nevertheless, the parameter estimation carried out by using PTxy information in shown in the following figures for the purpose of reference.

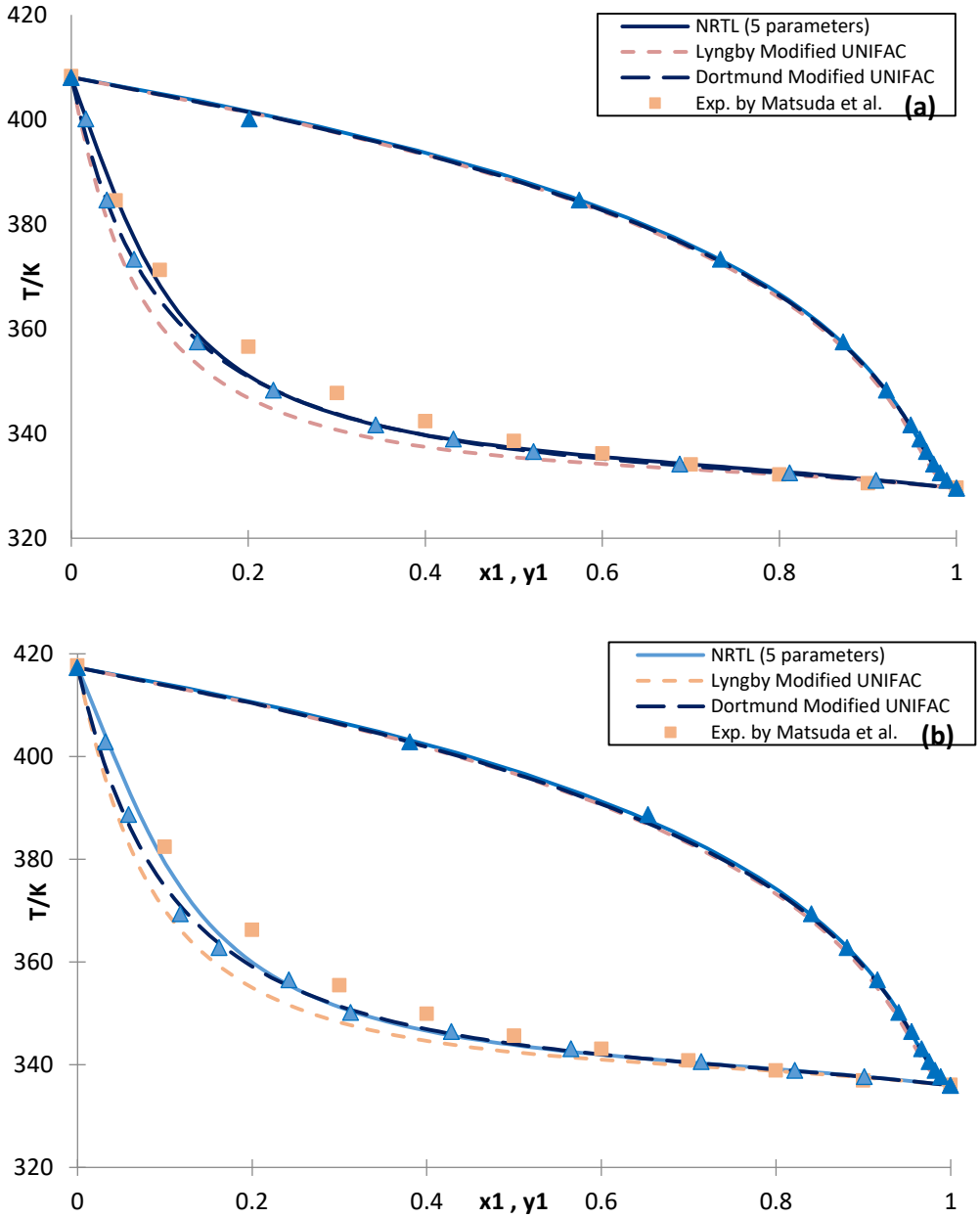

Figure D.1. PTxy diagram for [ethanol (1) + ethyl hexanoate (2)] at (a) 40 kPa and (b) 53.33 kPa (NRTL parameters were fitted on PTxy data measured in this work at 40 and 53.33 kPa: a_{12} = 9.74057; b_{12} /K = -2937.76; a_{21} = -5.96358; b_{21} /K = 2122.24; α_{12} = α_{21} = 0.5).

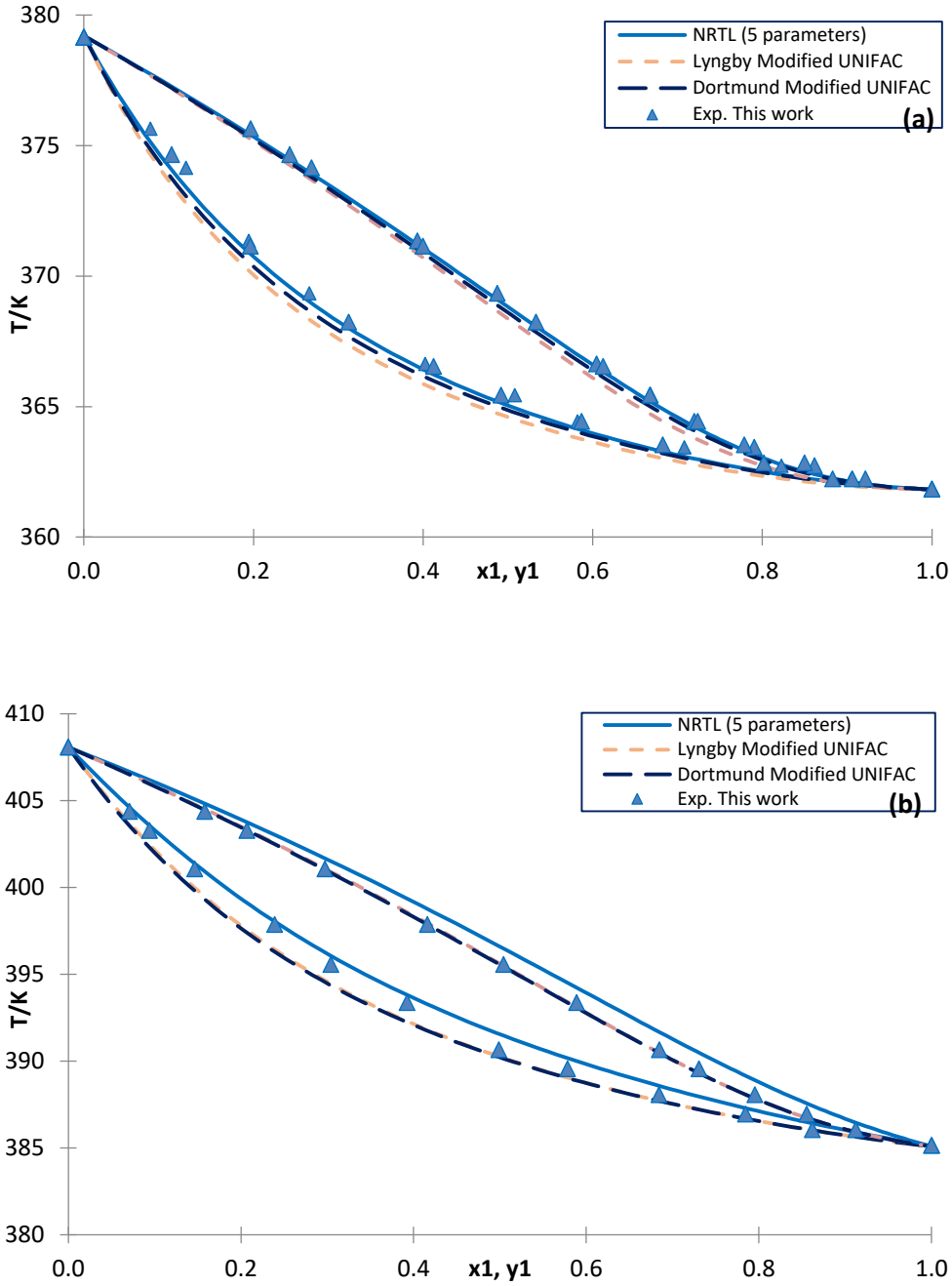

Figure D.2. PTxy diagram for [1-pentanol (1) + ethyl hexanoate (2)] at (a) 14.65 kPa and (b) 40 kPa (NRTL parameters were fitted on PTxy data measured in this work at 14.65 and 40 kPa: a_{12} = -5.09210; b_{12} /K = 2030.19; a_{21} = 1.10083; b_{21} /K = -345.249; α_{12} = α_{21} = 0.5).

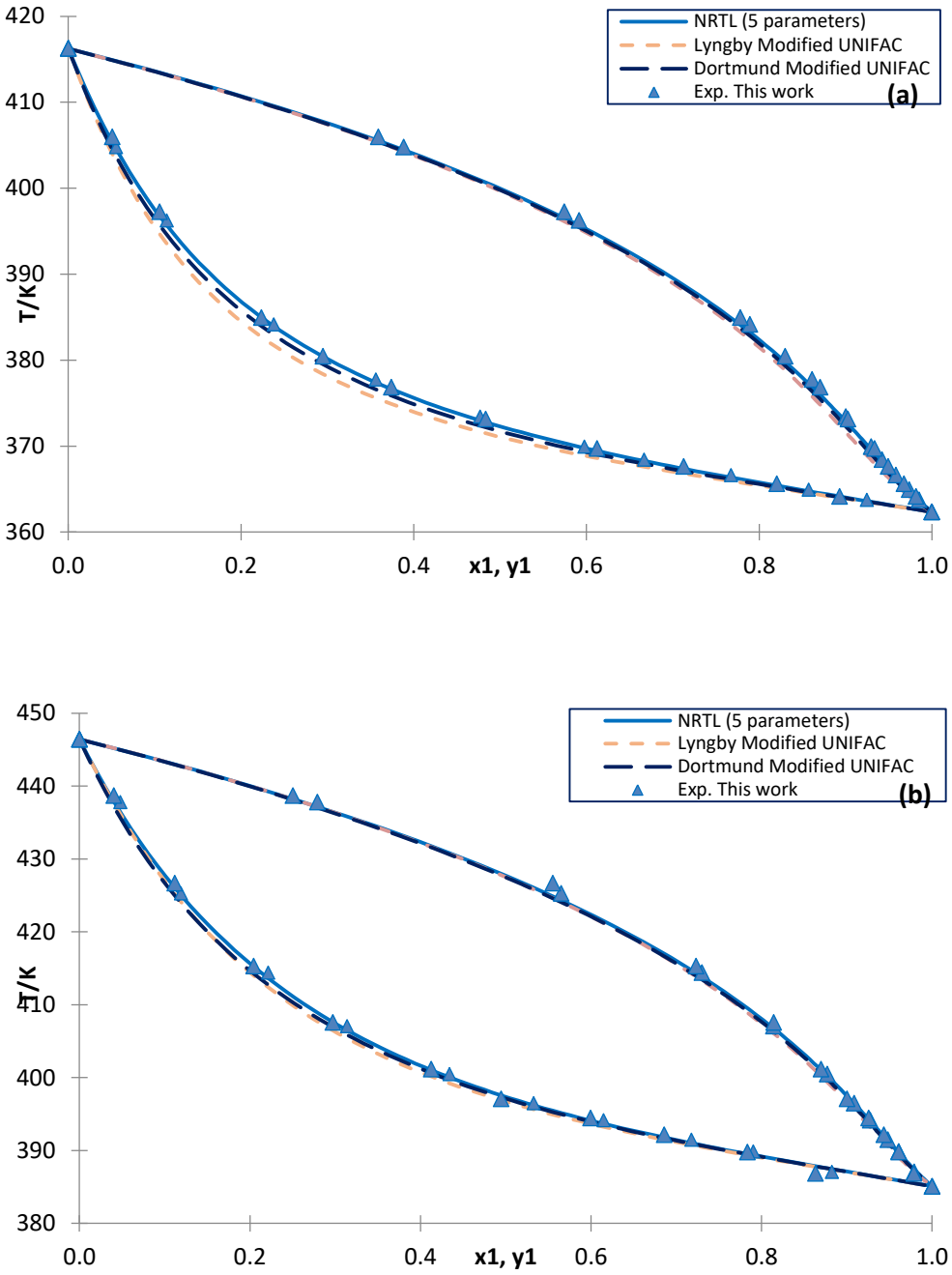

Figure D.3. PTxy diagram for [1-pentanol (1) + ethyl octanoate (2)] at (a) 15 kPa and (b) 40 kPa (NRTL parameters were fitted on PTxy data measured in this work at 15 and 40 kPa: a_{12} = 3.42889; b_{12} /K = -1035.93270; a_{21} = -3.25291; b_{21} /K = 1191.12747; α_{12} = α_{21} = 0.5).

Appendix E. Multicomponent – Prediction and Experimental Results

Table E.1. Multicomponent Prediction results with Dortmund Modified UNIFAC model

Stream (Summary)	UOM	FEED1	LIQ1	VAP1	FEED2	LIQ2	VAP2	FEED3	LIQ3	VAP3
Phase		Mixed	Liquid	Vapor	Mixed	Liquid	Vapor	Mixed	Liquid	Vapor
Thermodynamic System		UFT201	UFT201	UFT201	UFT201	UFT201	UFT201	UFT201	UFT201	UFT201
Total Molar Rate	kg-mol / hr	**1**	**0.93250166**	**0.06749834**	**1**	**0.93545797**	**0.06454203**	**1**	**0.93655475**	**0.06344525**
Temperature	K	**446.79**	**446.79**	**446.79**	**446.99**	**446.99**	**446.99**	**454.10**	**454.10**	**454.10**
Pressure	Pa	**7995.50**	**7995.50**	**7995.50**	**7995.50**	**7995.50**	**7995.50**	**9997.24**	**9997.24**	**9997.24**
Total Molecular Weight		**222.45**	**227.06**	**158.75**	**222.60**	**226.98**	**159.09**	**223.36**	**227.61**	**160.72**
					Total Molar Component Fractions					
OCTANOL		**0.1052**	**0.0745**	**0.5299**	**0.1023**	**0.0732**	**0.5240**	**0.0981**	**0.0709**	**0.4999**
DODA		**0.5134**	**0.5179**	**0.4506**	**0.5164**	**0.5205**	**0.4564**	**0.5158**	**0.5184**	**0.4780**
EPALMITATE		**0.0570**	**0.0608**	**0.0045**	**0.0570**	**0.0606**	**0.0046**	**0.0578**	**0.0614**	**0.0051**
ESTEARATE		**0.0423**	**0.0452**	**0.0016**	**0.0423**	**0.0451**	**0.0016**	**0.0429**	**0.0457**	**0.0018**
EOLEATE		**0.1139**	**0.1217**	**0.0059**	**0.1139**	**0.1213**	**0.0060**	**0.1154**	**0.1228**	**0.0067**
EVACCENATE		**0.0027**	**0.0029**	**0.0001**	**0.0027**	**0.0029**	**0.0001**	**0.0028**	**0.0030**	**0.0002**
ELINOLEATE		**0.1644**	**0.1758**	**0.0073**	**0.1643**	**0.1751**	**0.0073**	**0.1661**	**0.1768**	**0.0083**
EARACHIDATE		**0.0011**	**0.0012**	**0.0000**	**0.0011**	**0.0012**	**0.0000**	**0.0011**	**0.0012**	**0.0000**

Table E.1. (Continued)

Stream (Summary)	UOM	FEED4	LIQ4	VAP4	FEED5	LIQ5	VAP5	FEED6	LIQ6	VAP6
Phase		Mixed	Liquid	Vapor	Mixed	Liquid	Vapor	Mixed	Liquid	Vapor
Thermodynamic System		UFT201	UFT201	UFT201	UFT201	UFT201	UFT201	UFT201	UFT201	UFT201
Total Molar Rate	kg-mol / hr	**1**	**0.93157372**	**0.06842628**	**1**	**0.93211706**	**0.06788294**	**1**	**0.933261**	**0.066739**
Temperature	K	**455.10**	**455.10**	**455.10**	**461.01**	**461.01**	**461.01**	**461.41**	**461.41**	**461.41**
Pressure	Pa	**9997.24**	**9997.24**	**9997.24**	**11985.64**	**11985.64**	**11985.64**	**11985.64**	**11985.64**	**11985.64**
Total Molecular Weight		**223.91**	**228.46**	**161.94**	**224.42**	**228.89**	**163.06**	**224.60**	**228.95**	**163.68**
					Total Molar Component Fractions					
OCTANOL		**0.0946**	**0.0662**	**0.4809**	**0.0923**	**0.0652**	**0.4652**	**0.0892**	**0.0630**	**0.4550**
DODA		**0.5162**	**0.5177**	**0.4957**	**0.5149**	**0.5153**	**0.5091**	**0.5181**	**0.5180**	**0.5189**
EPALMITATE		**0.0584**	**0.0623**	**0.0054**	**0.0589**	**0.0628**	**0.0059**	**0.0590**	**0.0628**	**0.0060**
ESTEARATE		**0.0433**	**0.0463**	**0.0019**	**0.0438**	**0.0468**	**0.0021**	**0.0438**	**0.0468**	**0.0021**
EOLEATE		**0.1165**	**0.1245**	**0.0071**	**0.1176**	**0.1256**	**0.0077**	**0.1177**	**0.1256**	**0.0079**
EVACCENATE		**0.0028**	**0.0030**	**0.0002**	**0.0028**	**0.0030**	**0.0002**	**0.0028**	**0.0030**	**0.0002**
ELINOLEATE		**0.1671**	**0.1787**	**0.0088**	**0.1685**	**0.1801**	**0.0097**	**0.1683**	**0.1796**	**0.0099**
EARACHIDATE		**0.0011**	**0.0012**	**0.0000**	**0.0011**	**0.0012**	**0.0000**	**0.0011**	**0.0012**	**0.0000**

Table E.1. (Continued)

Stream (Summary)	UOM	FEED7	LIQ7	VAP7	FEED8	LIQ8	VAP8	FEED9	LIQ9	VAP9
Phase		Mixed	Liquid	Vapor	Mixed	Liquid	Vapor	Mixed	Liquid	Vapor
Thermodynamic System		UFT201	UFT201	UFT201	UFT201	UFT201	UFT201	UFT201	UFT201	UFT201
Total Molar Rate	kg-mol / hr	**1**	**0.92655969**	**0.07344031**	**1**	**0.92509322**	**0.07490678**	**1**	**0.93175643**	**0.06824357**
Temperature	K	**452.90**	**452.90**	**452.90**	**453.70**	**453.70**	**453.70**	**461.01**	**461.01**	**461.01**
Pressure	Pa	**7995.50**	**7995.50**	**7995.50**	**7995.50**	**7995.50**	**7995.50**	**9997.24**	**9997.24**	**9997.24**
Total Molecular Weight		**235.39**	**241.23**	**161.74**	**235.73**	**241.64**	**162.84**	**236.95**	**242.26**	**164.37**
				Total Molar Component Fractions						
OCTANOL		**0.0910**	**0.0583**	**0.5033**	**0.0874**	**0.0551**	**0.4864**	**0.0823**	**0.0541**	**0.4675**
DODA		**0.4173**	**0.4137**	**0.4637**	**0.4196**	**0.4148**	**0.4792**	**0.4163**	**0.4107**	**0.4938**
EPALMITATE		**0.0738**	**0.0790**	**0.0078**	**0.0740**	**0.0793**	**0.0081**	**0.0752**	**0.0801**	**0.0090**
ESTEARATE		**0.0548**	**0.0589**	**0.0027**	**0.0550**	**0.0592**	**0.0028**	**0.0559**	**0.0598**	**0.0032**
EOLEATE		**0.1472**	**0.1581**	**0.0101**	**0.1477**	**0.1588**	**0.0105**	**0.1502**	**0.1604**	**0.0117**
EVACCENATE		**0.0035**	**0.0038**	**0.0002**	**0.0035**	**0.0038**	**0.0002**	**0.0036**	**0.0038**	**0.0003**
ELINOLEATE		**0.2109**	**0.2267**	**0.0122**	**0.2113**	**0.2274**	**0.0127**	**0.2149**	**0.2296**	**0.0144**
EARACHIDATE		**0.0014**	**0.0015**	**0.0000**	**0.0014**	**0.0015**	**0.0000**	**0.0015**	**0.0016**	**0.0000**

Table E.1. (Continued)

Stream (Summary)	UOM	FEED10	LIQ10	VAP10	FEED11	LIQ11	VAP11	FEED12	LIQ12	VAP12
Phase		Mixed	Liquid	Vapor	Mixed	Liquid	Vapor	Mixed	Liquid	Vapor
Thermodynamic System		UFT201	UFT201	UFT201	UFT201	UFT201	UFT201	UFT201	UFT201	UFT201
Total Molar Rate	kg-mol / hr	**1**	**0.9191904**	**0.0808096**	**1**	**0.89796195**	**0.10203805**	**1**	**0.91875779**	**0.08124221**
Temperature	K	**462.81**	**462.81**	**462.81**	**466.31**	**466.31**	**466.31**	**471.31**	**471.31**	**471.31**
Pressure	Pa	**9997.24**	**9997.24**	**9997.24**	**7995.50**	**7995.50**	**7995.50**	**9997.24**	**9997.24**	**9997.24**
Total Molecular Weight		**237.18**	**243.37**	**166.76**	**244.52**	**251.88**	**179.78**	**244.16**	**250.00**	**178.13**
					Total Molar Component Fractions					
OCTANOL		**0.0787**	**0.0476**	**0.4321**	**0.0438**	**0.0202**	**0.2517**	**0.0449**	**0.0244**	**0.2766**
DODA		**0.4197**	**0.4104**	**0.5255**	**0.4057**	**0.3746**	**0.6797**	**0.4073**	**0.3852**	**0.6570**
EPALMITATE		**0.0753**	**0.0810**	**0.0099**	**0.0823**	**0.0898**	**0.0160**	**0.0819**	**0.0878**	**0.0154**
ESTEARATE		**0.0560**	**0.0606**	**0.0036**	**0.0617**	**0.0680**	**0.0059**	**0.0613**	**0.0662**	**0.0057**
EOLEATE		**0.1504**	**0.1625**	**0.0128**	**0.1654**	**0.1818**	**0.0207**	**0.1646**	**0.1774**	**0.0199**
EVACCENATE		**0.0036**	**0.0039**	**0.0003**	**0.0039**	**0.0043**	**0.0005**	**0.0039**	**0.0042**	**0.0005**
ELINOLEATE		**0.2148**	**0.2323**	**0.0158**	**0.2356**	**0.2595**	**0.0255**	**0.2345**	**0.2530**	**0.0249**
EARACHIDATE		**0.0015**	**0.0016**	**0.0000**	**0.0016**	**0.0018**	**0.0001**	**0.0016**	**0.0017**	**0.0001**

Table E.2. Experimental VLE results for multicomponent systems [Alcohols + EEBA] together with deviations in the liquid and vapor mole fractions predicted by Dortmund Modified UNIFAC model (mole fractions of the components in the global mixture (z), in the liquid and vapor phases (x and y)).

Component	P (Pa) = 7995.50 - T (K) = 446.79					P (Pa) = 7995.50 - T (K) = 446.99				
	z	x	Y	Δxi	Δyi	Z	x	y	Δxi	Δyi
1-Octanol	**0.1052**	**0.0763**	**0.5709**	**0.0019**	**0.0410**	**0.1023**	**0.0791**	**0.5688**	**0.0059**	**0.0448**
1-Dodecanol	**0.5134**	**0.5564**	**0.4173**	**0.0384**	**-0.0334**	**0.5164**	**0.5238**	**0.4190**	**0.0032**	**-0.0374**
Ethyl palmitate	**0.0570**	**0.0548**	**0.0035**	**-0.0060**	**-0.0010**	**0.0570**	**0.0592**	**0.0036**	**-0.0014**	**-0.0009**
Ethyl stearate	**0.0423**	**0.0407**	**0.0008**	**-0.0045**	**-0.0008**	**0.0423**	**0.0441**	**0.0008**	**-0.0010**	**-0.0007**
Ethyl oleate	**0.1139**	**0.1095**	**0.0026**	**-0.0122**	**-0.0034**	**0.1139**	**0.1185**	**0.0027**	**-0.0028**	**-0.0033**
Ethyl cis-vaccenate	**0.0027**	**0.0026**	**0.0000**	**-0.0003**	**-0.0001**	**0.0027**	**0.0028**	**0.0000**	**0.0000**	**-0.0001**
Ethyl linoleate	**0.1644**	**0.1586**	**0.0050**	**-0.0172**	**-0.0023**	**0.1643**	**0.1713**	**0.0051**	**-0.0038**	**-0.0022**
Ethyl Arachidate	**0.0011**	**0.0011**	**0.0000**	**-0.0001**	**0.0000**	**0.0011**	**0.0012**	**0.0000**	**0.0000**	**0.0000**
Average Absolute Deviation				**0.010**	**0.010**				**0.002**	**0.011**

Component	P (Pa) = 9997.24 - T (K) = 454.10					P (Pa) = 9997.24 - T (K) = 455.10				
	Z	x	Y	Δxi	Δyi	Z	X	y	Δxi	Δyi
1-Octanol	**0.0981**	**0.0785**	**0.5510**	**0.0076**	**0.0511**	**0.0946**	**0.0757**	**0.5270**	**0.0095**	**0.0461**
1-Dodecanol	**0.5158**	**0.5213**	**0.4354**	**0.0029**	**-0.0426**	**0.5161**	**0.5219**	**0.4585**	**0.0043**	**-0.0372**
Ethyl palmitate	**0.0578**	**0.0597**	**0.0040**	**-0.0016**	**-0.0011**	**0.0584**	**0.0603**	**0.0043**	**-0.0020**	**-0.0012**
Ethyl stearate	**0.0429**	**0.0444**	**0.0010**	**-0.0012**	**-0.0008**	**0.0433**	**0.0448**	**0.0010**	**-0.0016**	**-0.0009**
Ethyl oleate	**0.1154**	**0.1195**	**0.0030**	**-0.0033**	**-0.0037**	**0.1165**	**0.1204**	**0.0032**	**-0.0042**	**-0.0039**
Ethyl cis-vaccenate	**0.0028**	**0.0029**	**0.0000**	**-0.0001**	**-0.0002**	**0.0028**	**0.0029**	**0.0000**	**-0.0001**	**-0.0002**
Ethyl linoleate	**0.1661**	**0.1725**	**0.0056**	**-0.0043**	**-0.0027**	**0.1671**	**0.1729**	**0.0060**	**-0.0059**	**-0.0028**
Ethyl Arachidate	**0.0011**	**0.0012**	**0.0000**	**0.0000**	**0.0000**	**0.0011**	**0.0012**	**0.0000**	**0.0000**	**0.0000**
Average Absolute Deviation				**0.003**	**0.013**				**0.003**	**0.012**

Table E.2. (Continued)

Component	P (Pa) = 11985.64 - T (K) = 461.01					P (Pa) = 11985.64 - T (K) = 461.41				
	z	X	Y	Δxi	Δyi	Z	X	y	Δxi	Δyi
1-Octanol	**0.0923**	**0.0714**	**0.5157**	**0.0063**	**0.0505**	**0.0892**	**0.0701**	**0.5113**	**0.0071**	**0.0562**
1-Dodecanol	**0.5148**	**0.5179**	**0.4690**	**0.0026**	**-0.0401**	**0.5180**	**0.5222**	**0.4737**	**0.0042**	**-0.0452**
Ethyl palmitate	**0.0589**	**0.0615**	**0.0045**	**-0.0013**	**-0.0014**	**0.0590**	**0.0611**	**0.0044**	**-0.0017**	**-0.0016**
Ethyl stearate	**0.0438**	**0.0457**	**0.0011**	**-0.0011**	**-0.0010**	**0.0438**	**0.0455**	**0.0011**	**-0.0013**	**-0.0011**
Ethyl oleate	**0.1176**	**0.1229**	**0.0034**	**-0.0028**	**-0.0043**	**0.1177**	**0.1222**	**0.0034**	**-0.0034**	**-0.0045**
Ethyl cis-vaccenate	**0.0028**	**0.0030**	**0.0000**	**0.0000**	**-0.0002**	**0.0028**	**0.0029**	**0.0000**	**-0.0001**	**-0.0002**
Ethyl linoleate	**0.1685**	**0.1764**	**0.0063**	**-0.0037**	**-0.0034**	**0.1683**	**0.1748**	**0.0062**	**-0.0049**	**-0.0037**
Ethyl Arachidate	**0.0011**	**0.0012**	**0.0000**	**0.0000**	**0.0000**	**0.0011**	**0.0012**	**0.0000**	**0.0000**	**0.0000**
Average Absolute Deviation				**0.002**	**0.013**				**0.003**	**0.014**

Component	P (Pa) = 7995.50 - T (K) = 452.90					P (Pa) = 7995.50 - T (K) = 453.70				
	z	X	Y	Δxi	Δyi	Z	X	y	Δxi	Δyi
1-Octanol	**0.0910**	**0.0660**	**0.5584**	**0.0076**	**0.0552**	**0.0874**	**0.0622**	**0.5375**	**0.0071**	**0.0512**
1-Dodecanol	**0.4173**	**0.4186**	**0.4214**	**0.0049**	**-0.0424**	**0.4196**	**0.4188**	**0.4412**	**0.0039**	**-0.0380**
Ethyl palmitate	**0.0738**	**0.0771**	**0.0061**	**-0.0019**	**-0.0017**	**0.0740**	**0.0778**	**0.0064**	**-0.0016**	**-0.0016**
Ethyl stearate	**0.0548**	**0.0574**	**0.0015**	**-0.0015**	**-0.0013**	**0.0550**	**0.0578**	**0.0015**	**-0.0014**	**-0.0013**
Ethyl oleate	**0.1472**	**0.1542**	**0.0046**	**-0.0039**	**-0.0055**	**0.1477**	**0.1553**	**0.0049**	**-0.0035**	**-0.0056**
Ethyl cis-vaccenate	**0.0035**	**0.0037**	**0.0000**	**-0.0001**	**-0.0002**	**0.0035**	**0.0037**	**0.0000**	**-0.0001**	**-0.0002**
Ethyl linoleate	**0.2109**	**0.2215**	**0.0080**	**-0.0051**	**-0.0042**	**0.2113**	**0.2229**	**0.0084**	**-0.0045**	**-0.0043**
Ethyl Arachidate	**0.0014**	**0.0015**	**0.0000**	**0.0000**	**0.0000**	**0.0014**	**0.0015**	**0.0000**	**0.0000**	**0.0000**
Average Absolute Deviation				**0.003**	**0.014**				**0.003**	**0.013**

Table E.2. (Continued)

Component	P (Pa) = 9997.24 - T (K) = 461.01					P (Pa) = 9997.24 - T (K) = 462.81				
	Z	X	Y	Δxi	Δyi	Z	X	y	Δxi	Δyi
1-Octanol	**0.0823**	**0.0617**	**0.5099**	**0.0076**	**0.0424**	**0.0787**	**0.0572**	**0.4808**	**0.0096**	**0.0487**
1-Dodecanol	**0.4163**	**0.4175**	**0.4637**	**0.0068**	**-0.0301**	**0.4197**	**0.4205**	**0.4898**	**0.0101**	**-0.0357**
Ethyl palmitate	**0.0752**	**0.0780**	**0.0078**	**-0.0020**	**-0.0012**	**0.0753**	**0.0782**	**0.0087**	**-0.0028**	**-0.0012**
Ethyl stearate	**0.0559**	**0.0581**	**0.0020**	**-0.0017**	**-0.0012**	**0.0560**	**0.0583**	**0.0022**	**-0.0023**	**-0.0013**
Ethyl oleate	**0.1502**	**0.1560**	**0.0062**	**-0.0044**	**-0.0055**	**0.1504**	**0.1566**	**0.0070**	**-0.0059**	**-0.0058**
Ethyl cis-vaccenate	**0.0036**	**0.0037**	**0.0000**	**-0.0001**	**-0.0003**	**0.0036**	**0.0037**	**0.0000**	**-0.0002**	**-0.0003**
Ethyl linoleate	**0.2149**	**0.2235**	**0.0104**	**-0.0061**	**-0.0041**	**0.2148**	**0.2239**	**0.0115**	**-0.0083**	**-0.0043**
Ethyl Arachidate	**0.0015**	**0.0015**	**0.0000**	**-0.0001**	**0.0000**	**0.0015**	**0.0015**	**0.0000**	**-0.0001**	**0.0000**
Average Absolute Deviation				**0.004**	**0.011**				**0.005**	**0.012**

Component	P (Pa) = 7995.50 - T (K) = 466.31					P (Pa) = 9997.24 - T (K) = 471.31				
	Z	X	Y	Δxi	Δyi	Z	X	y	Δxi	Δyi
1-Octanol	**0.0438**	**0.0260**	**0.2947**	**0.0058**	**0.0430**	**0.0449**	**0.0338**	**0.3373**	**0.0094**	**0.0607**
1-Dodecanol	**0.4057**	**0.3889**	**0.6575**	**0.0144**	**-0.0222**	**0.4073**	**0.4012**	**0.6201**	**0.0160**	**-0.0369**
Ethyl palmitate	**0.0823**	**0.0870**	**0.0141**	**-0.0028**	**-0.0019**	**0.0819**	**0.0843**	**0.0126**	**-0.0035**	**-0.0027**
Ethyl stearate	**0.0617**	**0.0655**	**0.0038**	**-0.0025**	**-0.0021**	**0.0613**	**0.0632**	**0.0033**	**-0.0030**	**-0.0024**
Ethyl oleate	**0.1654**	**0.1757**	**0.0117**	**-0.0061**	**-0.0090**	**0.1646**	**0.1695**	**0.0103**	**-0.0079**	**-0.0096**
Ethyl cis-vaccenate	**0.0039**	**0.0042**	**0.0000**	**-0.0001**	**-0.0005**	**0.0039**	**0.0040**	**0.0000**	**-0.0002**	**-0.0005**
Ethyl linoleate	**0.2356**	**0.2509**	**0.0183**	**-0.0086**	**-0.0072**	**0.2345**	**0.2423**	**0.0163**	**-0.0107**	**-0.0086**
Ethyl Arachidate	**0.0016**	**0.0017**	**0.0000**	**-0.0001**	**-0.0001**	**0.0016**	**0.0017**	**0.0000**	**-0.0001**	**-0.0001**
Average Absolute Deviation				**0.005**	**0.011**				**0.006**	**0.015**